Thermo-Oxidative Degradation Of Polyamide 6

by

Michael Nathan Grigg

B. App. Sci. (Hons.)

A Thesis Submitted for the Degree of Doctor of Philosophy
At the School of Physical and Chemical Sciences
Queensland University of Technology
2006

To the most important people

in the world

my brother, my Nan,

the memory of my Grandad,

And my beautiful little Sarah

Declaration

The work submitted in this thesis has not been previously submitted for a degree or diploma at any other tertiary educational institution. To the best of my knowledge and belief, the material contained in this thesis contains no material previously published or written by any other person except where due reference is made.

M. N. Grigg……

January, 2006

Acknowledgments

First and foremost I would like to thank my supervisor, Prof. Graeme George, for providing me with the opportunity, insight, guidance and discussions as well as both moral and financial support through my PhD program. I can't express enough gratitude for his patience.

Thanks to the past and present members of the QUT Polymer Group including Idriss Blakey, Ben Goss, Heping Liu and Sue Hunt for their friendship. Additional gratitude goes to Idriss, Heping and Sue for instructing me on the CL apparatus, FTIR emission spectrometer and MALDI-TOF MS instrument respectively.

I thank Prof. Norman C. Billingham for allowing me to conduct research with his group at the University of Sussex (England) on two separate occasions and for his guidance, discussions, and financial assistance. For the friendship given by the members of his group including Christos, Laurent, Amiya and particularly Dave, who showed me the ropes of the CL Imager and the CL-DSC, I am truly grateful.

It must also be acknowledged that a Queensland University of Technology Postgraduate Research Award (QUT-PRA) and an ARC Grant (number A29803983) supported this project. The QUT Grants-In-Aid scheme, the Centre for Instrumental and Developemental Chemistry (QUT) and the RACI Polymer Division also provided additional financial support for domestic and international conferences and for research performed internationally.

Lastly, thanks to all of my dear friends for all their support and encouragement.

Relevant Publications/Conference Proceedings

M. Grigg, N.C. Billingham, G.A. George, "Chemiluminescence Imaging and Simultaneous Chemiluminescence/DSC of Nylon 6 Thermo-Oxidation." *World Chemistry Congress*, P93, 2001.

G.A. George, I. Blakey, B. Goss, M. Grigg, "Modeling, Experimental Evidence and Practical Consequences of the Infectious Spreading of Oxidative Degradation in Polymers." *Polymer Preprints (American Chemical Society, Division Of Polymer Chemistry)*, 2001, 42, 402-403.

M. Grigg, N.C. Billingham, G.A. George, "Effects of End Groups on the Thermo-Oxidative Degradation of Nylon 6." *24th Australian Polymer Symposium*, B6/3, 2001.

M. Grigg, S. Hunt, G.A. George, "Oxidation Analysis of Nylon by MALDI-TOF MS and Chemiluminescence." *MODEST*, proceedings, 2000.

G.A. George, I. Blakey, B. Goss, M. Grigg, H. Liu, "Evidence for the Infectious Spreading of Polymer Oxidation and the Implications for Polymer Lifetimes." *MODEST*, proceedings, 2000.

M. Grigg, S. Hunt, G.A. George, "MALDI-TOF Analysis of Nylon Degradation." *23rd Australian Polymer Symposium*, 1999, P1/19.

Abstract

The thermo-oxidative degradation of unstabilized polyamide 6 (PA-6) was investigated by a number of novel techniques in an attempt to achieve a better understanding of the mechanisms involved in the oxidative degradation of polymers. Particular attention was given to the influence of end groups on PA-6 oxidation by studying samples that terminated predominantly in carboxylic, amine or methyl end groups.

The changes occurring in the oxidative stabilities and mechanisms of PA-6 as a result of altering the end groups of PA-6 were investigated by a technique termed CL-DSC, which simultaneously measures the chemiluminescence (CL) and heat flow (DSC) from a sample. When amine end groups were abundant in the PA-6 sample a chemically induced electron exchange luminescence (CIEEL) mechanism could occur directly and the CL intensity was proportional to the heat flow curve of the DSC. However, when amine end groups were absent it was the first derivative of the CL intensity that was proportional to the heat flow curve because the CIEEL mechanism could not operate until an easily oxidisable luminescent oxidation product was formed.

Due to the dramatic effect end groups have on the oxidation mechanisms of PA-6 it was hypothesized that end groups could be sites analogous to the impurities in polyolefins that lead to heterogeneous oxidation. To test this hypothesis, CL Imaging was used to map the occurrence and extent of oxidation across samples of PA-6 to

display the influence end groups have on the homogeneous or heterogeneous nature of PA-6 oxidation.

Sequences of FTIES spectra collected at specified time intervals during the *in situ* oxidation of PA-6 samples terminating in the different end groups were turned into oxidation product profiles. The differences between spectra related to significant points on the oxidation profiles were compared in an attempt to elucidate the chemical or physical changes occurring in the samples during oxidation.

To identify the species involved in the mechanistically different oxidation processes resulting from the different end groups, methods for the MALDI-TOF analysis of non-oxidized and oxidized PA- 6 samples were developed via trial and error. It was only possible to detect the occurrence of degradation products by MALDI-TOF MS after considerable oxidation as measured by chemiluminescence, by which time the species were the result of a number of oxidative processes. Therefore, identification of the species formed was not possible.

Table of Contents

List of Figures

List of Tables

Preface

Polymeric materials constitute a major part of the materials used today and the number of applications utilizing polymers is continuously increasing. For example, polyamides are widely used in the textile industry and as engineering materials because of their good mechanical properties and high thermal resistance. Depending on their required use polymers can be expected to have a service life in excess of a decade. However, the lifetime of polymers is limited and if it were not for the addition of appropriate stabilizers the majority of polymers would be useless. Thermal oxidation of polymers is often the cause of detrimental changes to polymer properties and is therefore an important factor that determines the service life of many polymer products. The trend now is not to develop new polymers that offer long term stability and high temperature performance but rather to develop new additives such as stabilizers and fillers to enhance the already available polymers. Therefore, it is important to have an accurate understanding of the oxidation and degradation mechanisms responsible for the deterioration of polymers.

In early studies, oxidation was shown to proceed via a radical chain reaction commonly referred to as autoxidation. This scheme has since been applied by a great number of authors to the solid state oxidation of polymers. For example, oxidation kinetics have been modeled to enable the prediction of a polymer's serviceable lifetime. However, the classical approach to the modeling of polymer oxidation applies a homogeneous description based on liquid hydrocarbons to that of solid

polymers, which assumes that reactions occur homogeneously throughout the polymer. Recently, it has been proposed that the solid state oxidation of polymers is heterogeneous and should be modeled as such. To date, studies into the mechanistic aspects of polymer oxidative degradation has been largely base around polyolefins.

The aim of this work was to achieve a better understanding of the mechanisms involved in the oxidative degradation of polymers by investigating the processes occurring during the oxidation of polyamide 6 (PA-6). PA-6 is a condensation polymer that has none of the features of polyolefins except that it too is oxidatively unstable.

An introduction to polyamides and polymer oxidation is provided in **chapter 1**. Particular attention has been given to the oxidation of polyamides and the influence that end groups and hydroperoxides have on the oxidation mechanisms. Current methods for the stabilization of polyamides, related to the oxidative mechanisms, are also described. **Chapter 2** outlines the theory behind the various instrumental techniques used in the course of the study to enable a greater understanding of the results obtained.

The end groups of the polyamide chains have been shown to have a significant effect on the rate of polyamide oxidation. Therefore, three samples terminating in predominantly carboxylic, amine and methyl groups were required. The synthesis and characterization of the samples are discussed in **chapter 3**.

CL-DSC is a technique that simultaneously measures the chemiluminescence and the heat flow from a sample during oxidation. The results from this technique, displayed in **chapter 4**, made the differences in the oxidative mechanisms and stabilities as a result of the end groups obvious. Light was also shed on the mechanism for CL emission from polymers.

The oxidation of polyolefins has been shown to initiate from zones of impurities, such as residual Ziegler Natta catalyst, and progressively spread across the polymer. Polyamides do not contain the obvious impurities that cause the heterogeneous oxidation in polyolefins. However, in view of the results from chapter 4, it was hypothesized that the end groups in PA-6 could be considered to be impurities analogous to those of polyolefins, which cause heterogeneous oxidation. CL Imaging was utilized in **chapter 5** to test this hypothesis. Initially the oxidation of polyamide 6 appeared to be homogeneous regardless of the type of end groups present. However, further experiments indicated that oxidation can indeed start and spread from end groups.

In **chapter 6** FT-IES was used in an attempt to further elucidate the chemical or physical changes occurring in the samples during oxidation. A method was developed in **chapter 7** for the analysis of un-oxidized and oxidized samples of polyamide 6 by MALDI-TOF MS. This method was applied in **chapter 8** to identify the species present at different times during the oxidation of polyamide sample that terminated in predominantly different end groups. Conclusions and ideas for future work are then presented in **chapters 9** and **10** respectively.

1. Introduction

1.1 Polyamides

1.1.1 General

Polyamides (PA's), also referred to as nylons, are the class of thermoplastic polymers which contain the amide repeat linkage in the polymer backbone.[1] Carothers, and other scientists at Du Pont, developed PA's in the 1930's and in 1939 PA's became the first truly synthetic fiber to be commercialized.[2]

The regularity of the amide linkages along the polymer chain defines the two main classes of PA's: AB and AABB. AB polyamides are formed in a polycondensation reaction from cyclic amides (lactams). Type AABB, where the amide linkages alternate in orientation along the backbone, are formed from diacids and diamines in a polycondensation reaction.[3] Examples of AB and AABB types (Figure 1.1) are Polyamide-6 (PA-6) and Polyamide-6,6 (PA-6,6) respectively. Only PA-6 was used in this study.

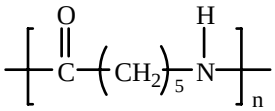

Polyamide 6

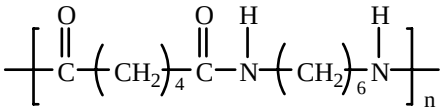

Polyamide 6,6

Figure 1.1: Repeating units of polyamide 6 and polyamide 6,6

PA-6 is produced by the ring opening polymerization of ε-caprolactam initiated by water. Small specific amounts of a monofunctional acid are added to the polymerization to control molecular weights and catalyze reactions.[4]

1.1.2 Properties

PA's are semicrystalline as they consist of crystalline and amorphous phases.[5] Crystallinity results from the polar amide groups, which undergo hydrogen bonding between the carbonyl and NH groups in adjacent sections of the PA chains. The regular spatial alignment of amide groups allows a high degree of hydrogen bonding to develop when chains are aligned together. The more random amorphous regions have a much lower degree of hydrogen bonding.[5]

A semicrystalline structure gives rise to a good balance of properties. The crystalline regions contribute to the hardness, yield strength, chemical resistance, creep resistance and temperature stability. The amorphous areas contribute to the impact resistance and high elongation. Because of their good chemical resistance, PA's are insoluble in common organic solvents at room temperature. However, they are soluble in formic acid, phenols, mineral acids, and fluorinated alcohols such as 2,2,2-trifluoroethanol.[6]

The high melting points of PA's are a function of the strong hydrogen bonding between the chains. PA-6 and PA-66 are isomers that share the same empirical

formula, density and other properties but differ in melting point. PA-6 melts at 225°C and PA-6,6 melts at 265°C. This is due to the differences in the alignment of molecular chains and crystallization behavior.

Polyamides are hygroscopic as water hydrogen bonds to the polar amide groups.[7,8] Water absorption is greater in the amorphous regions due to greater availability of amide groups. Moisture strongly affects properties of polyamides such as the glass transition temperature (T_g) and acts as a plasticiser increasing the flexibility and toughness. Polyamides also degrade by hydrolysis at elevated temperatures.[3]

1.1.3 Applications

Polyamides are significant commercial polymeric materials, representing approximately 4% of the total world consumption of principal polymers. PA-6 accounts for approximately 54% of polyamides produced while PA-6,6 accounts for approximately 36%.[3]

Almost 75% of polyamides are used as fibres while about 15% are used as engineering plastics. Fibre uses include carpet, apparel, home furnishings and industrial applications.[9] Engineering uses vary from wheel covers, handles, radiator end tanks and fuel hoses in the automotive industry to hair dryers, lawnmowers, gears and bearings.[10]

1.2 Oxidation of Polymers

The service life of polymers is limited by their degradation, which can be caused by a number of environmental factors, e.g. temperature, humidity, impurities, mechanical load, irradiation, microorganisms, chemicals and air. Degradation is an undesirable process in the majority of polymeric applications as it generally leads to changes in the chemical and physical structure of the polymer resulting in the loss of many useful properties, such as molecular weight[11], mechanical strength[12], impact resistance[13] and colour[14]. The understanding of degradation mechanisms is further complicated by factors such as morphology, diffusion processes and interactions of additives.

Oxidation is one of the most important of all degradation processes. Hoffman made the first report on oxidative degradation of polymers in 1861.[15] He found that the perishing of natural rubber involves absorption of oxygen. Since then the oxidation of polymers has been the subject of extensive studies and the continuous progress has been covered in several books.[16-21]

Oxidation can occur in every stage of the life cycle of a polymer: during manufacture and storage of the polymer resin, as well as during processing and end use of the plastic article produced. Numerous oxidation products are formed as the result of the degradation of polymers, such as peroxides, alcohols, ketones, aldehydes, acids, peracids, peresters and γ-lactones. Elevated temperatures, irradiation (e.g. UV) and catalysts such as metal ions increase oxidation rates. Also, most polymers have structural elements that are particularly prone to oxidative degradation reactions.[22]

1.2.1 Autoxidation

The definition of autoxidation is auto-initiated oxidation by molecular oxygen, but the word is commonly used to describe the reaction of oxygen with organic materials by a free radical process.[16] At ambient temperatures the oxidation of pure hydrocarbons is usually slow so it remains physically and chemically intact for a relatively long period of time. Autoxidation is often initiated thermally, photochemically or mechanically. In the presence of impurities, or when the polymer contains a high degree of branching, functional groups or unsaturation, the rate of oxidation increases markedly. Thus, polymer structure and the content of impurities are obviously important factors that determine the oxidative susceptibility of the polymer.

Structural defects and impurities cannot be excluded from a polymer sample. During processing (the melt, extrusion and injection/blow molding) peroxy radicals are formed by reaction with molecular oxygen under the conditions of high temperatures and mechanical shear.[23] Therefore, contaminants are present right from the start of the polymer's service life.

When a hydrocarbon polymer is exposed to oxygen it first goes through an apparent induction period during which the rate of formation of oxidation products does not seem to increase (Figure 1.2). A small concentration of hydroperoxides is formed during this time. However, when a certain concentration of hydroperoxides is reached, accelerated oxidation begins. The processes responsible for the production of hydroperoxides during the induction period are not yet fully understood.[23]

The useful life of polymers is generally a little longer than the induction period and failure often occurs within a short time after the onset of accelerated oxidation. Therefore, it is very important to study the reactions occurring during the early stages of oxidation in order to understand the subsequent accelerated phase of polymer oxidation.

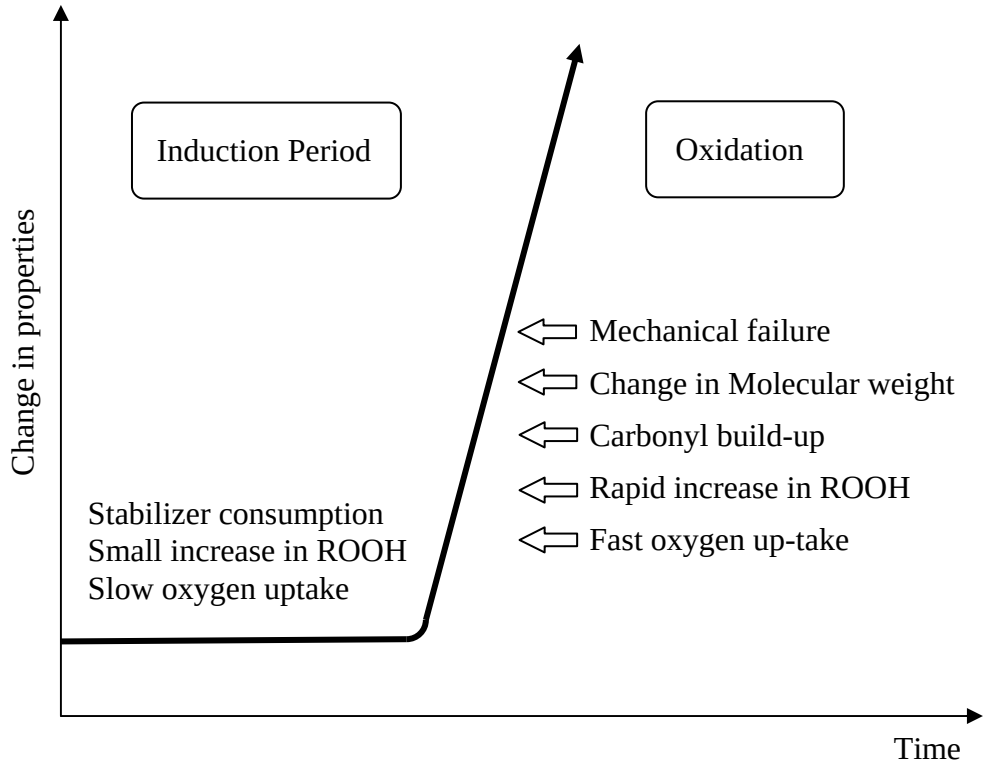

Figure 1.2: Changes in material properties during aging of polymers

The basic autoxidation scheme (BAS) was first developed by Bolland, Gee and Bateman in the 1940's.[24-26] It is based on free radical chain reaction theory obtained from studies on liquid hydrocarbons. This scheme has been modified[16], as displayed in Figure 1.3, to describe polymer oxidation.

Initiation:

Polymer $\longrightarrow$ $P^{\bullet}$ + $P^{\bullet}$ (1.1)

Propagation:

$P^{\bullet}$ + O_2 $\longrightarrow$ $POO^{\bullet}$ (1.2)

$POO^{\bullet}$ + PH $\longrightarrow$ POOH + $P^{\bullet}$ (1.3)

Chain Branching:

POOH $\longrightarrow$ $PO^{\bullet}$ + $^{\bullet}OH$ (1.4)

POOH + POOH $\longrightarrow$ $PO^{\bullet}$ + $POO^{\bullet}$ + H_2O (1.5)

PH + $^{\bullet}OH$ $\longrightarrow$ $P^{\bullet}$ + H_2O (1.6)

PH + $PO^{\bullet}$ $\longrightarrow$ $P^{\bullet}$ + POH (1.7)

Termination:

$P^{\bullet}$ + $P^{\bullet}$ $\longrightarrow$ Non Radical Products (1.8)

$P^{\bullet}$ + $POO^{\bullet}$ $\longrightarrow$ Non Radical Products (1.9)

$POO^{\bullet}$ + $POO^{\bullet}$ $\longrightarrow$ Non Radical Products + O_2 (1.10)

Figure 1.3: The basic autoxidation scheme (BAS) for hydrocarbon oxidation.

The basic steps in this scheme are free radical initiation, propagation, chain branching and termination, the cycle of which is displayed in Figure 1.4. At relatively larger extents of oxidation, secondary reactions may become important. Because this model is based on liquid solutions with homogeneous kinetics it should

be noted that the application of this model to solid state oxidation of polymers assumes that the oxidation takes place uniformly within the polymer and that the rate constants of the different reactions remain constant, irrespective of where the reaction takes place in the polymer. This has been reported to be unlikely in the oxidation of polypropylene.[27]

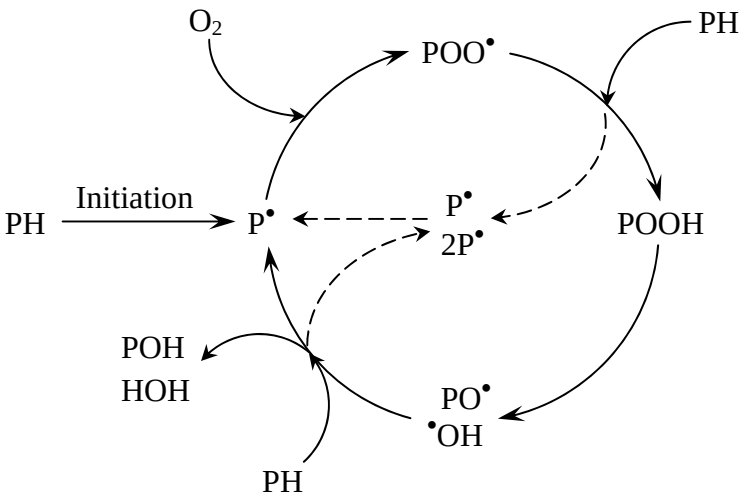

Figure 1.4: The cycle of autoxidation.

1.2.1.1 Initiation

The initiation reaction represents the 'primary' initiation. However, the method by which the primary alkyl radical $P^{\bullet}$ (eq. 1.1) is produced has not been fully determined.[22] The direct reaction of the polymer with molecular oxygen is not favoured due to thermodynamic and kinetic considerations. One explanation is that, in the course of polymerization, catalysts such as transition metals, radical initiators, impurities in the monomers, and minute amounts of oxygen react and form peroxy

radicals $POO^{\bullet}$ which abstract hydrogen from the polymer and form an alkyl radical and a hydroperoxide (eq. 1.3).[28,29] The hydroperoxides produced during polymerization decompose when heated or irradiated yielding free radicals that can initiate autoxidation. The decomposition can proceed homolytically (eq. 1.4) or bimolecularly (eq. 1.5), with the dominating reaction pathway depending on hydroperoxide concentration and reaction temperature.[17,23,30] The proximity of adjacent hydroperoxides has been found to be another important factor.[31-33]

Several authors have concluded that hydroperoxides are the major primary oxidation product.[31,34]. When the concentration builds up during oxidation, the decomposition of hydroperoxides becomes the predominant initiating step in the chain branching reactions. This hypothesis suggests that impurities, which are formed in the manufacturing and processing of the polymer, will have a significant effect on the rate of initiation and the overall rate of oxidation.

1.2.1.2 Propagation

ESR studies[35,36] have shown that the alkyl radicals produced during initiation (eq. 1.1) react almost instantly with molecular oxygen to form peroxy radicals (eq. 1.2). This reaction has little or no activation energy and is almost independent of temperature. However, the reaction does depend on the oxygen pressure and the radical structure.[37,38] The rate constant for the reaction of most alkyl radicals with oxygen is in the order of 10^7–10^9 $mol^{-1}s^{-1}$.[36]

The peroxy radical produced can abstract a hydrogen atom from the polymer resulting in a hydroperoxide and a new macro radical (eq. 1.3), which can start another propagation cycle. The abstraction may be either intramolecular by abstraction of a hydrogen atom from the same polymer chain or intermolecular by abstraction from an adjacent molecule.[39-41]

The abstraction of hydrogen by a peroxy radical requires the breaking of a C–H bond. This reaction has a significant activation energy and is the rate-determining step in autoxidation.[42] As the bond energy of the POO–H bond is approximately 376 kJ mol^{-1}[43], rapid hydrogen abstraction will occur if the bond strength of the P–H bond is similar or less. For that reason, the rate of hydrogen abstraction by peroxy radicals decreases in the following order: tertiary hydrogen > secondary hydrogen > primary hydrogen.[44-46] Hydroperoxides produced during thermal and photo oxidation have been detected via iodometry.[47-49]

Because the production of hydroperoxides has a high activation energy, an increase in oxidation temperature will increase the rate of reaction (of eq. 1.3) and subsequent yield of hydroperoxides, which results in an increase in the number of propagation cycles.[42] The number of propagation cycles before termination is known as the kinetic chain length.

1.2.1.3 Chain Branching

Chain branching occurs when hydroperoxides undergo thermolysis to produce alkoxy radicals and hydroxy radicals (eq, 1.4). These radicals can then abstract hydrogen from the polymer, which leads to degenerate chain branching.

The bond energies of the O–O in hydroperoxides and peroxides are around 200 $kJmol^{-1}$ or less.[50] Therefore, the O–O bond readily submits to chain scission under thermolysis to produce the alkoxy and hydroxy radicals. The bond energies of the O–H bonds in water[50] and alcohols[51] are approximately 500 $kJmol^{-1}$ and 435 $kJmol^{-1}$ respectively while the bond energies of the C–H bonds in polymers[50,52,53] are typically below 417 $kJmol^{-1}$. Consequently, the hydroxy and alkoxy radicals can abstract any hydrogen from the same or nearby polymer chain (eq's 1.6 and 1.7 respectively).

The homolytic decomposition of hydroperoxides (eq. 1.4) has a higher activation energy than the bimolecular decomposition of hydroperoxides (eq. 1.5) and is favoured at higher temperatures when decomposition can occur before two hydroperoxide groups have the opportunity to interact. However, bimolecular decomposition is favoured when hydroperoxides accumulate.[54,55] The hydroperoxide concentration will go through a maximum when the rate of hydroperoxide decomposition equals their formation rate. The autocatalytic effect of chain branching can be seen in Figure 1.4 and explains the auto-acceleration of the oxidation of polymers.

1.2.1.4 Termination

Termination of the propagation cycle occurs when two radicals recombine to yield non-radical products (eq's 1.8 to 1.10). When the oxygen pressure is high, the termination reactions occur almost exclusively by recombination of peroxy radicals (eq. 1.10). This usually proceeds via a tetroxide intermediate:

$$2PO_2^{\bullet} \longrightarrow POOOOP \longrightarrow Products$$

If both peroxy radicals were tertiary then the reaction would lead, via β-scission, to two alkoxy radicals and molecular oxygen or alternatively a molecule of oxygen and a peroxide linkage.[56-59] The peroxide linkage being thermolabile will eventually decompose to form alkoxy radicals which continue the propagation cycle.

If one of the peroxy radicals is primary or secondary, the intermediate tetroxide will decompose into a carbonyl, an alcohol and a molecule of oxygen.[60-62] This reaction is commonly referred to as the Russell mechanism (Figure 1.5).

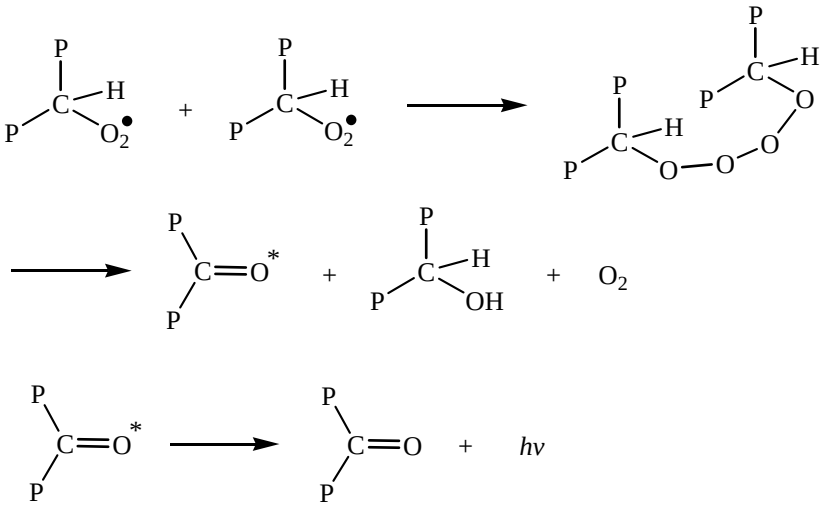

Figure 1.5: The Russell mechanism[60] for termination of peroxy radicals.

If the oxygen pressure is low, or the oxygen concentration is limited due to diffusion, then peroxy radicals also terminate with alkyl radials forming crosslinks (eq. 1.9).[63,64] If this is the case then autoxidation becomes a function of oxygen concentration. If oxygen is absent, then the dominant reaction is presumed to be the termination by recombination of two alkyl radicals[64,65], which result in carbon–carbon crosslinked products (eq. 1.8). However, if the oxygen concentration is intermediate then all three reactions will contribute to form products.[23]

It can be seen that both formation of crosslinks and chain scissions may occur in termination reactions. These reactions affect the mechanical strength, chemical resistance and toughness of the polymer and may also lead to discolouration. All of these bring about the premature end to the service life of the polymer.

1.3 Oxidation of Polyamides

The initial studies into the oxidation of PA's have been credited to Sharkley and Mochel[66], Levantovskaya[67], and Lock and Sagar[68]. These investigations showed there were three principal overall reactions:

(i) formation of N-acylamides (imides):

$$R–CO–NH–CH_2–R' \longrightarrow R–CO–NH–CO–R'$$

(ii) formation of N-formamides (formimides) as a result of C1-C2 scission:

$$R–CO–NH–CH_2–R' \longrightarrow R–CO–NH–CHO$$

(iii) oxidative dealkylation to yield carbonyl compounds:

$$R–CO–NH–CH_2–R' \longrightarrow R–CO–NH_2 + R'–CHO$$

The results also showed that products from the thermo-oxidation of aliphatic PA's were in agreement with the mechanistic study of model amides. Their conclusion was that either thermal oxidation or photooxidation is initiated by abstraction of a hydrogen atom from an N-vicinal methylene group and propagates by oxidation of the formed macroradical.

Support for the N-vicinal methylene group as the primary site of attack of oxygen on the polymer chain came from hydrolysis experiments on PA-6.[69] Homologous aliphatic normal monocarboxylic, dicarboxylic, valeric acid and adipic acid were the main products. There was also simultaneous production of N-alkylamines which indicates a parallel mechanism of degradation.

A revised mechanism for the thermo-oxidation of aliphatic PA's (Figure 1.6) was produced by Karstens and Rossbach[70] and is supported by many other authors[71-74]. The mechanism is again based on the primary attack on the N-vicinal methylene group.

The radical in the initial step forms at the N-vicinal methylene group then combines with oxygen to give a new radical, which may isomerize or follow various reaction pathways (each involving chain scission) resulting in formation of carbonyl and carboxy end-groups.

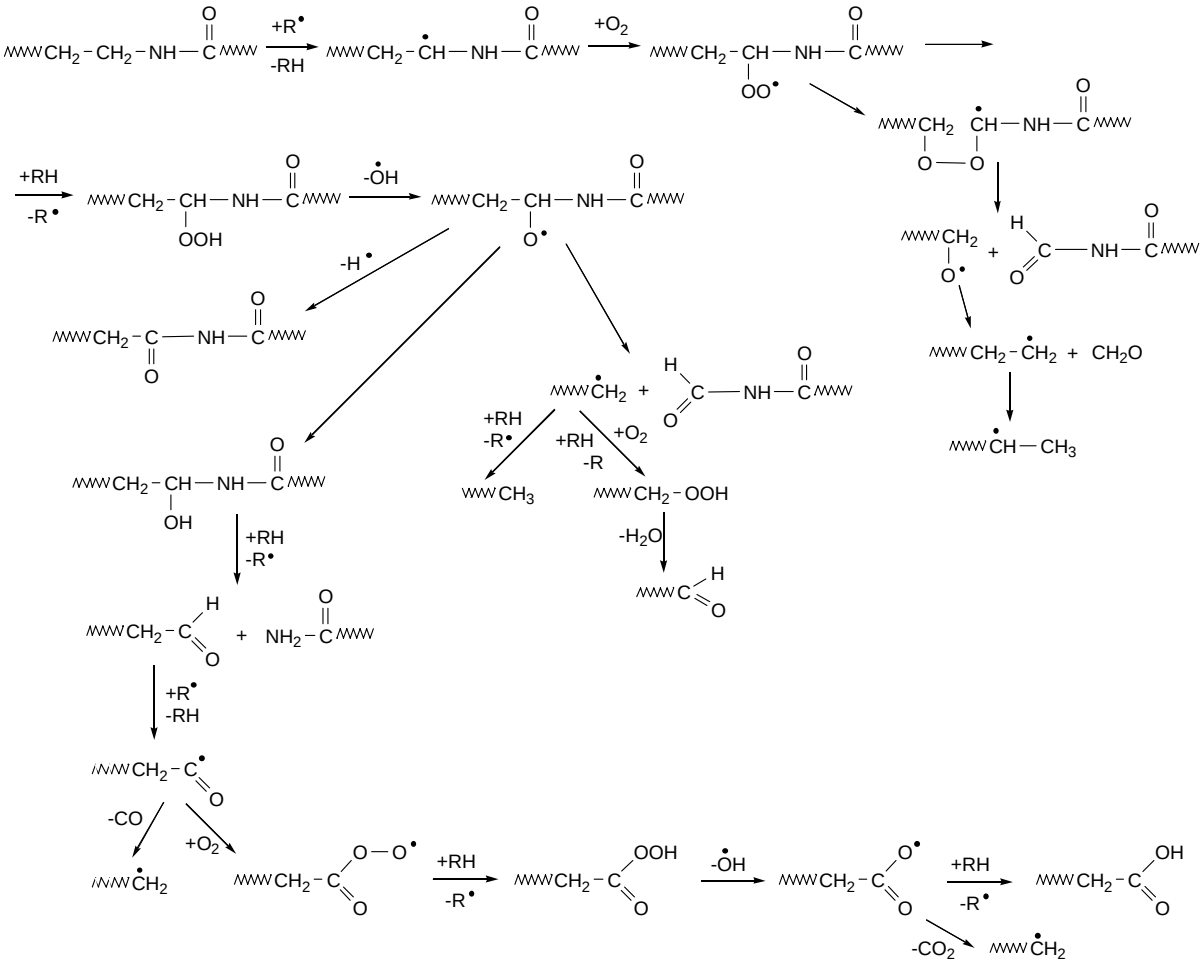

Figure 1.6: Mechanism for the thermo-oxidation of Polyamides.

It has also been suggested that any other methylene group can be oxidized in aliphatic PA's (Figure 1.7).[75-77] This can lead to β-scission, which results in an aldehyde and a free macroradical.

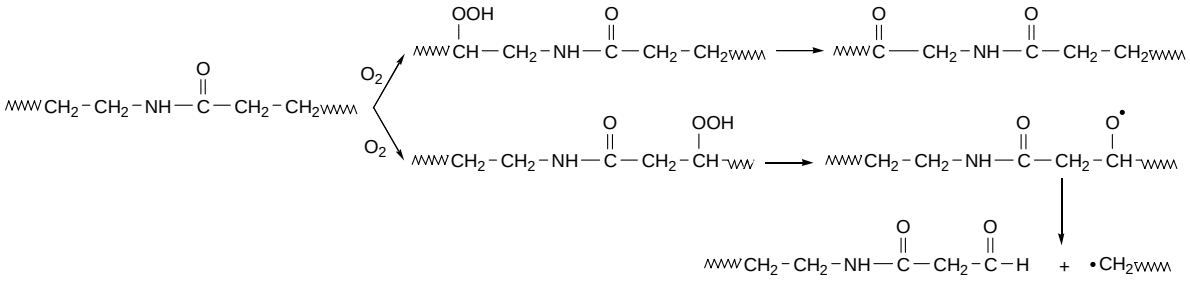

Figure 1.7: Oxidation of methylene groups in Polyamides.

It has been suggested that the N-acylamides (imides) formed during thermal oxidation of aliphatic PA's are unstable (Figure 1.8).[78] They cannot accumulate in the polymer, but dissociate into two radicals. Saturated aldehydes are formed by hydrogen abstraction, which then undergoe crotonization.

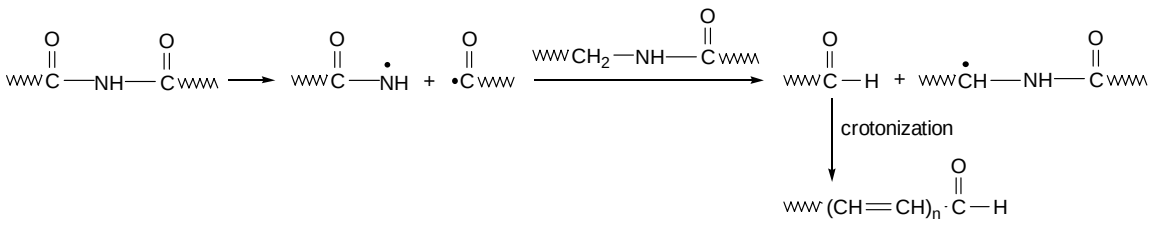

Figure 1.8: Dissociation of N-acylamides (imides).

EPR studies have shown the possibility of conjugated structures in thermally oxidized PA samples.[77,79,80] The EPR spectrum was attributed to a nitroxide radical (Figure 1.9) with four equivalent protons.

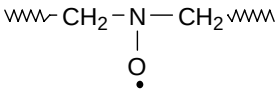

Figure 1.9: Nitroxyl radical formed during PA oxidation.

The formation of the nitroxide is attributed to a deamination reaction (Figure 1.10) followed by oxidation of the secondary amine.

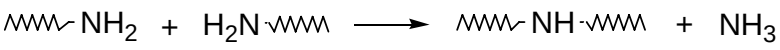

Figure 1.10: Deamination.

The EPR spectrum also showed the presence of a conjugated system with an unpaired electron (Figure 1.11).

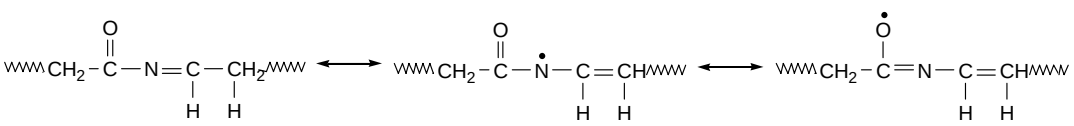

Figure 1.11: Occurrence of conjugation within PA's during thermo-oxidation.

Further oxidation of methylene groups after formation of N-acylamides has been supported by a number of research groups.[75-77,81,82] However, it has been noted that preferential attack by oxygen is likely to occur at the α-positioned methylene group (Figure 1.12).[81,82]

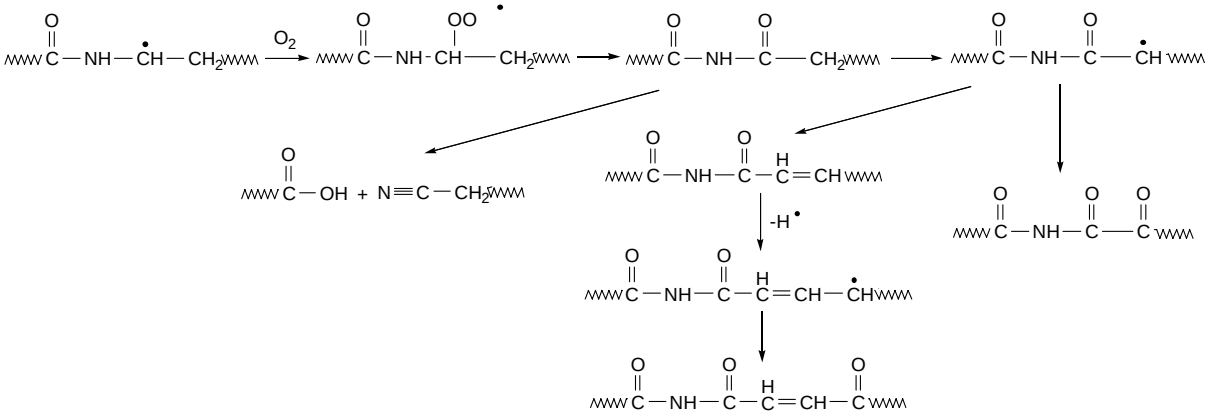

Figure 1.12: Subsequent oxidation of methylene groups during PA oxidation.

The N-acylamide group may be further degraded to acid and cyano groups, or subjected to continuing oxidation. Unsaturated N-acylamide can consequently become an α,β-unsaturated carbonyl.

A recent mechanism has been proposed to account for the yellowing of PA samples as they undergo thermo-oxidative degradation.[70,83] It suggests that UV/vis active chromophores in aliphatic PA's result from the consecutive reactions of azomethines (Figure 1.13).

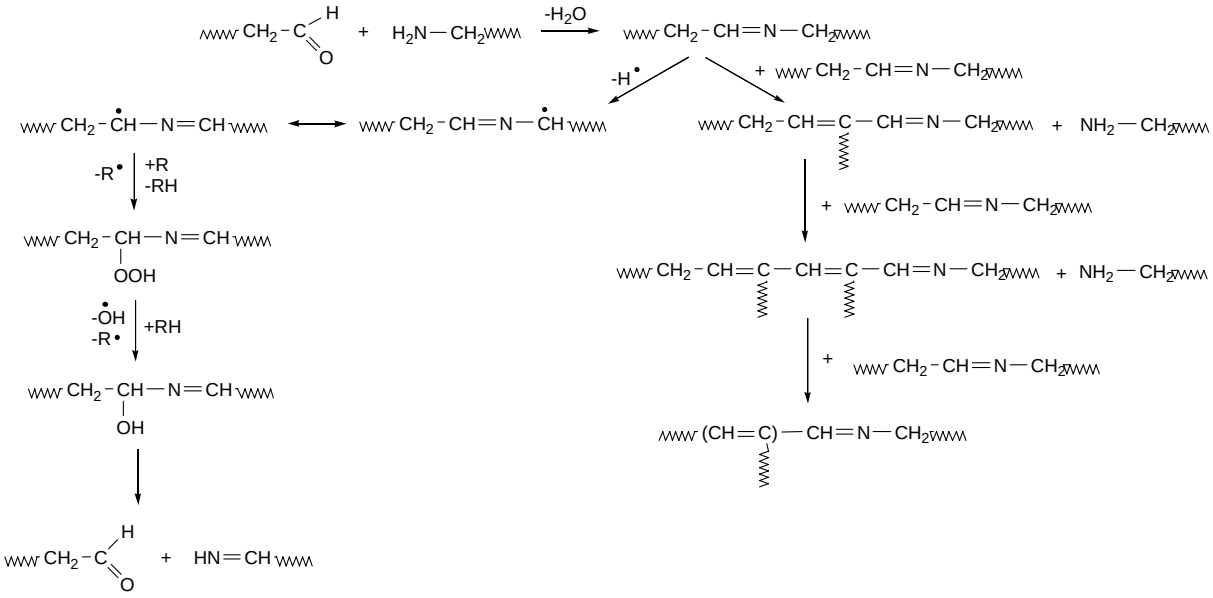

Figure 1.13: Mechanism for the yellowing of PA's during thermo-oxidation.

Ketone groups along the polymer backbone (e.g. in the β-position to the amide group) have been assumed to react by inter- and intra-chain condensation reactions (Figure 1.14).[76,77]

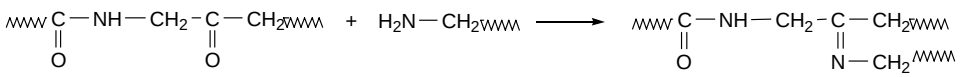

Figure 1.14: Inter-chain and intra-chain condensation reactions during PA oxidation.

Azomethine polycondensation is another suggested mechanism for cross-linking (Figure 1.15).[72]

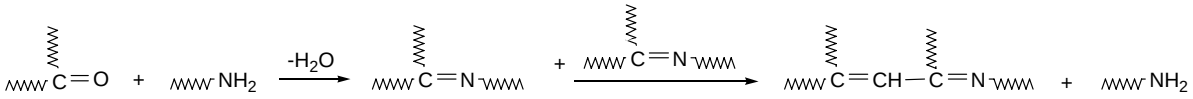

Figure 1.15: Azomethine polycondensation.

Although there was no detailed explanation, Fedotova et al[84] contributed the idea that N–N or C–C bridges can be formed between two aliphatic nylon chains (Figure 1.16).

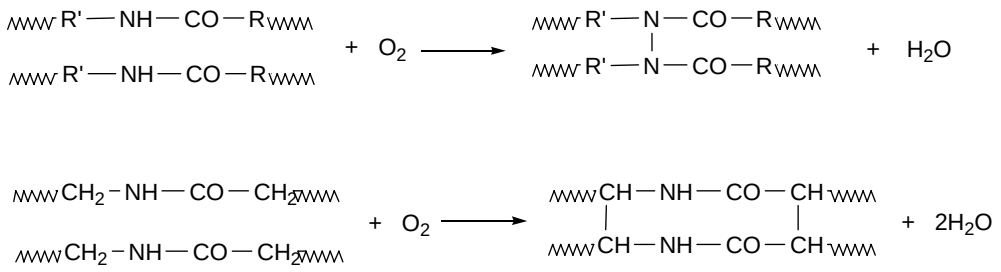

Figure 1.16: Cross-linking of PA's during oxidation via N–N and C–C bridges.

1.3.1 Initiation

The initiating step in PA oxidation is still under investigation because the radical initiating species is still unidentified.[70,73,77,78,85] Lemaire[86] has suggested that if chromophoric groups are absent then initiation of the oxidation of PA's could occur via radical attack from excited impurities or defects in the polymer.

The role of impurities towards the initiation of PA thermal and photo-oxidation was further investigated by Allen[76,77,87] at different wavelengths of incident energy. Initiation was credited to the direct scission of the C–N bond of the amide group during oxidation at wavelengths shorter than 290 nm. However, at wavelengths longer than 290 nm Allen postulated that the impurity responsible for initiation was a photosensitizer. Hydroperoxides and carbonyl groups (including α,β-unsaturated

groups) were identified as impurities. However, the part these groups played in the initiation was unknown. The role of α,β-unsaturated groups and α-keto imide groups have been considered by a number of authors.[76,85,88,89]

1.3.2 Influence of Hydroperoxides

During photo-oxidation the hydroperoxides formed in PA's, primarily in the α-position to the nitrogen atom are unstable above 60°C and do not initiate new oxidation chains, i.e. they do not show any photoinductive effect.[85,90] For wavelengths greater than 300 nm this has been attributed to homolysis of the hydroperoxide bond followed by reaction of the hydroxyl radical with the alkoxy radical in the cage to yield an imide and water which results in an autoretardant accumulation of hydroperoxides. However, during thermal oxidation of PA's, hydroperoxides appear to reach a maximum.[76,91,92] Here the oxidation products formed were associated with the successive decomposition of hydroperoxides. Samples of PA that contained a high initial concentration of hydroperoxides showed rapid chain scission from the commencement of oxidation, possibly due to the hydroperoxides inducing β-scission.[76]

1.3.3 Influence of Carboxylic and Amine End Groups

The content and ratio of carboxylic and amine end groups has been shown to have a significant effect on the rate of thermo-oxidation of PA's.[77,93-96,139] A higher

ratio of carboxylic end groups to amine end groups makes the polymer more sensitive to oxidation.

This has been attributed to the catalytic effect of carboxylic groups on the decomposition of hydroperoxides (Figure 1.17).[93]

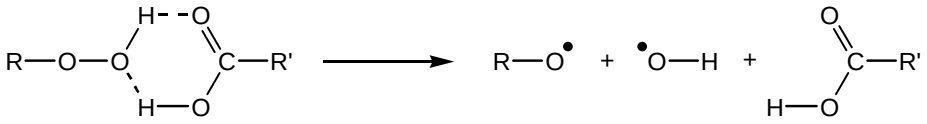

Figure 1.17: Acid-catalysed homolytic decomposition of hydroperoxides.

Conversely, amine end groups have been found to stabilize PA's.[94,97,98] This has been attributed to the ability of amine end groups to react with hydroperoxides and peroxy radicals by a similar mechanism to that of hindered amine stabilizers.[99] Amine end groups also condense with aldehydes and ketones, generated by oxidation, to form aldimines and azomethines respectively.[70,100] Additional oxidative stability has been attributed to this removal of oxidation products and higher tendency for crosslinking by amine end groups. However, it has been suggested that the consecutive reaction of azomethines results in sequences of conjugated double bonds, which gives rise to the chromophore that accounts for the observed yellowing of PA's during oxidation.[83]

1.4 Homogeneous and Heterogeneous Oxidation

The classical approach to the modeling of polymer degradative oxidation applies a homogeneous free radical kinetic description of oxidation, based on liquid hydrocarbons, to that of solid polymers.[101] This assumes that reactions occur homogeneously throughout the polymer. Recently, it has been proposed that the solid state oxidation of polymers is heterogeneous and should be modeled as such.[102] The view here is that there are distinct localized zones from where oxidation initiates. The oxidation then spreads from these zones so that an increasing fraction of polymer is oxidizing.

1.4.1 Homogeneous Aspects of Oxidation

The homogeneous kinetic models use the steady state approximation with the set of chemical equations that effectively represent the oxidation of the polymer. The chemical equations are derived from free radical oxidation schemes, like that of Figure 1.3, which are established from studies on liquid hydrocarbons. From this approach, it is possible to derive mathematical equations describing the consumption of oxygen or the formation of oxidation products.[101,103,104]

The evaluation of relative oxidation rates may be useful in some cases, however the kinetic parameters obtained have no real physical meaning. The measurements only relate to a homogeneous process as it is assumed the oxidation reactions may be described in terms of the concentrations of reactants and intermediates as would be

occurring is a liquid environment. Therefore, homogeneous modeling only provides the average information about the oxidation of the polymer. No account is made for any aspect of non-uniform degradation when applying a model used to describe the reactions occurring in the liquid state.

1.4.2 Heterogeneous Aspects of Oxidation

For obvious reasons, solid polymers are not well mixed liquid homogeneous systems. Simple chemical reactions cannot explain the complex physical changes occurring during oxidation. Factors affecting the oxidation of solid polymers include: the restricted mobility of radicals[64], morphological variations[105], diffusion limitations of oxygen[106], and the gas phase spreading of initiating species[107].

The localization of oxidation in polymers has been illustrated by a number of techniques and authors. Specific staining techniques in combination with ultraviolet microscopy have highlighted regions of extensive oxidation as highly discoloured areas.[108-111] Oxidation has been shown to spread through the gas phase from polymer particle to polymer particle[112,113] and through CL Imaging oxidation was seen to spread from an initially oxidized region of a polymer to the remainder of the polymer with time.[114] One experiment illustrated that an unstabilized film placed on the edge of a thin strip of stabilized film was able to infect the stabilized film.[115] The oxidation was perceived to spread down the film of oxidized polymer as the anti-oxidant was consumed.

1.4.2.1 Morphology

Semicrystalline polymers consist of amorphous and crystalline phases. Diffusion of oxygen is restricted to the amorphous region[27,116] and as a consequence the rate of oxidation has been found to be inversely proportional to the percent of crystallinity.[105,117] Chain defects and chain end groups as well as impurities produced during processing and polymerization such as chromophoric groups, peroxides and other oxygen containing groups also concentrate in the amorphous regions.[118] Such defects and impurities affect and increase the rate of oxidation; they form 'hot spots' of oxidation. Low molecular weight oxidation products would be formed at a greater rate in these hot spots. Oxidation products are known to initiate further oxidation and so these hot spots oxidize at an even greater rate than the rest of the polymer.

1.4.2.2 Mobility of Radicals

Clearly the mobility of radicals in solid polymers are far more restricted than those in a liquid phase. The main difference between the oxidation processes in the liquid and solid state is cage recombination of polymer peroxy radicals.[64,119,120] In the solid state peroxy radicals can only separate by slow segmental diffusion; they cannot quickly randomize like those radicals in the liquid state. This limited mobility of radicals leads to heterogeneous oxidation. The mobility of radicals also varies notably between the amorphous and crystalline phases.[121] The initiation efficiencies

in amorphous polymers were found to be up to ten times faster than those of semicrystalline polymers.

1.4.2.3 Diffusion Limited Oxidation

Bulk polymer samples show diffusion limited oxidation (DLO).[106,122,123] DLO occurs when the rate of oxygen diffusion becomes the rate-determining factor in the oxidation process; i.e. oxygen is consumed in oxidation reactions at a greater rate than the oxygen can be replenished by diffusion. This effect becomes greater as the temperature is increased because the rate of oxidation depends more strongly on temperature than does the diffusion of oxygen.[122] However, DLO has still been observed at ambient temperatures in highly unstabilized polymers.[124] DLO results in oxidation depth profiles, which have been measured by a number of techniques including FT-IR, density profiling and modulus profiling.[125]

1.4.2.4 Physical Spreading of Oxidation

As mentioned in section 1.2.1.2 oxidation occurs by hydrogen abstraction to form a macroradical, which reacts with oxygen to form a peroxy radical. The peroxy radical then abstracts a nearby hydrogen from either the same or a different chain. The spreading of oxidation could then be explained by the fact that radicals and reactive oxidation products react in the nearby vicinity. Oxidation then continues to spread from point to point across the polymer.[126]

Spreading of oxidation also occurs via the gas phase. The lifetime of stabilized polymers has been reduced significantly during oven aging experiments when unstabilized samples were also present in the oven.[107] Matisova-Rychla[127] identified formic acid and hydrogen peroxide in the gas phase of an oxidizing polymer and suggested that these could be the species responsible for the observed physical spreading. It should be noted that the species responsible for gas phase spreading need some degree of stability. A highly reactive species such as a radical, would react before it had the opportunity to diffuse out of the already oxidizing polymer. An 'infectious' species should not be reactive until it reaches the gas phase where it could be easily transformed into a reactive species by reacting with oxygen.

1.4.2.5 Infectious spreading model

George et al have proposed an infectious spreading model for the oxidation of polypropylene.[102] In this model, the polymer is considered to have discrete defect zones, such as the regions of the polymer containing catalyst residues, which are the sites for localized oxidation at a high rate. Thus while there is an apparent 'induction period' in which there is a low overall rate of oxidation, within the initiating zones there is a degenerately branched chain reaction leading to high extents of localized oxidation. The macroscopic oxidation process then corresponds to the spreading of the oxidation from these zones so that an increasing fraction of the polymer is oxidizing.

In the infectious spreading model, three distinct populations in the polymer may be assigned after a short time of oxidation:

1. The remaining or unoxidized fraction, p_r.
2. The infectious or oxidizing fraction, p_i.
3. The dead or oxidized fraction, p_d.

It is now believed that CL-time curves of polymers doped with energy acceptors (e.g. 9,10-diphenylanthracene) can measure the time development of the infectious fraction, p_i.[126] The measurement of oxidation products, such as carbonyl groups etc, is obtained by IR spectroscopy. This will only measure the non-radical species and thus measure the dead fraction p_d. The remaining fraction is then determined as 1-(p_i+p_d). It is assumed that the infection can spread only if a zone has uninfected material available within a contact distance that is proportional to the fraction p_r.

At time zero, there is a small fraction, p_o, of the total volume of the polymer in which oxidation is occurring. Within these highly reactive zones the formation of volatile reaction products and free radicals occur which increase the instantaneous oxidizing fraction of the polymer from p_o to some value p_i. At the same time the fraction of polymer which is unaffected will decrease from 1-p_o (~1) to some value p_r.

From these relationships, kinetic equations can be determined and typical values of the spreading and removal coefficients may be obtained from an analysis of either oxidation product concentration as a function of oxidation time or of chemiluminescence in the early stages of the oxidation.

1.5 Stabilization of Polymers

Appropriate stabilizers, otherwise known as antioxidants, can be added in small amounts (less than 2% w/w) either before or during processing to inhibit the oxidation of polymers. Antioxidants are added to the polymer to alter species already present or react with species formed during oxidation in an attempt to suppress the autocatalytic oxidation reactions and therefore extend the useful lifetime of the polymer.

Scavenging antioxidants are used to trap free radicals. These types of antioxidants are commonly referred to as chain-breaking acceptors (CB–A's) and chain-breaking donors (CB–D's).[22] CB–A's, of which hindered amine stabilizers (HAS)'s are a good example, are effective at scavenging carbon-centered radicals under oxygen deficient conditions. Therefore CB–A's are most useful during thermal processing of polymers or for the stabilization of the bulk polymer where alkyl radicals will be present due to low concentrations of oxygen.[128] They are ineffective in situations where oxygen is present as molecular oxygen attacks carbon centered radicals in a very fast reaction (section 1.2.1.2) with minimal activation energy. In this case CB–D's, for example H-donors such as phenols and aromatic amines, can be utilized. It is not possible for the CB–D's to scavenge the highly reactive alkoxy and hydroxy radicals, however they react with peroxy radicals to form a relatively stable hydroperoxide.[129]

Hydroperoxide decomposers (HD's) are another effective type of antioxidant, examples of which are organophosphites and organosulfur compounds. HD's transform hydroperoxides into non-radical, non-reactive and thermally stable products by competing with the thermolysis of the hydroperoxide group.[22] Therefore chain branching in the autoxidation cycle by the formation of alkoxy and hydroxy radicals is suppressed. HD's are usually used in combination with CB–D's.

1.5.1 Stabilization of Polyamides

There are limited publications in the literature to date that deal with the stabilization of PA's.[130-132] Aliphatic PA's are traditionally stabilized with small amounts of copper salts (> 50 ppm) in combination with halogen ions such as iodide and bromide.[73,133] The efficiency of this stabilizer system is remarkable considering copper ions are known to act as catalysts in the degradation of polyolefins principally by accelerating hydroperoxide decomposition. The mechanism for stabilization with copper/halogen compounds is still

subject to investigation. Aromatic amines are another classic stabilizer used for PA's however they lead to discolouration of the polymer. Phenolic antioxidants are added to stabilize PA's by improving initial colour.[22]

1.5.1.1 Copper/Iodine Salt

The mixture of copper acetate and potassium iodide is one of the most efficient stabilizers for aliphatic PA's.[134,138] Unfortunately its applications as an antioxidant are limited because it leads to premature colouration of the polymer. The mechanism for the stabilization of PA's by copper salts is still under investigation, however a two step mechanism as illustrated in Figure 1.18 has been proposed:[133]

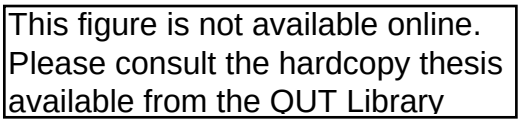

Figure 1.18: Suggested mechanism for Cu/I salt stabilization of polyamides.[133]

The first step is the reduction of a hydroperoxide group by iodine (I-) in the presence of an acid to give an alcohol. The alcohol is receptive to chain scission, which is possibly catalyzed by the presence of the transition metal, to give an amine end-group and an aldehyde. Chain scission does occur however autocatalytic initiation of new chains is prevented. Retardation of the free radical chain oxidation in PA's by copper/iodine salts is further supported by the chemiluminescence studies of Cerruti *et al*[138].

1.5.1.2 Sterically hindered phenols

As discussed in section 1.5, sterically hindered phenols are H-donors which fit into the radical scavenger class of stabilizers. Figure 1.19 displays the action of sterically hindered phenols.[135,136] The first and most important step is the formation of hydroperoxides by H-abstraction from the phenolic group with formation of the relatively stable phenoxy radical. The stability of the phenoxy radical is governed by the sterical hindrance of the substituents in the 2,6-position. A quinone ethide structure is formed by intramolecular rearrangement, regenerating the phenolic group. The abstraction of hydrogen from the polymer backbone does not readily occur until the external H-donor, or sterically hindered phenol, is consumed; thus the propagation cycle of autoxidation is retarded. Synergistic effects can be achieved when hindered phenols are mixed with a HD such as phosphites.[22]

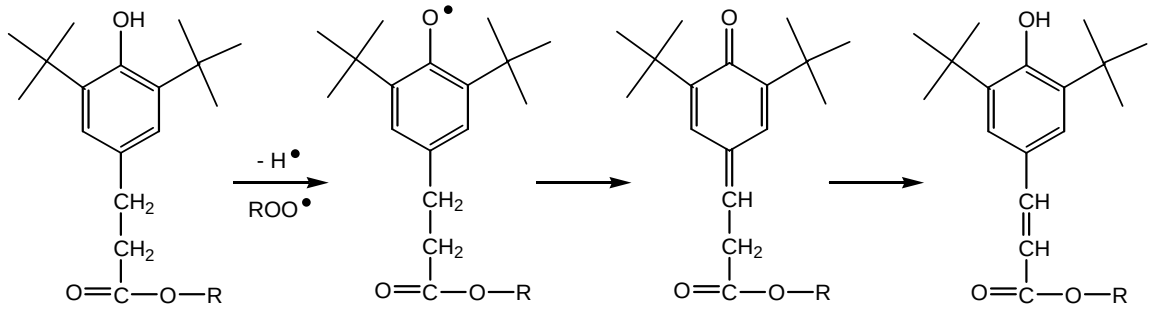

Figure 1.19: Mechanism for the action of sterically hindered phenols

1.5.1.3 Phosphites

Phosphites are the preferred HD for PA stabilization.[22] They are commonly used to prevent oxidation during processing and are quite effective at high temperatures. Phosphites compete with, and suppress, the chain branching reactions in the autoxidative cycle (eqs. 1.4 and 1.5) by decomposing hydroperoxides to non-radical products.[137] The hydroperoxide is reduced to an alcohol while the phosphite is oxidized in a stoichiometric reaction. Phosphites are typically used in combination with H-donors such as sterically hindered phenols.

1.6 References

(1) Kohan, M. I., *Nylon Plastics*, John Wiley & Sons, Inc., New York, 1973.

(2) Mark, H.; Whiby, G. S., *Collected Papers of Wallace Hume Carothers on High Polymeric Substances, High Polymers*, Interscience Publishers, New York, 1940.

(3) Kroschwitz, J. I.; Howe-Grant, M. (eds.), *Kirk-Othmer, Encyclopedia of Chemical Technology, 4th Ed.*, John Wiley & Sons, Inc., Brisbane, 1996.

(4) Schwartz, S. S.; Goodman, S. H., *Plastics Materials & Processes*, Van Bostrand Reinhold Company, 1982.

(5) Xenopoulos, A.; Clark, E. S., *Nylon Plastic Handbook*, ed. by Kohan, M. I., Hanser Publishers, Munich, 1995.

(6) Tuzar, Z., *Lactam-based Polyamides*, ed. by Puffr, R., Kubanek, V., CRC Press, Boca Raton, 1991.

(7) Weber, G., *Angew. Makromol. Chem.*, **74** (1978) 187.

(8) Smith, E. G., *Polymer*, **17** (1976) 7751.

(9) Meplestor, P., *Modern Plastics*, **74** (1997) 66.

(10) Dasgupta, S.; Hammond, W. B.; Goddard III, W. A., *J. Am. Chem. Soc.*, **118** (1996) 12291.

(11) Rychly, J.; Matisova-Rychla, L.; Csmorova, K.; Achimsky, L.; Audoin, L.; Tcharkhtchi, A.; Verdu, J., *Polym. Deg. Stab.*, **58** (1997) 269.

(12) Girois, S.; Delprat, P.; Audouin, L.; Verdu, J., *Polym. Deg. Stab.*, **56** (1997) 169.

(13 Ghaemy, M.; Scott, G., *Polym. Deg. Stab.*, **3** (1981) 233.

(14) Grassie, N.; Weir, N. A., *J. App. Polym. Sci.*, **9** (1965) 999.

(15) Hoffman, A. W., *J. Chem. Soc.*, **13** (1861) 87.

(16) Scott, G., *Atmospheric Oxidation and Antioxidants*, Elsevier Publishing Company, Amsterdam, 1965.

(17) Reich, L.; Stivala, S. S., *Autooxidation of Hydrocarbons and Polyolefins*, Dekker, New York, 1969.

(18) Ranby, B.; Rabek, J. F., *ESR Spectroscopy in Polymer Research*, Springer, Berlin, 1977.

(19) Jellinek, H. H. G., *Aspects of Degradation and Stabilisation of Polymers*, Elsevier Scientific Publishing Company, Amsterdam, 1978.

(20) Allen, N. S., *Degradation and Stabilisation of Poleolefins*, Applied Science Publishers Ltd., London, 1983.

(21) Clough, R. L.; Billingham, N. C.; Gillen, K. T., *Polymer Durability*, ASC Adv. Chem. Ser., 1996.

(22) Zweifel, H. (ed.), *Plastics Additives Handbook*, Hanser, Munich, 2001.

(23) Scott, G., *Atmospheric Oxidation and Antioxidants*, Elsevier Publishing Company, Amsterdam, 1993.

(24) Bolland, J. L.; Gee, G., *Trans. Farraday Soc.*, **42** (1946) 236.

(25) Bolland, J. L., *Q. Rev. (London)*, **3** (1949) 1.

(26) Bateman, L., *Quart. Rev. Chem. Soc.*, **8** (1954) 147.

(27) Knight, J. B.; Calvert, P. D.; Billingham, N. C., *Polymer*, **26** (1985) 1713.

(28) Scott, G., *Polym. Deg. Stab.*, **48** (1992) 315.

(29) Gugumus, F., *Polym. Deg. Stab.*, **62** (1998) 403.

(30) Bateman, L.; Hughes, H., *J. Chem. Soc.*, (1952) 4594.

(31) Chien, J. C.; Jabloner, H., *J. Polym. Sci., A-1*, **6** (1968) 393.

(32) Zolotova, N. V.; Denisov, E. T., *J. Polym. Sci., A-1*, **9** (1971) 3311.

(33) Gijsman, P.; Hennekens, J.; VBincent, J., *Polym. Deg. Stab.*, **42** (1993) 95.

(34) Dulog, L.; Radlman, E.; Kern, W., *Macromol. Chem.*, **80** (1964) 67.

(35) Chien, J. C.; Boss, C. R., *J. Polym. Sci., A-1*, **5** (1967) 3091.

(36) Ingold, K. U., *Acc. Chem. Res.*, **2** (1969) 1.

(37) Miller, A. A.; Mayo, F. R., *J. Am. Chem. Soc.*, **78** (1956) 1017.

(38) Hendry, D. G.; Russell, G. A., *J. Am. Chem. Soc.*, **86** (1964) 2371.

(39) Rust, F. F., *J. Am. Chem. Soc.*, **79** (1957) 4000.

(40) Van Sickle, D. E.; Mill, T.; Mayo, F. R.; Richardson, H.; Gould, C., *J. Org. Chem.*, **38** (1973) 4435.

(41) Van Sickle, D. E., *J. Org. Chem.*, **37** (1972) 755.

(42) Kamiya, Y.; Niki, E. G., *Aspects of Degradation and Stabilization of Polymers*, ed. by Jellineck, H. H. G., Elsevier Scientific Publishing Company, Amsterdam, 1978.

(43) Benson, S. W., *J. Am. Chem. Soc.*, **87** (1965) 972.

(44) Howard, J. A., *Free Radicals*, ed. by Kochi, J. K., Wiley, New York, 1973.

(45) Bolland, J. L., *Trans. Farady Soc.*, **46** (1950) 358.

(46) Leroy, G.; Nemba, R. M.; Sana, M.; Wilante, C., *J. Mol. Structure*, **198** (1989) 159.

(47) Lacoste, J.; Deslandes, Y.; Black, P.; Carlsson, D. J., *Polym. Deg. Stab.*, **49** (1995) 21.

(48) Scheirs, J.; Carlsson, D. J.; Bigger, S. W., *Polym. - Plast. Technol. Eng.*, **34** (1995) 91.

(49) Gijsman, P.; Kroon, M.; Vanoorschot, M., *Polym. Deg. Stab.*, **51** (1996) 3.

(50) McMillen, D. F.; Golden, D. M., *Ann. Rev. Phys. Chem.*, **33** (1982) 493.

(51) Moylan, C. R.; Brauman, J. I., *J. Phys. Chem.*, **88** (1984) 3175.

(52) Baldwin, R. R.; Drewery, G. R.; Walker, R. W., *J. Chem. Soc., Faraday Trans. 1*, **80** (1984) 2827.

(53) Castelhano, A. L.; Griller, D., *J. Am. Chem. Soc.*, **104** (1982) 3655.

(54) Gugumus, F., *Polym. Deg. Stab.*, **49** (1995) 29.

(55) Lemaire, J.; Arnaud, R.; Gardette, J. L., *Pure Appl. Chem.*, **55** (1983) 1603.

(56) Traylor, T. G.; Russell, C. A., *J. Am. Chem. Soc.*, **87** (1965) 2698.

(57) Bartlett, P. D.; Guaraldi, G. J., *J. Am. Chem. Soc.*, **89** (1967) 4799.

(58) Nangia, P. S.; Benson, S. W., *Int. J. Chem Kinetics*, **1** (1980) 29.

(59) Factor, A.; Russell, C. A., *J. Am. Chem Soc.*, **87** (1965) 3692.

(60) Russell, C. A., *J. Am. Chem. Soc.*, **79** (1957) 3871.

(61) Nakano, M.; Takayama, K.; Shimizu, Y.; Tsuji, Y.; Inaba, H.; Migita, T., *J. Am. Chem. Soc.*, **98** (1976) 1974.

(62) Howard, J. A.; Ingold, K. U., *J. Am. Chem. Soc.*, **110** (1968) 1056.

(63) Mantell, G.; Rankin, D.; Galiano, F., *J. Appl. Polym. Sci.*, **9** (1965) 3625.

(64) Rabek, J. F., *Photostabilization of Polymers*, Elsevier Applied Science, London, 1990.

(65) Beachell, H. C.; Nemphos, S. P., *J. Polym. Sci.*, **25** (1957) 173.

(66) Sharkley, W. H.; Mochel, W. E., *J. Am. Chem. Soc.*, **81** (1959) 3000.

(67) Levantovskaya, I. I.; Kovarskaya, B. M.; Dralyuk, G. V.; Neiman, M. B., *Vysokomol Soedin*, **6** (1964) 1885.

(68) Lock, M. V.; Sagar, B. F., *J. Chem. Soc. Part B*, (1966) 690.

(69) Valk, G.; Kruessmann, H.; Diehl, P., *Makromol. Chem.*, **107** (1967) 158.

(70) Karstens, T.; Rossbach, V., *Makromol. Chem.*, **190** (1989) 3033.

(71) Zimmerman, J., *Polyamides*, ed. by Kroschwitz, J. I., Wiley, New York, 1990.

(72) Marechal, P.; Legras, R.; Dekoninck, J. M., *J. Polym. Sci., Part A: Polym. Chem.*, **31** (1993) 2057.

(73) Gijsman, P.; Tummers, D.; Janssen, K., *Polym. Degrad. Stab.*, **49** (1995) 121.

(74) Lanska, B., *Polym. Degrad. Stab.*, **53** (1996) 89.

(75) Allen, N. S.; McKellar, J. F.; Phillips, G. O., *J. Polym. Sci., Polym. Chem. Ed.*, **12** (1974) 1233.

(76) Allen, N. S., *Polym. Degrad. Stab.*, **8** (1984) 55.

(77) Allen, N. S.; Harrison, M. J.; Follows, G. W.; Matthews, V., *Polym. Degrad. Stab.*, **19** (1987) 77.

(78) Fromageot, D.; Roger, A.; Lemaire, J., *Angew. Makromol. Chem.*, **170** (1989) 71.

(79) Bhuiyan, A. L., *Polymer*, **25** (1984) 1699.

(80) Chiang, T. C.; Sibilia, J. P., *J. Polym. Sci., Part A-1*, **10** (1972) 605.

(81) Do, C. H.; Pearce, E. M.; Bulkin, B. J.; Reimschuessel, H. K., *J. Polym. Sci., Part A: Polym. Chem.*, **25** (1987) 2301.

(82) Do, C. H.; Pearce, E. M.; Bulkin, B. J.; Reimschuessel, H. K., *J. Polym. Sci., Part A: Polym. Chem.*, **25** (1987) 2409.

(83) Rossbach, V.; Karstens, T., *Chemiefasern/Textilind.*, **40** (1990) E44.

(84) Fedotova, O. Y.; Gorokhov, V. I.; Korshak, V. V.; Freilin, G. N., *Trudy Mosk Teknolog Inst*, **70** (1972) 208.

(85) Roger, A.; Sallet, D.; Lemaire, J., *Macromolecules*, **19** (1986) 579.

(86) Tang, L.; Sallet, D.; Lemaire, J., *Macromolecules*, **15** (1982) 1432.

(87) Allen, N. S.; Harrison, M. J.; Ledward, M.; Follows, G. W., *Polym. Degrad. Stab.*, **23** (1989) 165.

(88) Postnikov, L. M.; Vichutinskaya, Y. V.; Lukomskaya, I. S., *Polym. Sci. USSR*, **27** (1985) 2442.

(89) Postnikov, L. M.; Vinogradov, A. V., *Polym. Sci., Ser. A*, **36** (1994) 25.

(90) Lemaire, J.; Gardette, J. L.; Rivaton, A.; Roger, A., *Polym. Deg. Stab.*, **15** (1986) 1.

(91) Lanska, B.; Sebenda, J., *Eur. Polym. J.*, **22** (1986) 199.

(92) Matisova-Rychla, I.; Lanska, B.; Rychly, J., *Angew. Makromol. Chem.*, **216** (1994) 169.

(93) Lanska, B., *Eur. Polym. J.*, **30** (1994) 197.

(94) Lanska, B.; Matisova-Rychla, L.; Brozek, J.; Rychly, J., *Polym. Degrad. Stab.*, **66** (1999) 433.

(95) Matisova-Rychla, L.; Lanska, B.; Rychly, J.; Billingham, N. C., *Polym. Degrad. Stab.*, **43** (1994) 131.

(96) Pavlov, N. N.; Kudryavtseva, G. A.; Abramova, I. M.; Vasil'eva, V. A.; Zezina, L. A.; Kazaryan, L. G., *Polym. Degrad. Stab.*, **24** (1989) 389.

(97) Reimschuessel, H. K.; Dege, G. J., *J. Polym. Sci., Part A-1*, **8** (1970) 3265.

(98) Lanska, B.; Doskocilova, D.; Matisova-Rychla, L.; Puffr, R.; Rychly, J., *Polym. Degrad. Stab.*, **63** (1999) 469.

(99) Allen, N. S., *Chem. Soc. Revs.*, **15** (1986) 373.

(100) Levchik, S. V.; Weil, E. D.; Lewin, M., *Polym. Int.*, **48** (1999) 532.

(101) Zlatkevich, L., *J. Polym. Sci. Polym. Phys.*, **23** (1985) 1691.

(102) George, G. A.; Celina, M.; Lerf, C.; Cash, G.; Weddell, D., *Macromol. Symp.*, **115** (1997) 69.

(103) Billingham, N. C.; George, G. A., *J. Polym. Sci. Polym. Phys.*, **28** (1990) 257.

(104) Zlatkevich, L., *J. Polym. Sci. Polym. Phys.*, (1990) 425.

(105) Hawkins, W. L.; Matreyek, W.; Winslow, F. H., *J. Polym. Sci.*, **41** (1959) 1.

(106) Clough, R. L.; Gillen, K. T., *Polym. Deg. Stab.*, **38** (1992) 47.

(107) Sedlar, J.; Pac, J., *Polymer*, **15** (1974) 613.

(108) Johnson, M.; Williams, M. E., *Eur. Polym. J.*, (1976) 843.

(109) Scheirs, J.; Delatycki, O.; Bigger, S. W.; Billingham, N. C., *Polym. Int.*, (1991) 187.

(110) Richters, P., *Macromolecules*, **3** (1970) 262.

(111) Billingham, N. C.; Calvert, P. D., *Inst. Phys. Conf. Ser.*, **98** (1989) 571.

(112) Celina, M.; George, G. A.; Billingham, N. C., *Polym. Deg. Stab.*, **42** (1993) 335.

(113) Ahlblad, G.; Reitberger, T.; Terselius, B.; Sternberg, B., *Polym. Deg. Stab.*, **65** (1999)

(114) Celina, M.; George, G. A.; Lacey, D. J.; Billingham, N. C., *Polym. Deg. Stab.*, **47** (1995) 311.

(115) Dudler, V.; Lacey, D. J.; Krohnke, C., *Polym. Deg. Stab*, **51** (1996) 115.

(116) Billingham, N. C., *Makromol. Chem., Macromol. Symp.*, **28** (1989) 145.

(117) Gedde, U. W., *Polymer Physics*, Chapman & Hall, London, 1995.

(118) Buchachenko, A. L., *J. Polym. Sci. Symp.*, **57** (1976) 299.

(119) Garton, A.; Carlsson, D. J.; Wiles, D. M., *Makromol. Chem.*, **181** (1980) 1841.

(120) Carlsson, D. J.; Chan, K. H.; Garton, A.; Wiles, D. M., *Pure & Appl. Chem.*, **52** (1980) 389.

(121) Chien, J. C. W.; Wang, D. S. T., *Macromolecules*, **8** (1975) 920.

(122) Billingham, N. C.; Walker, T. J., *J. Polym. Sci., Polym. Chem. Ed.*, **13** (1975) 1209.

(123) Cunliffe, A. V.; Davis, A., *Polym. Deg. Stab.*, **4** (1982) 17.

(124) Gillen, K. T.; Celina, M.; Clough, R. L.; Wise, J., *TRIP*, **5** (1997) 250.

(125) Gillen, K. T.; Clough, R. L., *Handbook of Polymer Science and Technology. Vol. 2: Performance Properties of Plastics and Elastomers*, ed. by Cheremisinoff, N. P., Marcel Dekker, New York, 1989.

(126) Blakey, I.; George, G. A., *Polym. Deg. Stab.*, **70** (2000) 269.

(127) Matisova-Rychla, L.; Rychly, J.; Verdu, J.; Audouin, L.; Csomorova, K., *Polym. Deg. Stab.*, **49** (1995) 51.

(128) Grassie, N.; Scott, G., *Polymer Degradation and Stabilization*, Cambridge University Press, Cambridge, 1985.

(129) Allen, N. S.; Edge, M., *Fundamentals of Polymer Degradation and Stabiliztion*, 1st Edition, Elsevier Applied Science, London, 1992.

(130) Berger, W.; Otto, C.; Ahlers, K. D.; Kuprat, D., *Faserforsch. Textiltech.*, **23** (1972) 512.

(131) Brassat, B.; Buuysch, H. J., *Kunstsoffe*, **70** (1980) 833.

(132) Matusevich, Y. I.; Krul, L. P., *Thermochim. Acta.*, **97** (1986) 351.

(133) Janssen, K.; Gijsman, P.; Tummers, D., *Polym. Degrad. Stab.*, **49** (1995) 127.

(134) Gugumus, F., *Plastic Additives*, 3rd Edition, ed. by Gachter, R., Muller, H., Hanser Publishers, Munich, 1990.

(135) Pospisil, J., *Polym. Deg. Stab.*, **34** (1991) 85.

(136) Scheirs, J.; Pospisil, J.; O'Connor, M. J.; Bigger, S. W., *Adv. Chem. Ser.*, **248** (1996) 359.

(137) Schwetlick, K.; Konig, T.; Ruger, C.; Pionteck, J.; Habicher, W. D., *Polym. Deg. Stab.*, **15** (1986) 97.

(138) Cerruti, P.; Rychly, J.; Matisova-Rychla, L.; Carfagna, C., *Polym. Deg. Stab.*, **84** (2004) 199.

(139) Cerruti, P.; Carfagna, C.; Rychly, J.; Matisova-Rychla, L., *Polym. Deg. Stab.*, **82** (2003) 477.

2. Instrumental Techniques

2.1 Infrared Emission Spectroscopy

Vibrational spectroscopy measures the electromagnetic radiation absorbed or emitted by molecules or other chemical species that is associated with the changes in their vibrational energy states.[1] To absorb or emit radiation, a molecule must produce an oscillating dipole moment.[2] The molecule does not need to have a permanent dipole; only a change in dipole is required. These bond vibrations are generally described by symmetric and anti-symmetric stretching, bending, twisting and rocking (Figure 2.1).[3] The frequency at which the vibrations are observed depends on the nature of the functional group producing them.[4]

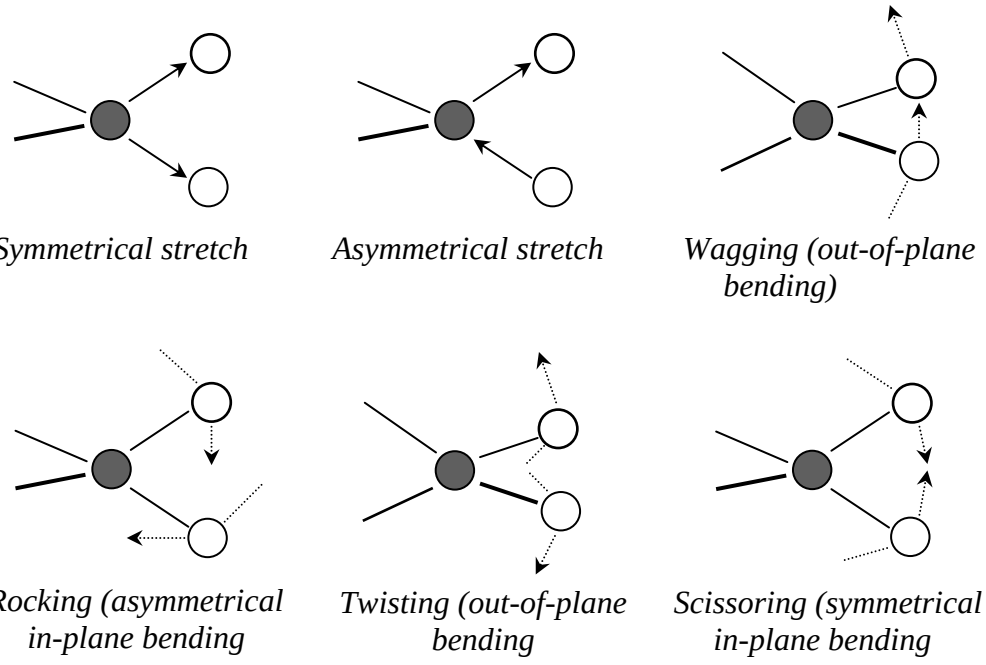

Figure 2.1: Examples of vibrational modes for the methylene group.

The allowed energies of vibrational states of a harmonic oscillator are given by[5]:

$$E = (v + ½)\, h\nu_m \qquad \ldots(2.1)$$

where: v = the vibrational quantum number (0, 1, 2…),

h = Planck's constant

ν_m = the vibrational frequency of the bond.

Transitions between vibrational states are allowed only if the quantum number is changed by one, i.e. $\Delta v = \pm 1$.

When molecules composed of several atoms vibrate according to the bending and stretching motions overtones of these frequencies can be obtained.[1] When one bond vibrates, the remainder of the molecule is also involved. The overtone vibrations have a frequency that represents multiples of the fundamental frequency. A combination band is the sum or difference of the frequencies of two or more fundamental vibrations.[3] Intensities of both overtone and combination bands are much smaller than those of the fundamental bands.[2] The multiplicity of vibrations occurring simultaneously produces a highly complex spectrum that is uniquely characteristic of the molecule.[4]

The infrared (IR) region of the electromagnetic spectrum includes radiation with wavenumbers ranging from 14000 to 20 cm^{-1}.[3] This region is conveniently divided into three ranges: near-IR (4000-14000 cm^{-1}), mid-IR (200-4000 cm^{-1}) and far-IR

(20-200 cm^{-1}). The mid-IR is the region most commonly used for analysis of organic samples as most of the fundamental vibrations are found in this range.[4]

Infrared Emission Spectroscopy (IES) is a technique used to measure the infrared radiation emitted as vibrationally excited molecules relax to their ground state.[6,7] Samples are heated to above ambient temperatures to populate the higher energy states. Energy emitted as the molecule returns to the ground state is then detected by a spectrometer.

The absorption and subsequent emission of photons corresponding with a molecule's energy levels with vibrational quantum numbers of v = o and v is represented by[6]:

$$A_{vo} = \frac{8\pi h\nu^3}{c^3} B_{ov} = 8\pi h\bar{\nu}^3 B_{ov} \qquad \ldots(2.2)$$

where: A_{vo} = Einstein coefficient for spontaneous emission

B_{ov} = Einstein coefficient for stimulated absorption

$\bar{\nu}$ = wavenumber of the spectral transition.

c = speed of light

The intensity of emission depends on the number of molecules in the excited state so the Boltzmann distribution (Eq. 2.3) is used to determine the population of the excited energy level, N_v, relative to the ground state, N_o[6].

$$N_v = N_o e^{\left(\frac{-hc\bar{\nu}}{kT}\right)} \qquad \ldots(2.3)$$

By combining equations 2.2 and 2.3 the intensity of emission can be described by:

$$E_{vo} = A_{vo}N_v = 8\pi h\bar{v}^3 B_{ov}N_o e^{\left(\frac{-hc\bar{v}}{kT}\right)} \quad \ldots(2.4)$$

The Planck distribution (Eq. 2.5) gives the intensity of radiation emitted by a black body, E_{bb}, at a given temperature, T.[6]

$$E_{bb} = \frac{8\pi h\bar{v}^3}{e^{\left(\frac{hc\bar{v}}{kT}\right)} - 1} \quad \ldots(2.5)$$

The ratio of the intensity of emission from the sample to that of the black body is known as the emissivity, $\in_{vo}$, i.e.[6]:

$$\in_{vo} = \frac{E_{vo}}{E_{bb}} \quad \ldots(2.6)$$

By substituting from equations (2.4) and (2.5), then for $hcv >> kT$, the emissivity can be related to the intensity of radiation absorbed at wavenumber, $\bar{v}$, by the simple relation:

$$\in_{vo} \cong B_{ov}N_o \quad \ldots(2.7)$$

Therefore, the emission spectrum is theoretically equivalent to the absorption spectrum. However this relationship breaks down when samples reach a thickness that allows reabsorption of the emitted radiation.[6-8]

IES is a single beam technique; therefore the signal observed by the detector is a combination of the absorption and emission spectra of all the components of the IR emission spectrometer that the beam comes into contact with, e.g. mirrors, beam splitter and hotplate.[7] The ratio of the sample spectrum to the background spectrum from a polished platinum surface is calculated to obtain the relative emissivity of the sample.[6-8]

Consequently, $\in_{vo}$ is in practice determined by[7]:

$$\in_{vo} = \frac{E_{vo} - E_{Pt}}{E_{bb} - E_{Pt}} \qquad \ldots(2.8)$$

Figure 2.2 displays the IES spectra for a black body, platinum, a sample of PA-6 and a corrected sample spectrum determined with the use of equation 2.8.

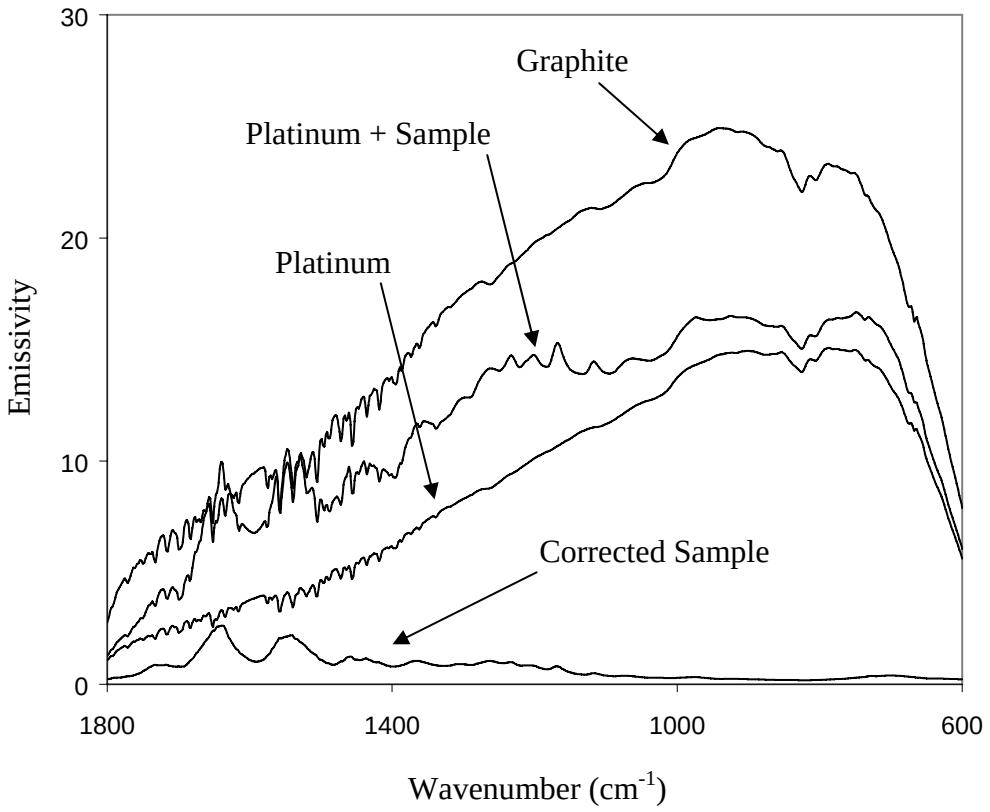

Figure 2.2: FTIR emission from a black body (graphite), platinum and a PA-6 sample as well as the corrected sample spectrum determined after application of equation 2.8.

2.2 Chemiluminescence

Luminescence is the general term used for the emission of light from an electronically excited substance. Fluorescence and phosphorescence result from excitation by light[9] and triboluminescence is a result of mechanical excitation while chemiluminescence (CL) originates from chemical reactions.[10]

For a chemical reaction to produce a photon in the visible spectrum from 400 nm to 700 nm the reaction must produce at least 171-299 kJ mol^{-1} of energy. The product of the reaction must also have an accessible excited state that equates to this energy. Such excited states are typically available in carbonyl and aromatic compounds.[11] The emission of a photon occurs when the reaction product relaxes from the excited state to the ground state. The required energy to promote the reaction product to the excited state primarily comes from the heat of reaction with contribution from the activation energy.[12,13] Therefore, only very exothermic reactions are able to produce CL.

Quantum yields of CL depend in part on both the efficiency of chemical excitation, ϕ_{CE}, and the efficiency of emission, ϕ_{EM}.[14,15] They are also governed by the geometry of the excited state in relation to the transition state.[11] Molecular rearrangements occur relatively slowly compared with energy level transitions so for the probability of excited state formation to be high the geometry of the excited state species needs to be similar to that of the transition state. If more molecular restructuring is required then the time for energy to dissipate will be extended and

this could result in the remaining energy being insufficient to produce the excited state.

The CL intensity, I_{CL}, is proportional to the rate of the luminescent reaction, R_{CL}. A general expression relating I_{CL} to R_{CL} is equation 2.9.[16]

$$I_{CL} = G\phi_{CL}R_{CL} \qquad \ldots(2.9)$$

where: I_{CL} = Measured CL intensity

G = Geometric factor

ϕ_{CL} = Overall efficiency factor for the formation and emission of excited species, i.e. $\phi_{CE} \times \phi_{EM}$.

R_{CL} = Geometric factor

Because I_{CL} changes with time it is common to plot curves of I_{CL} versus reaction time[17] as displayed in Figure 2.3.

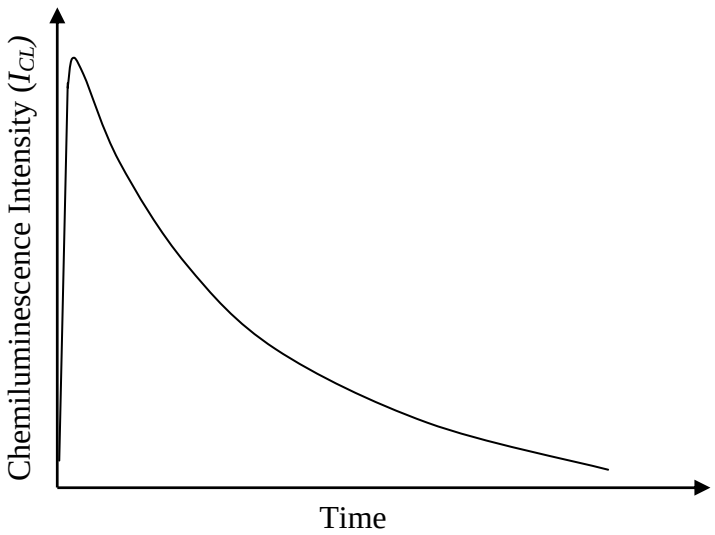

Figure 2.3: Schematic drawing of a time dependent light emission (i.e. a CL curve).

2.2.1 Chemiluminescence From Polymers

In 1961 Ashby reported that light was emitted from polymers heated in air.[18] He described this phenomenon as oxyluminescence as he concluded that oxygen had to be present for light emission to occur and that the light intensity was in fact proportional to the concentration of oxygen present. Such luminescence is now commonly referred to as CL and has been observed for numerous polymers.[19-22] CL measurements have been used to probe polymer oxidation reactions in real time with high sensitivity[23] while kinetic equations derived from CL curves have been used to determine activation energies, induction periods and stabilities.[24,25]

CL techniques are not yet used for the routine analysis of polymer oxidation, as the mechanism to produce CL is still uncertain. Quantum yields of CL reactions are relatively low for polymers (10^{-8} to 10^{-15}) especially compared to the bioluminescence of a firefly (0.88).[14,15] The low quantum efficiencies of polymer CL contributes to the uncertainty regarding the mechanism because parallel non-chemiluminescent reactions that form the majority of the autoxidative reactions obscure the processes that result in CL.

Evidence suggests that the mechanism for CL involves peroxidic groups or radicals that are produced during peroxide decomposition.[26] Spectral distributions of the CL emissions during the oxidation of some common polymers such as PA's, polypropylene and epoxy resins show the majority of photons emitted are approximately in the 360-500 nm region.[23,27-30] This region is consistent with

emission resulting from the relaxation of triplet carbonyls to the ground state.[11] CL studies showed that polymers emit light when heated in an inert atmosphere and that the area under the CL emission curve, denoted the total luminescence intensity (TLI), was proportional to the hydroperoxide concentration in the early stages of oxidation.[16,31] The CL emission also decreased with treatment of a peroxide-destroying agent, e.g. sulfur dioxide, indicating that the emission resulted from hydroperoxides.[32] The effect of triplet sensitizers on emitted light intensity[33,34] and quenching of CL by oxygen[35,36] indicates that relaxation of a triplet-excited state is a source of light emission.

Several mechanisms capable of generating the energy required to populate a carbonyl triplet state, which is at least 290-340 kJ mol^{-1} [17], have been suggested.[37] Direct homolysis of hydroperoxides[38-40], disproportion of alkoxy radicals[41] and β-scission of alkoxy radicals[42] are all sufficiently exothermic. The most widely accepted mechanism is the highly exothermic (460 kJ mol^{-1}) bimolecular termination of primary or secondary alkyl peroxy radicals, i.e. the Russell mechanism.[14,16,23,43,44]

Blakey and George recently discovered that the CL profile is related to the carbonyl concentration,[45,46] which contradicts peroxy termination or direct hydroperoxide decomposition as the source of CL. They proposed that CL is the result of chemically induced electron exchange luminescence (CIEEL) from reactions involving hydroperoxides.[46]

2.2.1.1 Decomposition of Hydroperoxides

Hydroperoxides are formed as impurities during processing (section 1.2.1.1) and are produced during the propagation step (Eq. 1.3) in the autoxidation cycle of polymers. It has been proposed that decomposition of hydroperoxides is responsible for the CL observed during oxidation (Figure 2.4).[38-40]

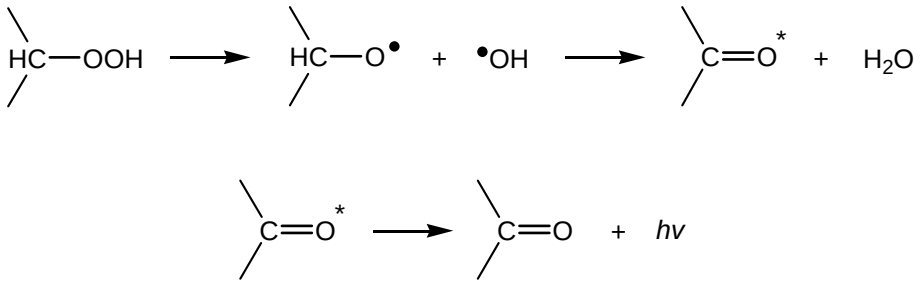

Figure 2.4: Chemiluminescence from the decomposition of hydroperoxides.

Support for this mechanism comes from Achimsky *et al.*[47] who proposed that the linear dependency of CL intensity (I_{CL}) on the oxygen concentration was evidence for CL to be the result of hydroperoxide decomposition. However, this mechanism is not widely accepted due to its unfavourable energetics. The bimolecular decomposition of hydroperoxides[48] has also been suggested as a source of CL, however no supporting mechanism has been proposed.

2.2.1.2 The Russell Mechanism

The Russell mechanism (Figure 1.5), discussed in section 1.2.1.4, is the most widely accepted mechanism for the formation of an excited carbonyl and the subsequent emission of CL. [14,16,23,43,44] This termination reaction between two peroxy radicals, which yields a carbonyl together with an alcohol and a molecule of oxygen, generates more than 400 kJ mol^{-1}. Either the carbonyl or the oxygen produced can be in the excited state; therefore both species may give rise to light emission by relaxation.

Considerable experimental evidence supporting the Russell mechanism can be found throughout the literature. Both singlet oxygen[44,49-51] and triplet carbonyls[14,29,52] have been detected during the decomposition of model hydroperoxides and during the autoxidation of hydrocarbons and polymers. The tetroxide intermediate was detected for secondary[51] and tertiary[53,54] peroxy radicals. A deuterated derivative effect has been observed for recombination of secondary radicals showing involvement of the α–hydrogen.[43,50,55]The six-member cyclic transition state also favours the reaction.

2.2.1.3 Chemically Induced Electron Exchange Luminescence

Kinetic analysis of both the Russell mechanism and hydroperoxide decomposition illustrates that I_{CL} should be proportional to the hydroperoxide concentration and the integral of I_{CL} should be proportional to accumulation of carbonyls.[45] Both these

relationships must be valid if either mechanism is to account for production of CL. However, Blakey and George have recently shown via simultaneous CL-FTIES of polypropylene that I_{CL} is not proportional to the hydroperoxide concentration, but is directly proportional to the carbonyl concentration or some oxidation product that is produced at a similar rate to that of the carbonyls.[45] Therefore, they believe that the Russell mechanism or the direct decomposition of hydroperoxides cannot account for the production of CL. Instead they proposed that CL originates from either an energy transfer mechanism (Figure 2.5) or by chemically induced electron exchange luminescence (CIEEL) involving hydroperoxides reacting with an easily oxidised species such as an aromatic hydrocarbon (Figure 2.6).

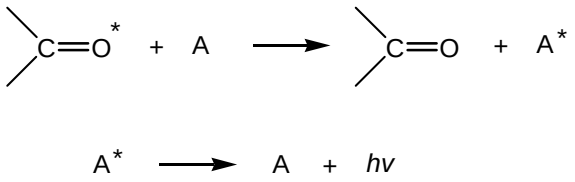

Figure 2.5: Energy transfer mechanism to explain proportionality between rate of light emission and carbonyl concentration, where A is the energy accepting species.

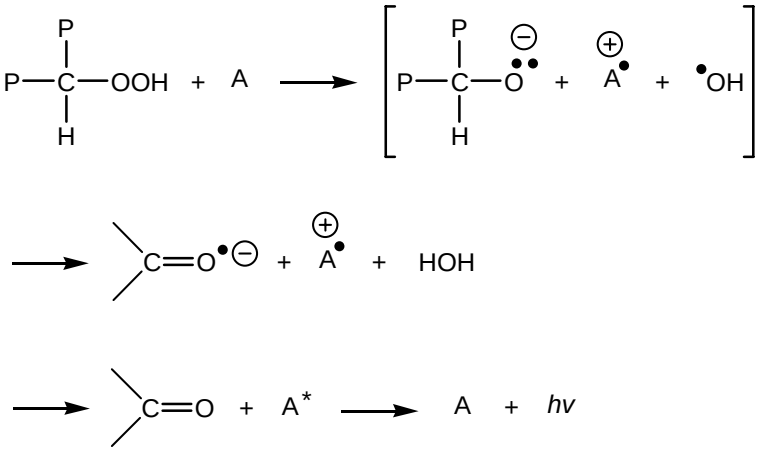

Figure 2.6: Proposed CIEEL mechanism to account for CL, where A is some luminescent oxidation product.

Separate polypropylene samples were doped with an energy acceptor (9,10-dibromoanthracene {DBA}) and a CL activator (9,10-diphenylanthracene {DPA}) respectively to determine the contribution of each proposed mechanism.[46] DBA had little effect on the shape of the I_{CL} versus time curve, while DPA had a significant effect. Under the influence of DPA the integrated I_{CL} versus time curve was proportional to the accumulation of carbonyls, which suggests the I_{CL} versus time curve was proportional to the hydroperoxide concentration. Their conclusion was that CL occurs via a CIEEL mechanism (Figure 2.6).

2.2.2 Photon Counting

An extremely sensitive device commonly based on a photomultiplier tube (PMT)[3] is used to count the photons emitted during CL. A high voltage supply is connected to the PMT's light sensitive cathode and the anode of the PMT is connected to a pulse height discriminator and a counter. The PMT photo-cathode, with an applied potential, is connected to a series of dynodes that are held at progressively higher potentials. When a photon hits the photo-cathode a photoelectron is emitted and accelerated under a potential gradient to the first dynode. Because of the potential gradient the electron hits the first dynode with a relatively high kinetic energy causing the emission of secondary electrons from the dynode. These secondary electrons are accelerated to the next dynode causing emission of further secondary electrons. This process is continued through the remaining dynodes and results in a discrete pulse of electrons, with a certain height, at the anode. The pulse height is determined by the kinetic energy of the initial electrons emitted at the cathode.

Spurious emissions of electrons arising from cosmic ray interactions or thermal emission from the dynodes gives rise to electron pulses of different heights to those resulting from CL photons. The relevant pulses are selected by pulse height discrimination. The discriminator converts these pulses to a digital signal, which is integrated by the counter to give a photon count per unit of time.

2.2.3 Chemiluminescence Imaging

The development of sophisticated position sensitive photon detectors and advances in digital image processing has enabled the measurement of both the intensity and the position of the emitted photons resulting from CL, i.e. CL imaging.[29,56-60] For CL imaging a charge-coupled device (CCD) camera replaces the PMT.

The CCD consists of an array of pixels assembled on a wafer of silicon crystal. Each pixel is a metal oxide semiconductor so when photons, focused by a lens, hit a pixel on the CCD electrons are liberated. These electrons are transferred to potential wells in the silicon wafer. Each pixel has its own well and they are emptied into a register and counted at a pre-determined rate. The signal obtained from each well is processed and the positions of the detected photons are transformed into an image.

2.3 Differential Scanning Calorimetry

Differential scanning calorimetry (DSC) has become the most widely used thermal analysis technique.[3] It measures the heat flow to or from a sample, as a function of time, with results typically displayed as heat flow versus time (heat flow curve).[61] The time integral of the heat flow curve represents the amount of heat evolved in an exothermic process or absorbed in an endothermic process, which provides a measure of the physical or chemical transformations the sample has undergone.[62] Physical transformations may include glass transition, melting or crystallization, while chemical transformations can include curing and oxidation reactions.

In DSC, the sample and a reference are placed in separate pans that sit on raised platforms on a disk.[63] The sample and the reference are subjected to either a precise temperature (isothermal mode) or a programmed temperature change (ramped mode). Heat is transferred separately to the sample and reference via the disk. The differential heat flow to the sample and reference is monitored by thermocouples that are used to measure the temperatures of the sample and reference directly.[3]

The change in enthalpy, ΔH, of the sample is equal to the difference between the heat flow to or from the sample, Q_s, and the heat flow to or from the reference, Q_r[61]:

$$\Delta H = Q_s - Q_r \qquad \ldots(2.10)$$

The heat flow, Q, is proportional to the temperature difference ($T_2 - T_1$) and inversely proportional to the thermal resistance, R_{th}:

$$Q = \frac{T_2 - T_1}{R_{th}} \qquad \ldots(2.11)$$

Combining (2.10) and (2.11):

$$\Delta H = Q_s - Q_r = \frac{T_c - T_s}{R_{th}} - \frac{T_c - T_r}{R_{th}} \qquad \ldots(2.12)$$

where T_c is a constant temperature external to the sample and reference, T_s is the sample temperature, and T_r is the reference temperature. DSC instruments are designed so that the two T_c and the two R_{th} values are equal.[61] Therefore:

$$\Delta H = -\frac{T_s - T_r}{R_{th}} \qquad \ldots(2.13)$$

The measured voltage from the thermocouple is proportional to the temperature difference ($T_s - T_r$).

For isothermal processes the measured heat evolved, Q_m, can be related to the extent of reaction, ξ, by measuring the heat flow at time t, ϕ_m, and at the end of the reaction, ϕ_{end}:[64]

$$Q_m = \int_0^t \phi_m - \phi_{end} = \Delta H \int_0^{\xi} \frac{d\xi}{dt} \qquad \ldots(2.14)$$

Therefore, by measuring the area under the heat flow curve and correcting for the sample size the extent of reaction can be determined.

The heat flow at time t can be related to the rate of reaction, ω, by taking the derivative of equation 2.14[64]:

$$\frac{\Delta Q_m}{dt} = \phi_m - \phi_{end} = \Delta H \omega \qquad \ldots(2.14)$$

It should be noted that DSC is a non-specific technique that monitors a heat flow comprising the contributions from all simultaneous exothermic and endothermic processes of a sample.[61,62,64] This makes the interpretation of heat flow during processes such as oxidation difficult. DSC cannot distinguish between the large number of reactions occurring simultaneously during oxidation. DSC can only provide an overall rate of all chemical reactions. However, the overall shape and position of a heat flow curve is a very good indicator of the overall oxidation process. Heat flow curves can be used to compare oxidation induction times (OIT's) and therefore make comparisons between the relative stabilities of different polymer samples.[62]

2.4 Matrix Assisted Laser Desorption/Ionization Time of Flight Mass Spectrometry

Hillenkamp and Karas developed Matrix assisted laser desorption/ionization time of flight mass spectrometry (MALDI-TOF MS) in 1988 for the analysis of large biomolecules.[65,66] The first investigation of polymers with MALDI-TOF MS was not performed until 1992.[67-69] MALDI-TOF MS is reputed to be a soft ionization technique that allows the measurement of intact molecular ions. Unlike some other MS techniques, MALDI-TOF MS can measure molecular ions above 100,000 Da

with virtually no fragmentation.[67-70]

A typical sample preparation procedure for MALDI-TOF MS measurements[70-72] is displayed in Figure 2.7. The analyte and matrix are dissolved in appropriate and preferably identical solvents and mixed. Metal ions are often added in salt form to enhance cationization.[73-75] A small amount (approx. 1μL) of this mixture is applied to a holder and dried.

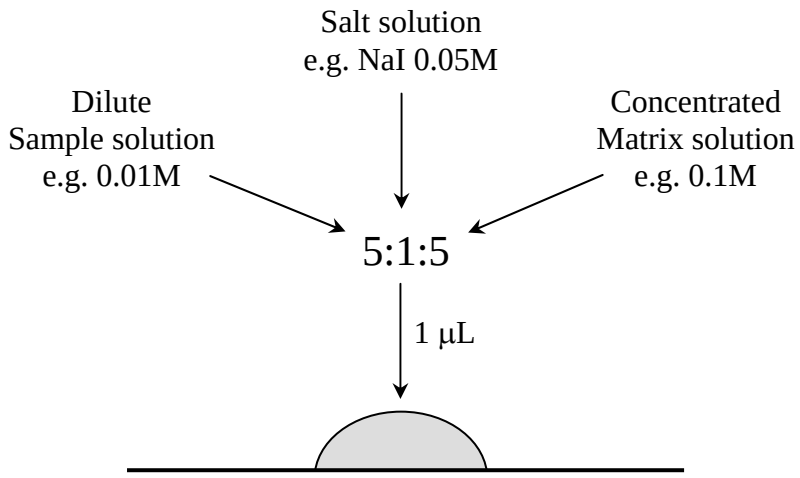

Figure 2.7: Sample preparation for MALDI-TOF MS.

The sample is then placed into the ion source under vacuum (approx 10^{-10} bar) and irradiated by a pulsed UV laser (Figures 2.7 and 2.8).

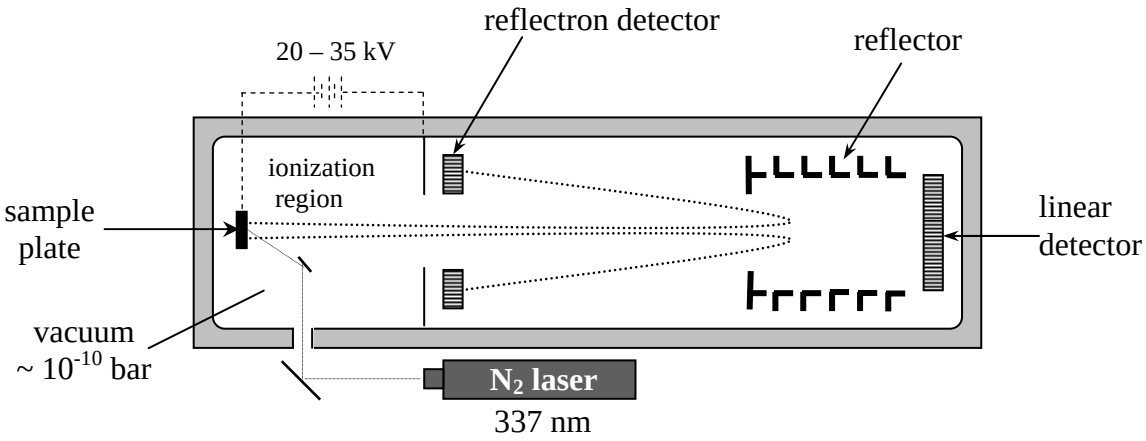

Figure 2.8: Schematic diagram of a MALDI-TOF MS instrument

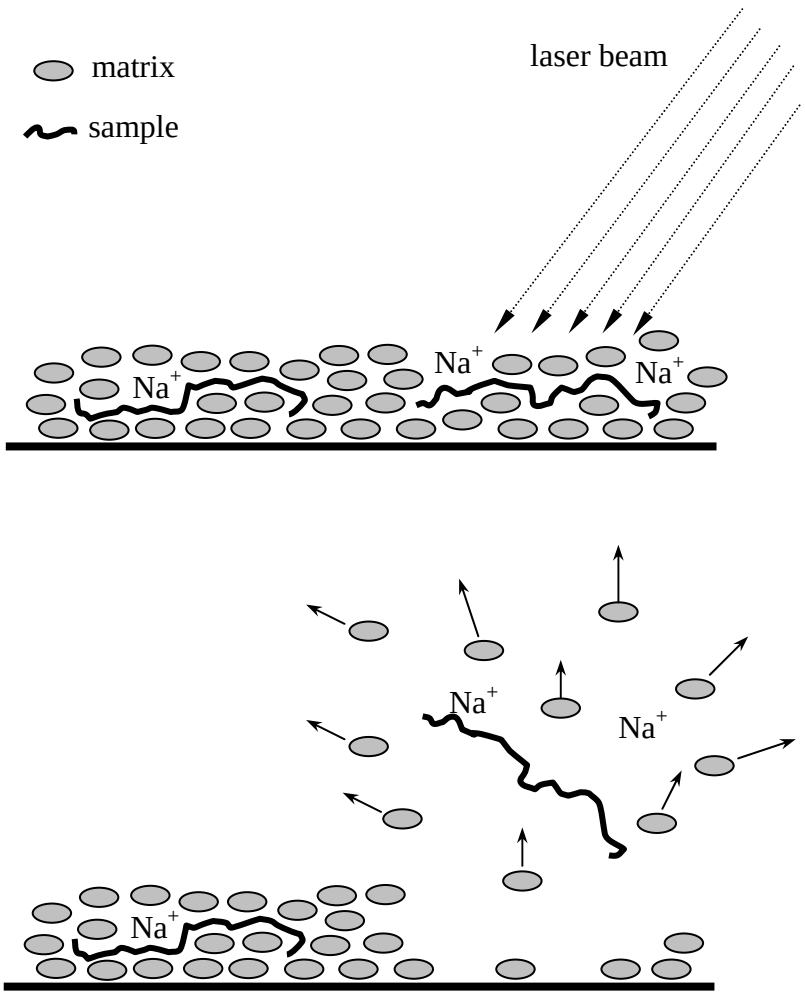

Figure 2.9: Schematic representation of ionization in MALDI-TOF MS.

The energy from the laser beam is absorbed by the matrix, which rapidly volatilizes and carries the sample molecules into the gas phase. The ions formed (mechanisms for ion formation are discussed in section 2.4.1) after a laser pulse are accelerated from the ionization region by a static electric field of up to 35 kV into a field free drift region. The accelerated ions then drift toward the detector with a velocity proportional to their mass. The lighter ions will reach the detector before the heavier ions (time of flight mass spectrometry (TOF MS) is discussed in section 2.4.2). The ions are therefore separated by time and masses are determined by the time that elapses between the laser being fired and the ion impinging on the detector.

MALDI-TOF MS spectra of polymers can provide a great deal of important information in the mass range where single polymers chains are resolved, e.g. mass of the constituent repeating units, composition of end groups, chemical distributions (i.e. different functional groups, different sequences of monomers or different sequence length), and structural heterogeneities (i.e. linear, cyclic, grafted or branched parts).[76-80]

2.4.1 Ion Formation

Radical cations, protonated pseudo-molecular ions and cationized pseudo-molecular ions (i.e. metal ion adducts) are the only common observed ions in positive ion MALDI. The formation of these ions in MALDI is still being investigated, however a number of mechanisms for ion formation have been suggested. These include multiphoton ionization[81], energy pooling[82], desorption of preformed ions[83],

ion–molecule reactions[84], disproportionation[85], excited state proton transfer[86] and thermal ionization[87]. It is very unlikely that a single mechanism can explain all of the ions formed in a single experiment.[87] It should also be noted that the overall ion-to-neutral ratio in MALDI experiments is approximately 10^{-4}, which means the proposed mechanisms are to account for the minority species in the process.[88]

There are two main types of ionization: primary and secondary. Primary ionization includes the processes that generate the first ions from neutral molecules, while secondary ionization results in analyte ions produced from processes other than primary processes. The most important secondary ionization processes are those which lead to protonated and cationized analytes. Only the common ion formation mechanisms directly related to polymer studies will be discussed. Ion formation mechanisms relevant to other analytes can be found elsewhere.[85-87]

2.4.1.1 Primary Ionization

Multiphoton Ionization

The matrix (M) is elevated to an excited state when it absorbes a photon after UV laser irradiation (Eq. 2.15). The excited state exists for a period of time that allows another photon to be absorbed, resulting in a matrix radical cation and a free electron (Eq. 2.15).[81,89,90]

$$M \xrightarrow{h\nu} M^* \xrightarrow{h\nu} M^{+\bullet} + e^- \qquad \ldots(2.15)$$

Statistically only one photon can participate in each step of equation 2.15 because the MALDI irradiance is typically 10^6 – 10^7 Wcm^{-2}.[91] Therefore, two laser photons must excite the matrix molecule from its ground state to above its ionization potential. Evidence indicates that matrix ionization potentials are above the energy reached by two laser photons.[91] However, it has been suggested that the additional energy might be supplied from heat produced in the plume.[92]

Energy Pooling

Once matrix molecules are elevated to an excited state two or more excited matrix molecules pool their energy to yield one matrix radical cation (Eq. 2.16). A polymer radical cation could also be formed if the excited matrix molecules are in close proximity to a polymer molecule (Eq. 2.17).[82,93,94]

$$2M \xrightarrow{2h\nu} 2M^* \longrightarrow M + M^{+\bullet} + e^- \qquad \ldots(2.16)$$

$$2M^* + P \longrightarrow 2M + P^{+\bullet} + e^- \qquad \ldots(2.17)$$

Desorpton of Preformed Ions

This mechanism assumes that the ions observed in a MALDI spectrum are already present in the solid sample and are simply released by the laser pulse. For example, the preformed ion could be a complex of the neutral polymer with a cation from added salts (i.e. cationization agent).[83]

2.4.1.2 Secondary Ionization

The primary ions, discussed in the previous section, are combined with neutral matrix and polymer molecules in the plume. Secondary ion formation is the result of numerous collisions between all species, which occurs before the ions are extracted into the drift region of the mass spectrometer.[87] Mechanisms occurring during such collisions are gas phase proton transfer and gas phase cationization.

Gas Phase Proton Transfer

When the primary ion is a radical cation then proton transfer can lead to a protonated molecule (Eq.'s 2.18 and 2.19).[89,95]

$$M^{+\bullet} + M \longrightarrow MH^{+} + (M - H)^{\bullet} \quad \ldots(2.18)$$

$$P^{+\bullet} + M \longrightarrow PH^{+} + (M - H)^{\bullet} \quad \ldots(2.19)$$

Generally polymers have a higher proton affinity than matrix molecules. Therefore if a protonated matrix molecule is in the proximity of a polymer molecule the interaction will result in a protonated polymer molecule (Eq. 2.20).[96]

$$MH^{+} + P \longrightarrow M + PH^{+} \quad \ldots(2.20)$$

Gas-Phase Cationization

Ion–molecule interactions in the gas phase, where a polymer complexes with a metal ion, result in cationized molecules (also known as pseudo-molecular ions) (Eq. 2.21).[81,84]

$$P + Na^+ \longrightarrow PNa^+ \qquad \ldots(2.21)$$

In MALDI, cations do not need to be added to the sample as Na^+ and K^+ impurities are sufficient to provide strong cationized signals.[87] However, it is common to add ions such as K^+, Na^+ and Ag^+ as their salts in order to provide a cationization agent.[97] It has been shown that Na^+ is well solvated by polymer molecules in the gas phase, further confirming viability of such ion-molecule interactions.[98]

2.4.2 Time of Flight

The ions formed in the source region (of length *s*) of the MALDI-TOF mass spectrometer are accelerated by an electric field, *E*, into a longer field-free drift region (of length *D*). The kinetic energy, *KE*, of the ions entering the drift region is given by[99]:

$$KE = zeEs = zeV_{acc} \qquad \ldots(2.22)$$

where *e* is the charge on an electron and *z* is the number of charges.

The classical equation for kinetic energy is:

$$KE = \tfrac{1}{2}mv^2 \qquad \ldots(2.23)$$

where m is the mass of the of the ion and v is the velocity of the ion.

Therefore:

$$\tfrac{1}{2}mv^2 = zeV_{acc} \qquad \ldots(2.24)$$

$$v = \left(\frac{2zeV_{acc}}{m}\right)^{1/2} \qquad \ldots(2.25)$$

Because $v = D/t$, the time required for the ion to travel the length of the drift region is given by:

$$t = \left(\frac{m}{2zeV_{acc}}\right)^{1/2} D \qquad \ldots(2.26)$$

Therefore, the time spectrum can be directly converted to a mass spectrum:

$$\frac{m}{z} = 2eV_{acc}\left(\frac{t}{D}\right)^2 \qquad \ldots(2.27)$$

However, in practice more exact values for the mass scale can be obtained by calibration against flight times of ions with known masses and equation 2.28[100].

$$\frac{m}{z} = at^2 + b \qquad \ldots(2.28)$$

where the constants *a* and *b* are determined by measuring the flight times of two ions with known masses.

TOF mass spectrometers generally use pulsed ionization to obtain the timing information regarding ion formation, which is why TOF MS is ideal for MALDI. [99,100]

2.5 References

(1) Lin-Vien, D.; Colthup, N. B.; Fateley, W. G.; Grasselli, J. G., *The Handbook of Infrared and Raman Characteristic Frequencies of Organic Molecules*, 1st ed., Academic Press, San Diego, 1991.

(2) George, W.; McIntyre, P., *Infrared Spectroscopy*, John Wiley and Sons, London, 1986.

(3) Willard, H.; Merritt, L.; Dean, J.; Settle, F., *Instrumental Methods of Analysis*, 7th ed., Wadsworth Inc., California, 1988.

(4) Kemp, W., *Organic Spectroscopy*, 3rd ed., Macmillan, London, 1992.

(5) Atkins, P., *Physical Chemistry*, 5th ed., Oxford University Press, Oxford, 1994.

(6) George, G. A.; Vassallo, A. M.; Cole-Clarke, P. A.; Celina, M., *Die Angew. Makromol. Chem.*, **232** (1995) 105.

(7) Celina, M.; Ottesen, D. K.; Gillen, K. T.; Clough, R. L., *Polym. Degrad. Stab.*, **58** (1997) 15.

(8) George, G. A.; Celina, M.; Vassallo, A. M.; Cole-Clarke, P. A., *Polym. Deg. Stab.*, **48** (1995) 199.

(9) Allen, N. S.; Owen, E. D., *Luminescence Techniques in Solid State Polymer Research*, L. Zlatkevich (ed), Dekker, New York, 1989.

(10) McCapra, F.; Perring, K. D., *Chemi and Bioluminescence*, J. G. Burr (ed), Dekker, New York, 1989.

(11) Schuster, G. B.; Schmidt, S. P., *Advances in Organic Chemistry*, V. Gold, D. Bethell (eds), Academic Press, London, 1982.

(12) Lissi, E., *J. Am. Chem. Soc.*, **98** (1976) 3386.

(13) Wilson, E. B., *J. Am. Chem. Soc.*, **98** (1976) 3387.

(14) Kellogg, R. E., *J. Am. Chem. Soc.*, **91** (1969) 5433.

(15) Vassil'ev, R. F., *Opt. i Spectry.*, **18** (1964) 131.

(16) Billingham, N. C.; Then, E. T.; Gijsman, P., *Polym. Deg. Stab.*, **34** (1991) 263.

(17) George, G. A., *Luminescence Techniques in Solid State Polymer Research*, L. Zlatkevich (ed), Marcel Dekker Inc, New York, 1989.

(18) Ashby, G. E., *J. Polym. Sci.*, **50** (1961) 99.

(19) David, D. J., *Thermochim. Acta*, **3** (1972) 277.

(20) Schard, M. P.; Russell, C. A., *Journal of applied polymer science*, **8** (1964) 985.

(21) Wendlandt, W. W., *Thermochim. Acta*, **68** (1983) 383.

(22) Wendlandt, W. W., *Thermochim. Acta.*, **72** (1984) 363.

(23) George, G. A., *Developments in Polymer Degradation - 3*, N. Grassie (ed), Applied Science Publishers, London, 1981.

(24) Zlatkevich, L., *J. Polym. Sci. Polym. Lett.*, **21** (1983) 571.

(25) Zlatkevich, L., *Luminescence Techniques in Solid State Polymer Research*, L. Zlatkevich (ed), Marcel Dekker, New York, 1989.

(26) Chien, J. C.; Boss, C. R., *J. Polym. Sci., A-1*, **5** (1967) 3091.

(27) George, G. A., *Polym. Degradation Stab.*, **1** (1979) 217.

(28) George, G. A.; Schweinsberg, D. P., *J. Appl. Polym. Sci.*, **33** (1987) 2281.

(29) Lacey, D. J.; Dudler, V., *Polym. Deg. Stab.*, **51** (1996) 109.

(30) Tiemblo, P.; Gomez-Elvira, J. M.; Teyssedre, G.; Massines, F.; Laurent, C., *Polym. Deg. Stab.*, **65** (1999) 113.

(31) Kron, A.; Stenberg, B.; Reitberger, T.; Billingham, N. C., *Polym. Deg. Stab.*, **53** (1996) 119.

(32) Billingham, N. C.; Burdon, J. W.; Kakulska, I. W.; O'Keefe, E. S.; Then, E. T. H., *Proc. Int. Symp. Lucerne*, **2** (1988) 11.

(33) Phillips, D.; Anisimov, V.; Karpukhin, O.; Shiliaintokh, *Nature*, **215** (1967) 1163.

(34) Hofert, M., *Photochem. Photobiol.*, **9** (1969) 427.

(35) Beutel, *J. Am. Chem. Soc.*, **93** (1971) 2615.

(36) Vassil'ev, R. F., *Nature*, **196** (1962) 668.

(37) Matisova-Rychla, L.; J., R., *Polymer Durability - Degradation, Stabilization and Lifetime Prediction*, L. C. Roger, N. C. Billingham, K. T. Gillen (eds), Am. Chem. Soc., Washington DC, 1996.

(38) Reich, L.; Stivala, S. S., *Die Macromol. Chem.*, **103** (1967) 74.

(39) Matisova-Rychla, L.; Rychly, J.; Vavrekova, M., *Eur. Polym. J.*, **14** (1978) 1033.

(40) Zlatkevich, L., *J. Polym. Sci. Polym. Phys.*, **23** (1985) 1691.

(41) Quinga, E. M. Y.; Mendenhall, G. D., *J. Am. Chem. Soc.*, **105** (1983) 6520.

(42) Aoudin-Jirackova, L.; Verdu, J., *J. Polym. Sci.*, **25** (1987) 1205.

(43) Russell, C. A., *J. Am. Chem. Soc.*, **79** (1957) 3871.

(44) Lee, S. H.; Mendenhall, G. D., *J. Am. Chem. Soc.*, **91** (1988) 4318.

(45) Blakey, I.; George, G. A., *Macromolecules*, **34** (2001) 1873.

(46) Blakey, I.; Billingham, N. C.; George, G. A., *Macromolecules*, accepted 2001.

(47) Achimsky, L.; Audouin, L.; Verdu, J.; Rychla, L.; Rychly, J., *Eur. Polym. J.*, **35** (1999) 557.

(48) Matisova-Rychla, L.; Rychly, J., *Polym. Deg. Stab.*, **67** (2000) 515.

(49) Nakano, M.; Takayama, K.; Shimizu, Y.; Tsuji, Y.; Inaba, H.; Migita, T., *J. Am. Chem. Soc.*, **98** (1976) 1974.

(50) Howard, J. A.; Ingold, K. U., *J. Am. Chem. Soc.*, **110** (1968) 1056.

(51) Bogan, D. J.; Celii, F.; Sheinson, R. S.; Coveleskie, R. A., *J. Am. Chem. Soc.*, **25** (1984) 409.

(52) Lloyd, R. A., *Trans. Faraday Soc.*, **61** (1965) 2182.

(53) Bartlett, P. D.; Guaraldi, G. J., *J. Am. Chem. Soc.*, **89** (1967) 4799.

(54) Miller, A. A.; Mayo, F. R., *J. Am. Chem. Soc.*, **78** (1956) 1017.

(55) Russell, G. A., *J. Am. Chem. Soc.*, **80** (1958) 6699.

(56) Fleming, R. H.; Craig, A. Y., *Polym. Deg. Stab.*, **37** (1992) 173.

(57) Hosoda, S.; Seki, Y.; Kihara, H., *Polymer*, **34** (1993) 4602.

(58) Lacey, D.; Dudler, V., *Polym. Deg. Stab.*, **51** (1996) 115.

(59) Lacey, D.; Dudler, V., *Polym. Deg. Stab.*, **51** (1996) 101.

(60) Ablblad, G.; Stenberg, B.; Terselius, B.; Reitberger, T., *Polym. Test.*, **16** (1997) 59.

(61) Wendlandt, W., *Thermal Methods of Analysis*, 3rd ed., John Wiley, New York, 1986.

(62) Billingham, N. C.; Bott, D. C.; Manke, A. S., *Developments in Polymer Degradation - 3*, N. Grassie (ed), Applied Science Publishers, London, 1981.

(63) Gill, P., *Am. Lab.*, **17** (1985) 34.

(64) Hohne, G. W. H.; Hemminger, W.; Flammershein, H. J., *Differential Scanning Calorimetry an Introduction for Practitioners*, 1st ed., Springer, Berlin, 1996.

(65) Karas, M.; Bachmann, D.; Bahr, U.; Hillenkamp, F., *Int. J. Mass Spectrom. Ion Processes*, **78** (1987) 53.

(66) Hillenkamp, F.; Karas, M.; Beavis, R. C.; Chait, B. T., *Anal. Chem.*, **63** (1991) 1193.

(67) Danis, P. O.; Karr, D. E.; Mayer, F.; Holle, A.; Watson, C. H., *Org. Mass Spectrom.*, **27** (1992) 843.

(68) Karas, M.; Bahr, U.; Deppe, A.; Stahl, B.; Hillenkamp, F., *Macromol. Chem., Macromol. Symp.*, **61** (1992) 397.

(69) Danis, P. O.; Karr, D. E.; Westmoreland, D. G.; Piton, M. C.; Christie, D. I.; Clay, P. A.; Kable, S. H.; Gilbert, R. G., *Macromolecules*, **26** (1993) 6684.

(70) Schriemer, D. C.; Li, L., *Anal. Chem.*, **68** (1996) 2721.

(71) Pasch, H.; Resch, M., *GIT Fachz. Lab.*, **3** (1996) 189.

(72) Lehrle, S.; Sarson, D. S., *Polym. Deg. Stab.*, **51** (1996) 197.

(73) Deery, M. J.; Jennings, K. R.; Jasieczek, C. B.; Haddleton, D. M.; Jackson, A. T.; Yates, H. T.; Scrivens, J. H., *Rapid Commun. Mass Spectrom.*, **11** (1997) 57.

(74) Bahr, U.; Deppe, A.; Karas, M.; Hillenkamp, F.; Giessmann, U., *Anal. Chem.*, **64** (1992) 2866.

(75) Spickermann, J.; Martin, K.; Rader, H. J.; Mullen, K.; Schlaad, H.; Muller, A. H. E.; Kruger, R. P., *Eur. Mass Spectrom.*, **2** (1996) 161.

(76) Pasch, H.; Unvericht, R.; Resch, M., *Angew. Makromol. Chem.*, **212** (1993) 191.

(77) Schadler, V.; Spickermann, J.; Rader, J.; Wiesner, U., *Macromolecules*, **29** (1996) 4865.

(78) Spickermann, J.; Rader, H. J.; Mullen, K.; Muller, B.; Gerle, M.; Fischer, K.; Schmidt, M., *Macromol. Rapid Commun.*, **17** (1996) 885.

(79) Montaudo, G.; Montaudo, M. S.; Puglisi, C.; Samperi, F., *J. Polym. Sci., Part A: Polym. Chem.*, **34** (1996) 439.

(80) Kruger, R. P., *GIT Fachz Lab.*, **3** (1995) 189.

(81) Liao, P. C.; Allison, J., *J. Mass Spectrom.*, **30** (1995) 408.

(82) Karas, M.; Bahr, U.; Stah-Zeng, J. R., *Large Ions: Their Vaporization, Detection and Structural Analysis*, T. Baer, C. Y. Ng, I. Powis (eds), Wiley, London, 1996.

(83) Lehmann, E.; Knochenmuss, R.; Zenobi, R., *Rapid Commun. Mass Spectrom.*, **11** (1997) 1483.

(84) Wang, B. H.; Dreisewerd, K.; Bahr, U.; Karas, M.; Hillenkamp, F., *J. Am. Mass Spectrom.*, **4** (1993) 393.

(85) Breuker, K.; Knochenmuss, R.; Zenobi, R., *Int. J. Mass Spectrom. Ion. Proc.*, **184** (1999) 25.

(86) Splengler, B.; Kaufmann, R., *Analusis*, **20** (1992) 91.

(87) Zenobi, R.; Knochenmuss, R., *Mass Spectrom. Rev.*, **17** (1998) 337.

(88) Puretzky, A. A.; Geohegan, D. B., *Chem. Phys. Lett.*, **286** (1997) 425.

(89) Ehring, H.; Karas, M.; Hillenkamp, F., *Org. Mass Spectrom.*, **27** (1992) 427.

(90) Quist, A. P.; Huth-Fehre, T.; Sunqvist, B. U. R., *Rapid Commun. Mass Spectrom.*, **8** (1994) 149.

(91) Karback, V.; Knochenmuss, R., *Rapid Commun. Mass Spectrom.*, **12** (1998) 968.

(92) Allwood, D. A.; Dyer, P. E.; Dreyfus, R. W., *Rapid Commun. Mass Spectrom.*, **11** (1997) 499.

(93) Johnson, R. E., *Int. J. Mass Spectrom. Ion Proc.*, **139** (1994) 25.

(94) Ehring, H.; Sundqvist, B. U. R., *J. Mas Spectrom.*, **30** (1995) 1303.

(95) Harrison, A. G., *Chemical Ionization Mass Spectrometry*, CRC Press, Boca Raton, 1992.

(96) Bokelmann, V.; Spengler, B.; Kaufmann, R., *Eur. Mass Spectrom.*, **1** (1995) 81.

(97) Rader, H. J.; Schrepp, W., *Acta Polym.*, **49** (1998) 272.

(98) von Helden, G.; Wyttenbach, T.; Bowers, M. T., *Science*, **267** (1995) 1483.

(99) Cotter, R. J., *Anal. Chem.*, **64** (1992) 1027A.

(100) Cotter, R. J., *Time-of-flight Mass Spectrometry*, ACS Symposium Series, Vol. 549, American Chemical Society, Washington D.C., 1994.

3. Synthesis and Characterization of Samples

3.1 Introduction

The effect of end groups on the thermo-oxidative stability of PA's was discussed in section 1.3.3. A considerable number of studies[1-8] illustrate that end groups play a significant role in the oxidation of PA's, e.g. higher ratios of carboxylic end groups to amine end groups make PA's more sensitive to oxidation. Proposals have been made to account for such observed differences (refer to section 1.3.3) however, apart from work by Lanska[1,4], very little experimental evidence has been obtained to support these proposals. The mechanisms for end group interactions during PA oxidation remain unclear.

During this study on the thermo-oxidation of PA-6 the effect of end groups was investigated with the aim of gaining further insight into their role in the oxidation process. Accordingly, separate PA-6 samples terminating in predominantly carboxylic and amine groups respectively were required, as was a sample terminated in methyl groups to represent the oxidation of PA-6 without a significant contribution from end group effects arising from the precursor acid or amine of the PA.

Commercial PA's are typically terminated with a carboxylic group at one end of a chain and an amine group at the other. They can also contain cyclic oligomers. When heated above their melting point, PA's react with diacids or diamines resulting in a loss of molecular weight.[9,10] The PA is degraded by chain scission and the new chain ends will be determined by the added species: i.e. carboxylic terminated PA can be obtained from heating PA with diacids and amine terminated PA can be obtained from heating PA with diamines. Eichhorn[11] showed that PA degraded in this fashion produces a similar size exclusion chromatography (SEC) line shape to that of non-degraded PA, which indicates that this type of degradation is a controlled process with products possessing normal molecular weight distributions. Therefore, this type of reaction provided a suitable pathway for achieving the desired carboxylic terminated and amine terminated samples for this study. As well as providing the desired end groups, shortened chain lengths make the effect of end groups on PA oxidation more significant. Any cyclic oligomers should also be opened into linear chains thereby improving the uniformity of the samples.

Based on work by Fester[12], Lanska has obtained methyl terminated PA's by the deamination of amine terminated samples.[1,6] This methodology was utilized to obtain methyl terminated PA-6 for this study.

3.2 Materials

All basic materials were analytical grade commercial products. High molecular weight PA-6 (M_w = 43,000), adipic acid, diphenylsulphone (DPSO), hexamethylenediamine (HMDA), 2,2,2-trifluoroethanol (TFE) and 2-(4-hydroxyphenylazo)benzoic acid (HABA) were all supplied by Sigma-Aldrich Chemical Company (Australia). Methanol, sodium nitrite ($NaNO_2$), glacial acetic acid (CH_3COOH), potassium hydroxide (KOH) and hydrochloric acid (HCl) were all supplied by Ajax chemicals (Australia). PA-6 was dried at 50°C under vacuum for 24 h prior to all reactions.

3.3 Synthesis

3.3.1 Carboxylic Terminated PA-6

PA-6 terminated with carboxylic acid groups at both ends was obtained by degradation of Aldrich PA-6 with adipic acid. Aldrich PA-6, adipic acid and DPSO were placed into a 250 mL round bottom flask in the ratio of 4:1:4 (w/w/w) respectively. The flask was evacuated and filled with argon 3 times to remove all oxygen. The mixture was gently stirred at 235°C for 20 min under a stream of argon, then cooled before refluxing in methanol for 2 h. The solid residue was filtered and washed with fresh methanol. Any remaining impurities were removed by soxhlet

extraction in methanol for 6 h before the carboxylic terminated PA-6 was dried at 50°C under vacuum for 24 hours.

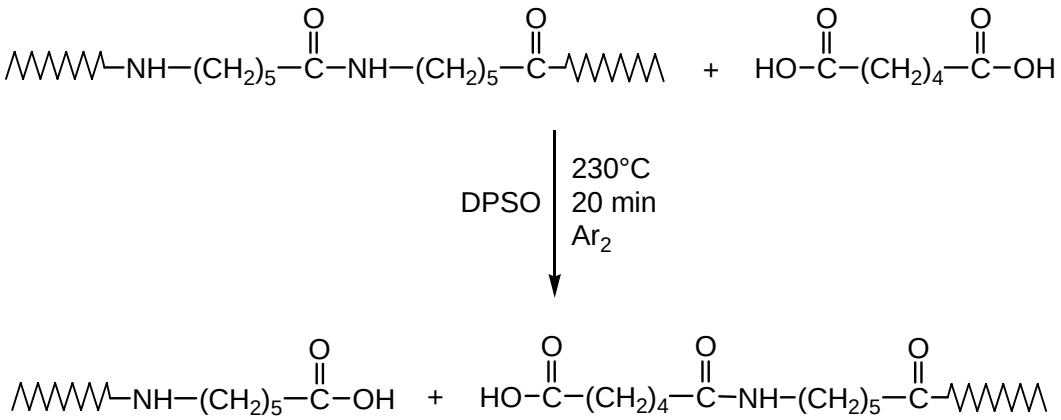

Figure 3.1: Synthesis of Carboxylic Terminated PA-6

3.3.2 Amine Terminated PA-6

PA-6 terminated with primary amine groups at both ends was obtained by degradation of Aldrich PA-6 with HMDA. Aldrich PA-6, HMDA and DPSO were placed into a 250 mL round bottom flask in the ratio of 1:1:1 (w/w/w) respectively. The flask was evacuated and filled with argon 3 times to remove all oxygen. The mixture was gently stirred at 235°C for 1 h under argon, then cooled before refluxing with methanol for 2 h. The solid residue was filtered and washed with fresh methanol. Any remaining impurities were removed by soxhlet extraction in methanol for 6 h before the amine terminated PA-6 was dried at 50°C under vacuum for 24 hours.

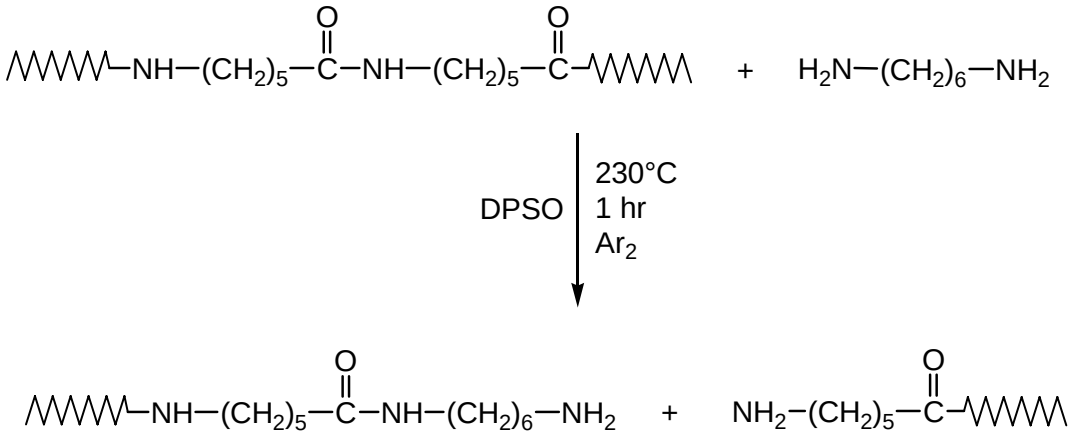

Figure 3.2: Synthesis of Amine Terminated PA-6

3.3.3 Methyl Terminated PA-6

PA-6 terminated with methyl groups at both ends was obtained by the deamination of amine terminated PA-6. A solution of 0.1 M $NaNO_2$ in 0.1 M CH_3COOH (aq) was prepared no more than 1 h before required. Amine terminated PA-6, synthesized in section 3.3.2, was added to this solution in the ratio of approximately 1g of amine terminated PA-6 per 200 mL of solution. This mixture was refluxed at 80°C for 4 h while being gently stirred. The sample was filtered before being boiled in deionized water 3 times for 10 min each time. The methyl terminated PA-6 was soxhlet extracted with methanol for 6 hours to remove any remaining impurities and then dried at 50°C under vacuum for 24 hours.

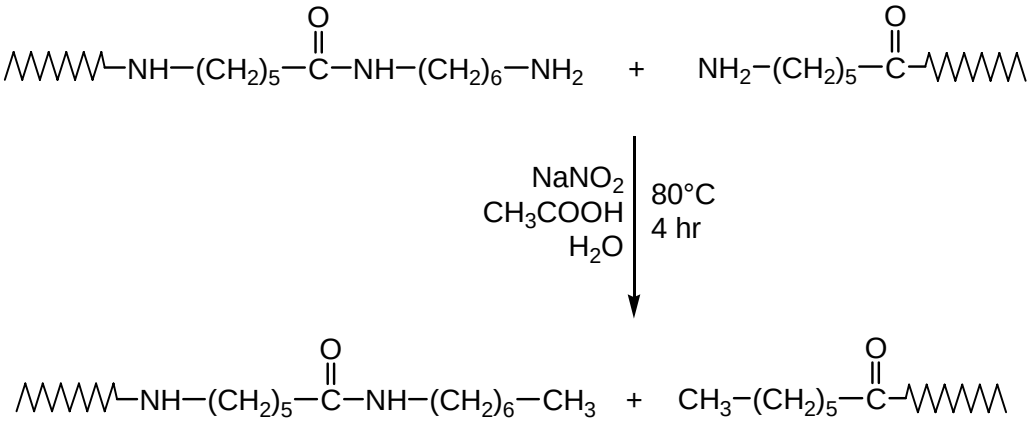

Figure 3.3: Deamination of amine terminated PA-6 to produce methyl terminated PA-6.

3.4 Characterization

3.4.1 MALDI-TOF Mass Spectra

For the development of the sample preparation method refer to chapter 7. PA-6 samples were prepared to a concentration of 10 mg/mL in TFE as was the matrix (HABA). Equal amounts of the sample and matrix solutions were mixed thoroughly. A 2 μL aliquot of this combined solution was applied to a stainless steel target plate and air-dried.

MALDI-TOF MS spectra were obtained with a Micromass TOF Spec E spectrometer equipped with a nitrogen laser operating at 337 nm. An accelerating voltage of 25 kV was used. All samples were measured in reflectron mode and the spectra generated by summing a minimum of 200 laser shots. External mass calibration was used, based on a number of points that both bracketed and fell within the mass range of interest.

The MALDI-TOF mass spectra for carboxylic, amine and methyl terminated PA-6 samples are displayed in Figures 3.4, 3.5 and 3.6 respectively. Peak assignments verify the composition of each sample.

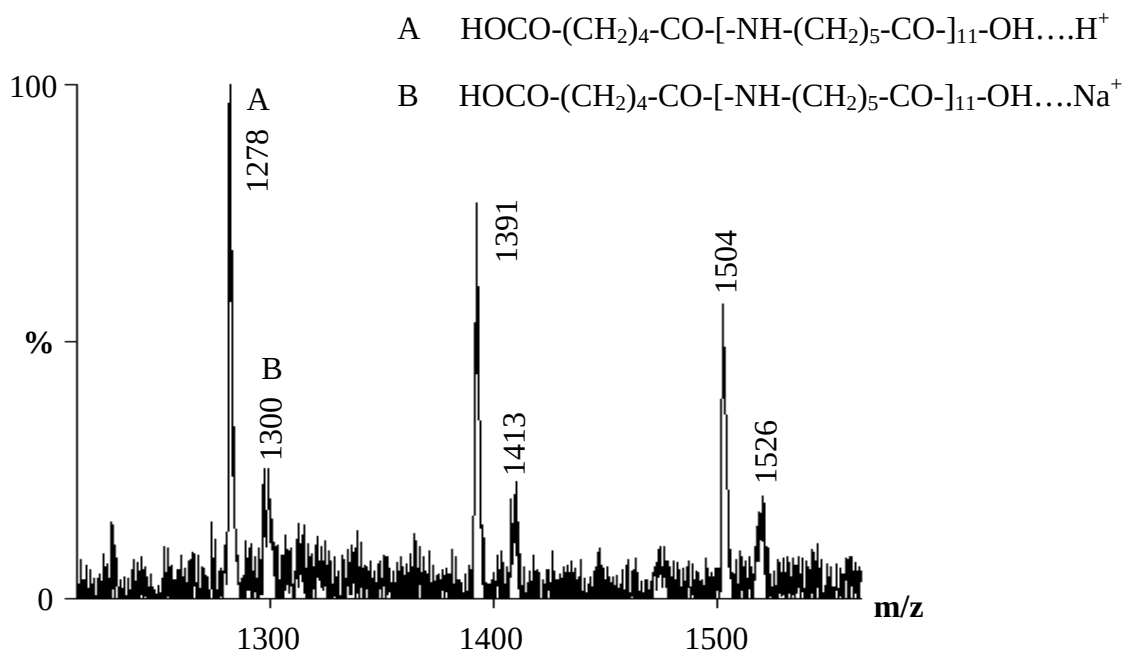

Figure 3.4: MALDI-TOF mass spectrum of carboxylic terminated PA-6, where the series A peaks (m/z 1278 +n113) are due to protonated chains and the series B peaks (m/z 1300 +n113) are due to sodium cationized chains.

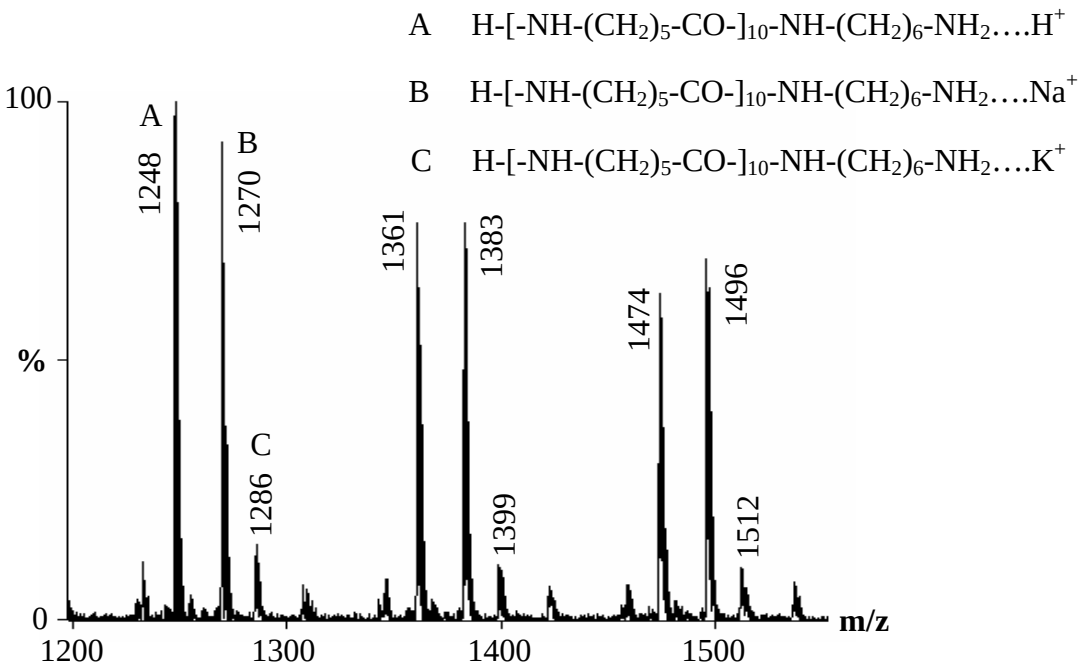

Figure 3.5: MALDI-TOF mass spectrum of amine terminated PA-6, where the series A, B and C peaks represent protonated, sodium cationized and potassium cationized chains.

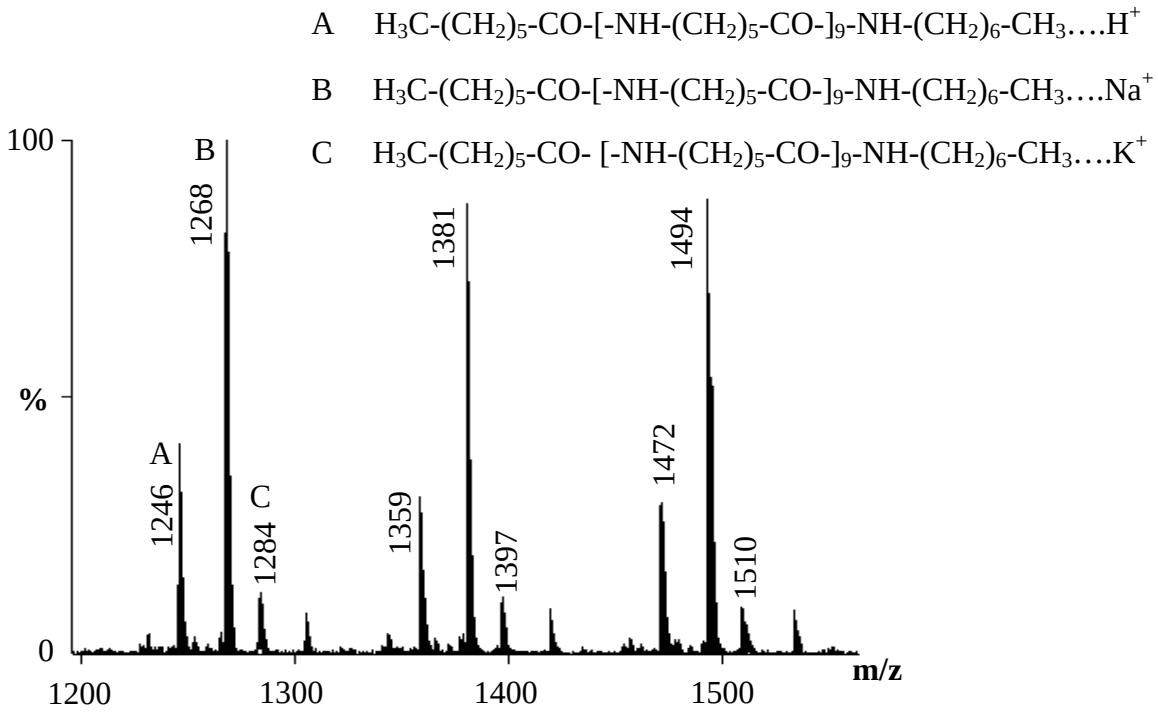

Figure 3.6: MALDI-TOF mass spectrum of methyl terminated PA-6, where the series A, B and C peaks represent protonated, sodium cationized and potassium cationized chains.

3.4.2 End Group Analysis

The concentration of end groups was determined by conventional end group titrations. The concentration of carboxylic end groups was determined by potentiometric titration using a 0.01 *N* KOH in methanol solution. The concentration of amine end groups was determined by potentiometric titration using a 0.01 *N* HCl in methanol solution. In both cases 0.5 g of PA-6 sample was dissolved in 20 mL of a TFE/methanol (1:1, v/v) solution for titration. The end group concentrations (mmol/kg) for each type of sample are summarized in table 3.1.

3.4.3 Molecular Weight Analysis

Number average molecular weights, M_n, were estimated from the end group concentration values, while viscosity measurements were used to determine the viscosity average molecular weights, M_v.

To determine the value of M_v for the different PA-6 samples, a series of solutions of each PA-6 sample in TFE, ranging in concentration (c) from 1 g/L to 10 g/L, was prepared. The flow times of pure TFE, t_0, and the PA-6 solutions, t, were measured using an Ostwald viscometer at 25°C. The specific viscosity, η_{sp}, was determined by:

$$\eta_{sp} = (t/t_0) - 1 \qquad \ldots(3.1)$$

η_{sp}/c was plotted against c and the intrinsic viscosity $[\eta]$ was determined from the intercept where c = 0.

M_v was determined by:

$$M_v = ([\eta]/K)^{1/a} \qquad \ldots(3.2)$$

Where the Mark-Houwink coefficients K and a in TFE at 25°C, are 5.36 x 10-2 mL/g and 0.75 respectively. [13]

The values of M_n and M_v for each type of sample are summarized in table 3.1.

Table 3.1: Properties of PA-6 samples

Sample	**[COOH]** (mmol/kg)	**[NH_2]** (mmol/kg)	M_n (kDa)	M_v (kDa)
COOH terminated	114	6	16.6	17.4
NH_2 terminated	10	193	9.8	11.2
CH_3 terminated	10	8	9.8	11.2

3.5 Comparison of Samples

Peak assignments in the MALDI-TOF spectra (Figures 3.4 to 3.6) show three distinct samples have been produced: one primarily terminated with carboxylic groups, one primarily terminated with amine groups and one primarily terminated with methyl groups. There appears to be no significant contamination in the samples from cyclic oligomers.

From the titration data (Table 3.1), it appears that some contamination from non-desired end groups does occur, e.g. there is 10 mmol/kg of carboxylic end groups in the amine terminated sample. However, as the concentrations of the contaminating end groups are low compared to the desired end groups they should not play a significant part in the oxidation of the various samples. Any differences observed in

the oxidation of the samples should be attributable to the primary end groups. It should be noted that the concentration determined for NH_2 end groups also includes other basic end groups such as imines, which are impurities produced during processing. The actual concentration of NH_2 groups can be calculated by subtracting the NH_2 concentration after deamination from the NH_2 concentration before deamination.

The molecular weights of the amine terminated and the methyl terminated PA-6 samples (Table 3.1) are the same, indicating that no other degradation occurred during deamination. Therefore, any difference observed in the oxidation of the respective samples is assumed primarily to be due to the end groups. The molecular weight of the carboxylic terminated sample is slightly larger than the other samples, however the effect of the carboxylic end groups on the oxidation of the sample should still be comparable to the other samples and therefore other end groups.

3.6 References

(1) Lanska, B.; Doskocilova, D.; Matisova-Rychla, L.; Puffr, R.; Rychly, J., *Polym. Degrad. Stab.*, **63** (1999) 469.

(2) Lanska, B.; Matisova-Rychla, L.; Brozek, J.; Rychly, J., *Polym. Degrad. Stab.*, **66** (1999) 433.

(3) Lanska, B.; Sebenda, J., *Eur. Polym. J.*, **22** (1986) 199.

(4) Lanska, B., *Eur. Polym. J.*, **30** (1994) 197.

(5) Allen, N. S.; Harrison, M. J.; Follows, G. W.; Matthews, V., *Polym. Degrad. Stab.*, **19** (1987) 77.

(6) Matisova-Rychla, L.; Lanska, B.; Rychly, J.; Billingham, N. C., *Polym. Degrad. Stab.*, **43** (1994) 131.

(7) Pavlov, N. N.; Kudryavtseva, G. A.; Abramova, I. M.; Vasil'eva, V. A.; Zezina, L. A.; Kazaryan, L. G., *Polym. Degrad. Stab.*, **24** (1989) 389.

(8) Reimschuessel, H. K.; Dege, G. J., *J. Polym. Sci., Part A-1*, **8** (1970) 3265.

(9) Kroschwitz, J. I.; Howe-Grant, M., *Kirk-Othmer, Encyclopedia of Chemical Technology, 4th Ed.*, , John Wiley & Sons, Inc., Brisbane, 1996.

(10) Montaudo, G.; Montaudo, M. S.; Puglisi, C.; Samperi, F., *J. Polym. Sci., Part A: Polym. Chem.*, **34** (1996) 439.

(11) Eichhorn, K. J.; Lehmann, D.; Voight, D., *J. Appl. Polym. Sci.*, **62** (1996) 2053.

(12) Fester, W., *Z. Ges Textilind*, **66** (1964) 955.

(13) Bandrup, J; Immergut, E.H. (eds), *Polymer Handbook, 3rd Ed.*, John Wiley & Sons, New York, 1989.

4. Simultaneous CL/DSC

4.1 Abstract

A technique that simultaneously measures chemiluminescence (CL) and heat flow (DSC) was used to study the isothermal oxidation of unstabilized PA-6 at temperatures ranging from 140°C to 160°C. PA-6 samples which terminated in predominantly carboxylic, amine or methyl end groups respectively were tested to examine what influence end groups have on PA-6 oxidation.

The differences in the oxidative mechanisms and stabilities for each type of sample as a result of the end groups were highlighted. In the case of amine terminated PA-6 samples the CL intensity was proportional to the heat flow curve. When amine end groups were absent it was the first derivative of the CL intensity that was proportional to the heat flow curve. Thus in the case of amine terminated PA-6 a CIEEL mechanism occurred directly and the CL profile was that of [ROOH] versus time. In the absence of amine end groups, the CIEEL mechanism could not operate until an easily oxidisable luminescent oxidation product was formed.

4.2 Introduction

CL and DSC are rate sensitive techniques used to study the oxidation of polymers. The techniques of CL and DSC were discussed in detail in sections 2.2 and 2.3 respectively.

DSC measures the heat flow to or from a sample as a function of time.[1] It is a non-specific technique that monitors the contributions from all simultaneous exothermic and endothermic processes of a sample[1-3] and provides a measure of the physical or chemical transformations the sample has undergone.[3] Physical transformations may include glass transition, melting or crystallization, while chemical transformations can include oxidation reactions such as hydrogen abstraction by oxy radicals or hydroperoxide decomposition. DSC cannot distinguish between the large number of reactions occurring simultaneously during oxidation. It can only provide an overall rate of all chemical reactions. However, the shape and position of a heat flow curve is a very good indicator of the overall oxidation process and the relative stabilities of different polymer samples.[3]

CL measures the luminescence resulting from chemical reactions. The mechanism for CL is unclear and dependent on the polymer type and degree of purity. For PP Blakey and George have proposed that CL intensity is directly proportional to the carbonyl concentration, or to some oxidation product that is produced at a similar rate to that of the carbonyls.[4] Matisova-Rychla et al[21] have attempted to relate CL curves to the thermal oxidation of Polyolefins and Polyamides. They suggest the

kinetics of the CL curves can be approximated by equations based on the bimolecular decomposition of hydroperoxides. However, CL studies on lactams (model PA's) indicate that bimolecular reactions of lactam peroxy radicals are a weak source of luminescence.[22] Instead, stronger light emission appears to come from the excited state of the cyclic hydrogen-bonded associate of lactam hydroperoxide with the aldehyde of the amide of the respective acid.

Lanska *et al*[23] report that CL data collected during the oxidation of PA's is not proportional to the oxygen consumption or more importantly to changes in polymer properties experienced during oxidation. Distinct luminescence does not appear until a significant reduction of mechanical properties is observed.[22,23] Although CL does not appear to provide an accurate method for following the level of physical change in the polymer resulting from oxidation it has been widely used to study the effects of stabilizers on PA oxidation.[23,24,25] CL has also been used to investigate the effects of impurities (e.g. end-groups) on polymer oxidation.[23,26]

Forsstrom et al have recently compared the heat flow curve (from microcalorimetry) and the CL curve of unstabilized PA-6 in air at the oxidation temperature of 110°C. They concluded that the two curves did not directly relate to each other and that different processes dominate the output of the two techniques. The DSC and CL curves were obtained from different samples from the same source of PA-6. Therefore, the differences observed could have been due to factors such as heterogeneity of the samples, slightly different measurement temperatures, oxygen pressures or possibly timing discrepancies.

In this study the results of simultaneous CL/DSC for unstabilised PA-6 samples will be presented. Because both the CL and DSC curves are obtained in real time from the same sample any differences between the two types of curves will be due only to the different processes of oxidation that might dominate their output. The effect of end groups on these processes and therefore on the differences between the CL and DSC curves are also investigated.

4.3 Experimental

4.3.1 Materials

Three distinct PA-6 samples terminating predominantly in carboxylic, amine or methyl groups respectively were used. The synthesis and characterization of the samples are discussed in chapter 3.

4.3.2 CL/DSC of PA-6 Samples

The simultaneous monitoring of CL intensity and heat flow from a sample has been made possible by Professor Billingham's polymer group at the University of Sussex. A Mettler Toledo DSC 821^e differential scanning calorimeter was modified to allow a photomultiplier tube connected to a photon counting device to be positioned above the sample chamber. Samples are normally contained in capped pans for DSC

analysis, however for this type of experiment the pans are uncapped to allow detection of CL.

1.00 ± 0.01 mg of PA-6 powder was placed in an aluminium DSC pan and an empty aluminium pan was used as a reference. The sample was heated to 105°C under nitrogen for 1 h to remove any absorbed water. The temperature was then elevated to the desired oxidation temperature while still under a nitrogen atmosphere. When the temperature had stabilized the gas was switched to pure oxygen with a flow rate of 50 mL/min. Oxidations were performed at 140°C, 145°C, 150°C, 155°C and 160°C. The photon counter in the CL apparatus was set to integrate over 10 second intervals with results normalized to counts per second, while the DSC measured heat flow every second.

Only 1 mg of a PA sample was used in each experiment as this provided a very thin but complete layer of sample over the bottom of the DSC pan. This small mass of sample results in a less than optimum signal to noise ratio for the DSC curves. More importantly though, this mass avoids the contributions towards the CL and DSC curves that arise from increased sample thickness, which were observed when optimizing the mass of sample. For example, broadening of curves was observed when greater amounts of samples were used.

4.4 Results and Discussion

4.4.1 Effect of End Groups on the CL of PA-6 Samples

Figure 4.1 displays the CL curves for PA-6 samples terminating in predominantly different end goups (i.e. COOH, NH_2 or CH_3 groups) when oxidized at 150°C.

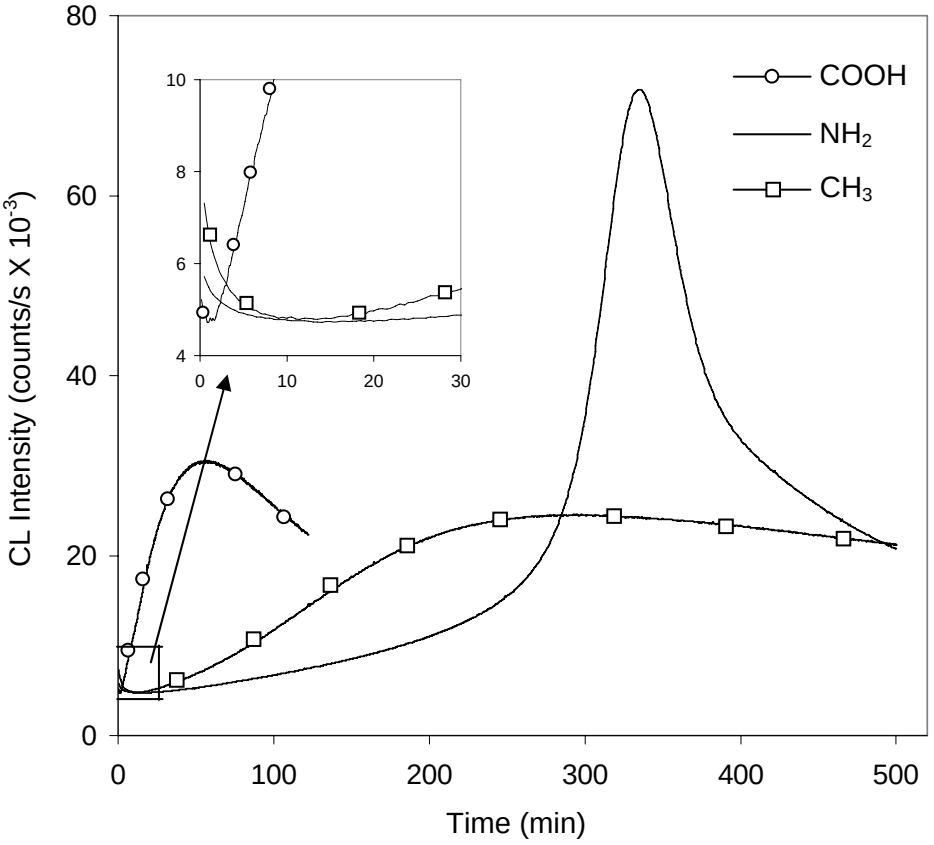

Figure 4.1: CL curves for PA-6 samples predominantly terminating in carboxylic, amine or methyl groups respectively at 150°C under oxygen.

The three types of samples have the same repeat unit and comparable molecular weights; the only notable difference is their end groups. However, the CL curves

for all three types of samples are significantly different from each other. Therefore, Figure 4.1 illustrates the consequential effect the type of end group has on the overall oxidation of PA-6.

In the proposed mechanism for the thermo-oxidation of aliphatic PA's (see Figure 1.6) the radical in the initial step forms at the N-vicinal methylene group. This macro-radical then combines with oxygen to give a new radical, which may isomerize or follow various reaction pathways (each involving chain scission) resulting in the formation of oxidation products which typically contain carbonyl and carboxy end-groups.[5-9] The CL curve in Figure 4.1 for the methyl terminated sample should reflect this mechanism, as the initial end groups of that sample should not affect the rate or the mechanism of oxidation.

The overall rate of oxidation for the carboxylic terminated sample is greater than for the other samples in Figure 4.1, which is in agreement with other studies.[10-14] Lanska[10] has suggested that carboxylic groups have a catalytic effect on the decomposition of hydroperoxides (see Figure 1.17) during PA oxidation. If this were so then the mechanism displayed in Figure 1.6 would not alter, only the rate at which it occurs would change. This seems to be the case in Figure 4.1 because the CL curve for the carboxylic terminated sample appears to be of the same basic shape as the CL curve for the methyl terminated sample but with a shift to an increased rate of oxidation. Furthermore, when the oxidation time expressed as a fraction of that to the maximum signal is plotted against the corresponding CL intensity expressed as a fraction of the maximum intensity for the different samples (Figure 4.2) the curves for the carboxylic terminated sample and the methyl terminated sample are very

similar. This similarity indicates that the carboxylic end groups do not change the mechanism governing the oxidation of PA-6 and therefore supports the catalytic decomposition of hydroperoxides by carboxylic groups.

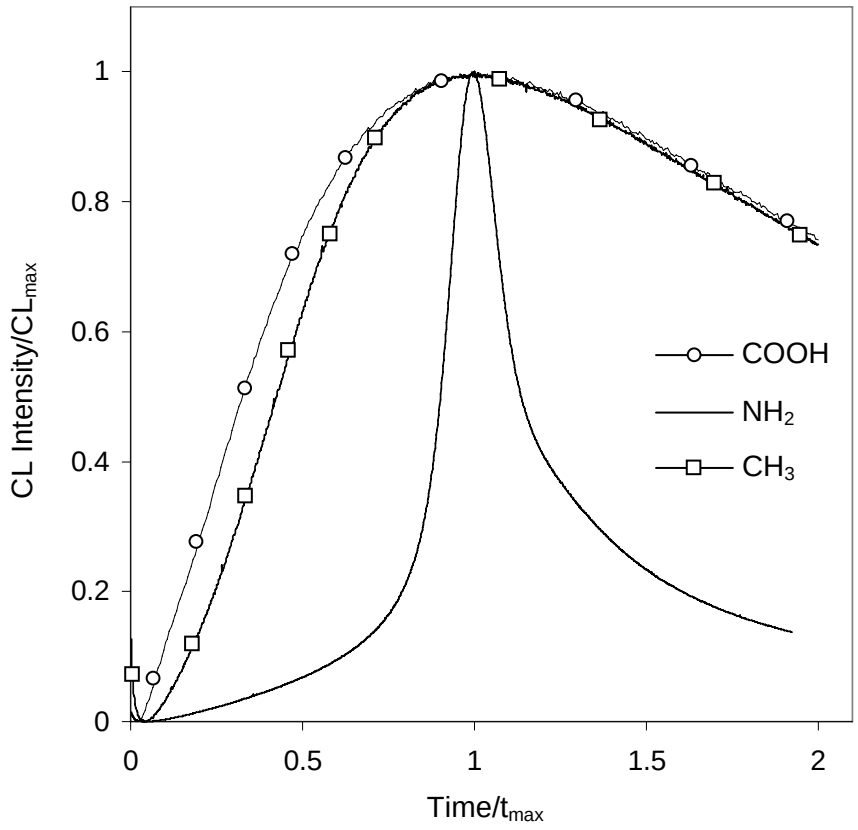

Figure 4.2: CL curves for PA-6 samples predominantly terminating in carboxylic, amine or methyl groups respectively at 150°C under oxygen, normalized to the point of maximum signal.

The curves representing the amine terminated sample in Figures 4.1 and 4.2 are significantly different to the curves for the methyl terminated and carboxylic terminated samples. There is a long induction time for the amine terminated sample, which is not evident for the other samples. This induction period is followed by a more intense rise to the maximum signal, which has a far greater intensity than the

maxima of the other samples. The decline in CL signal after the maximum is also considerably greater than was observed for the other samples. The disparity between the curves of the amine terminated sample and the curves for the other samples indicates that the amine end groups either change the mechanism governing the oxidation of PA-6, or the mechanism of CL so that the CL profile for the different samples reflects different reactions in the oxidation pathway.

Amine end groups have previously been found to stabilize PA's.[11,15,16] This has been attributed to the ability of amine end groups to react with hydroperoxides and peroxy radicals by a similar mechanism to that of hindered amine stabilizers.[17] Amine end groups also condense with aldehydes and ketones, generated by oxidation, to form aldimines and azomethines respectively.[5,18] Additional oxidative stability has been attributed to this removal of oxidation products and higher tendency for crosslinking by amine end groups. It has been suggested that the consecutive reaction of azomethines results in sequences of conjugated double bonds, which gives rise to the chromophore that accounts for the observed yellowing of PA's during oxidation.[19] Sufficient amine end groups are present to react with the hydroperoxides and the carbonyl oxidation products until the end of the oxidation induction time. However, when the end of the induction time is reached there are insufficient amine end groups to prevent a high rate of oxidation. At this point the sample is no longer PA-6 but a complex network of cross-linked polymer, the oxidation of which is considerably different to that of typical PA-6 samples.

It should be noted that when oxygen is admitted a burst of CL intensity occurs for each sample (see inset in Figure 4.1). This phenomena has previously been

reported[12,20] for PA's with the authors suggesting that some products are formed during annealing which readily oxidize on the admission of oxygen. The intensity of this CL burst increases in the following order: COOH < NH_2 < CH_3. This order also relates to the amount of time each sample was kept at an elevated temperature during synthesis. Therefore, the more reaction time (at an elevated temperature) required to produce a sample, the more products are formed which readily oxidize on the admission of oxygen to produce the burst of CL.

4.4.2 Simultaneous CL/DSC

The CL and DSC curves collected simultaneously for carboxylic terminated PA-6 oxidized at 140°C, 145°C, 150°C, 155°C and 160°C respectively are shown in Figure 4.3. The time to maximum intensity for each curve is listed in Table 4.1. The basic shapes of the two types of curves differ from each other at each temperature, although the pattern of the curves remains the same over the range of temperatures investigated. The time to maximum intensity for the CL and DSC curve differs significantly at each temperature. For example, at 150°C the maximum of the CL curve is reached at 58 minutes, while the DSC curve reaches the maximum at 16 minutes. Therefore, the difference between the maxima of the two curves is approximately 72% with respect to the CL curve. The relative difference between the CL and DSC times to maximum appears to decrease with increasing oxidation temperature.

The CL and DSC curves collected simultaneously for amine terminated PA-6 oxidized at 140°C, 145°C, 150°C, 155°C and 160°C respectively are shown in Figure 4.4. The time to maximum intensity for each curve is listed in Table 4.1. Unlike the carboxylic terminated sample, the basic shapes of the CL and DSC curves for the amine terminated sample are similar to each other at each temperature and the pattern of the curves remains the same over the range of temperatures investigated. In this case the time to maximum intensity for the CL and DSC curve do not differ significantly. For example, at 150°C the maximum of the CL curve is reached at 335 minutes, while the DSC curve reaches the maximum at 331 min; a difference of only 1.2% between the maxima of the two curves. The relative difference between the CL and DSC times to maximum does appear to again decrease with increasing oxidation temperature.

The amine terminated sample is the only one that has an obvious oxidation induction time. Oxidation induction times can be determined from the CL and the DSC curves by drawing a tangent to the 'linear' region of the curves (see curves at 150°C in Figure 4.4). It seems that the oxidation induction times determined by the DSC curves occur slightly before the OIT's determined by the CL curves.

The CL and DSC curves collected simultaneously for methyl terminated PA-6 oxidized at 140°C, 145°C, 150°C, 155°C and 160°C respectively are shown in Figure 4.5 and the time to maximum intensity for each curve is listed in Table 4.1. The signal to noise ratio of the DSC curves for the other PA-6 samples at 140°C was low, but a pattern in the DSC resulting from oxidation could still be observed. However,

in this case oxidation cannot be detected via DSC until at least 150°C with obvious signs of oxidation not apparent until 155°C. Therefore, comparisons between the two types of curves cannot be made until at least 155°C. CL curves of the methyl terminated sample clearly detect oxidation at 140°C, which shows that CL has the far superior limit of detection in regards to the oxidation of PA's.

Once DSC can detect oxidation occurring in the methyl terminated sample, i.e. at temperatures of 155°C and 160°C, the DSC and CL curves behave in a manner very similar to the carboxylic terminated sample. The basic shapes of the two different types of curves are similar to each other at each temperature and the time to maximum intensity for the CL and DSC curve differs significantly. At 155°C the difference between the two types of curves is approximately 83% with respect to the CL maximum.

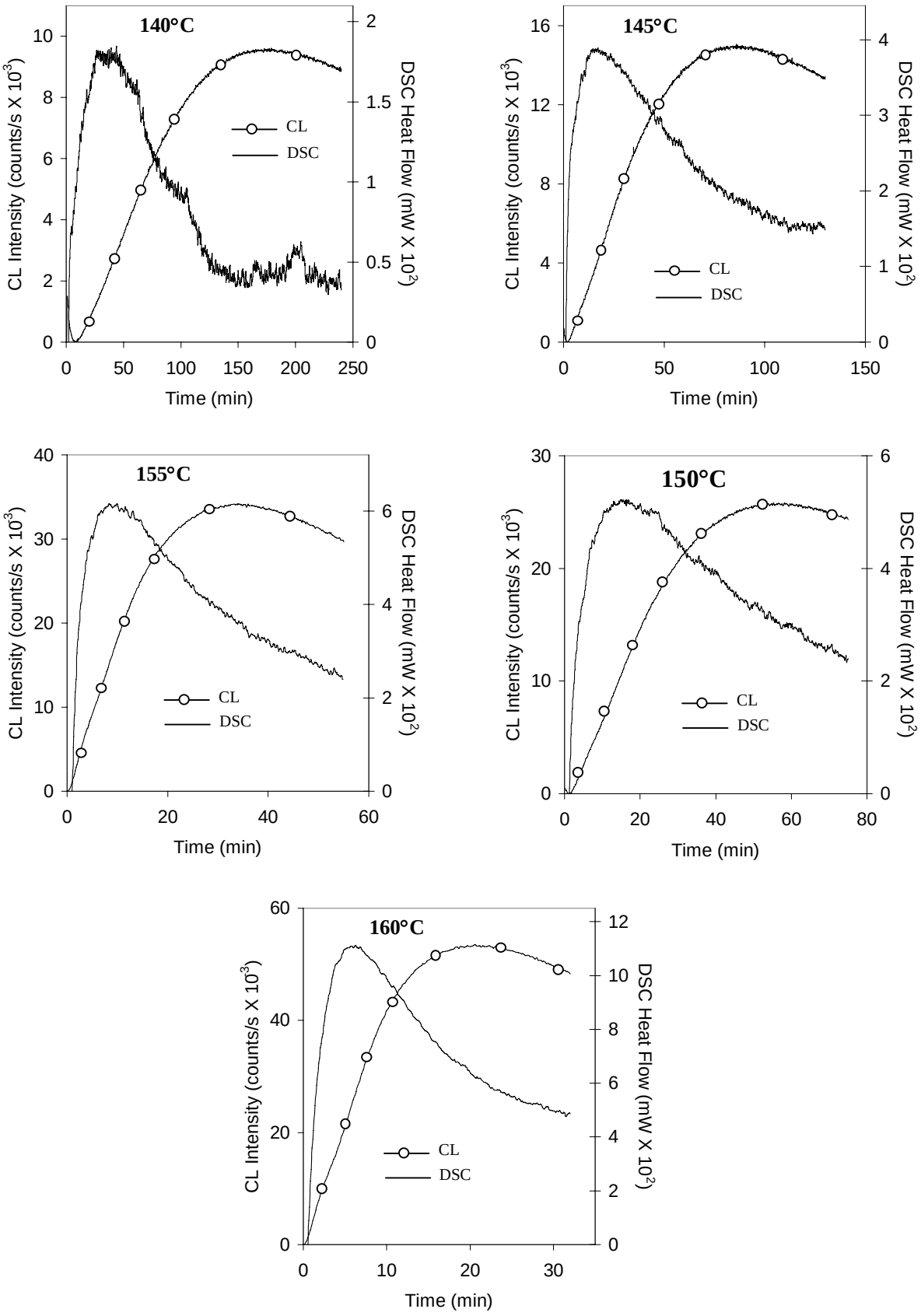

Figure 4.3: Simultaneous CL/DSC of carboxylic terminated PA-6 under oxygen at 140°C, 145°C, 150°C, 155°C and 160°C.

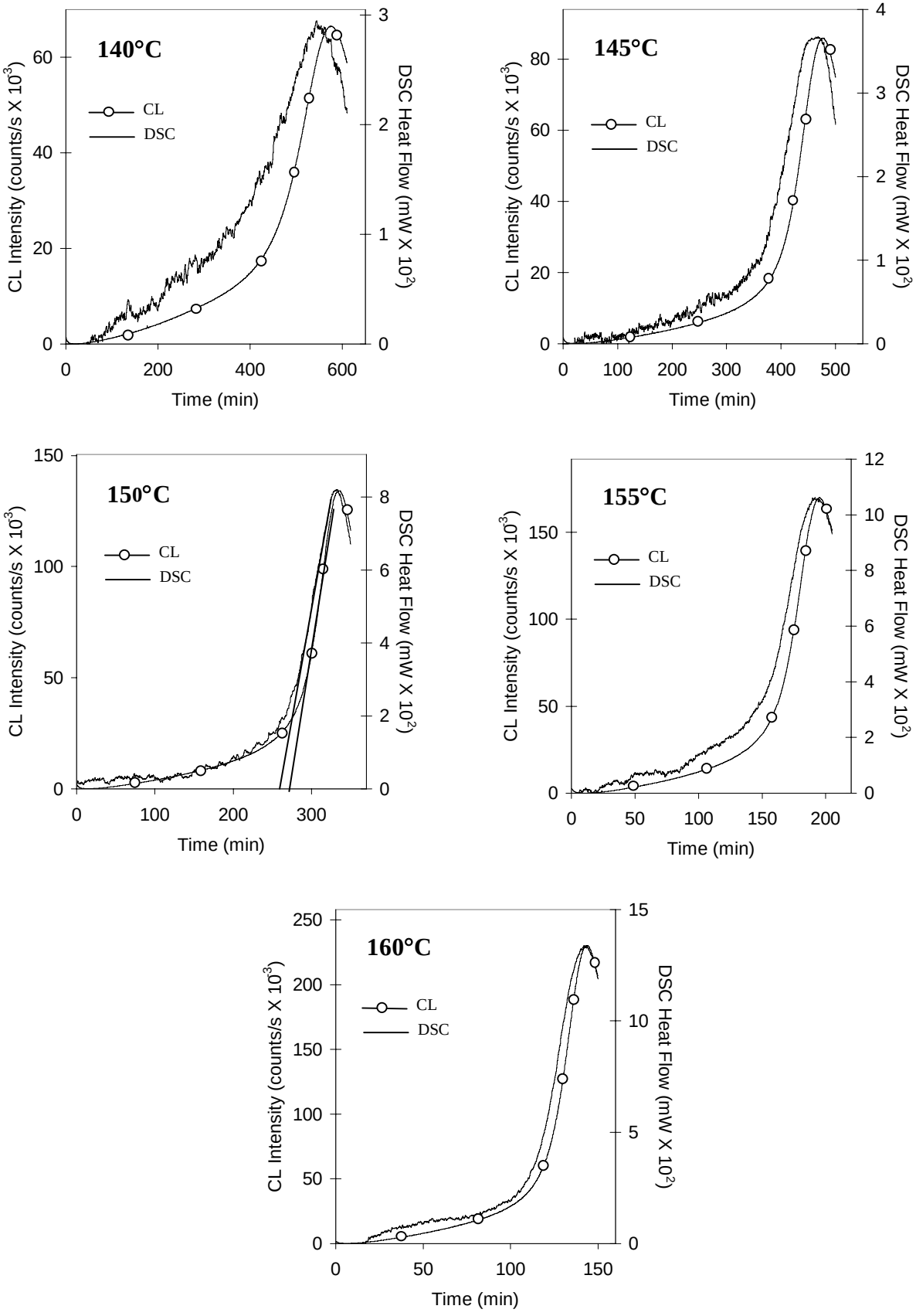

Figure 4.4: Simultaneous CL/DSC of amine terminated PA-6 under oxygen at 140°C, 145°C, 150°C, 155°C and 160°C.

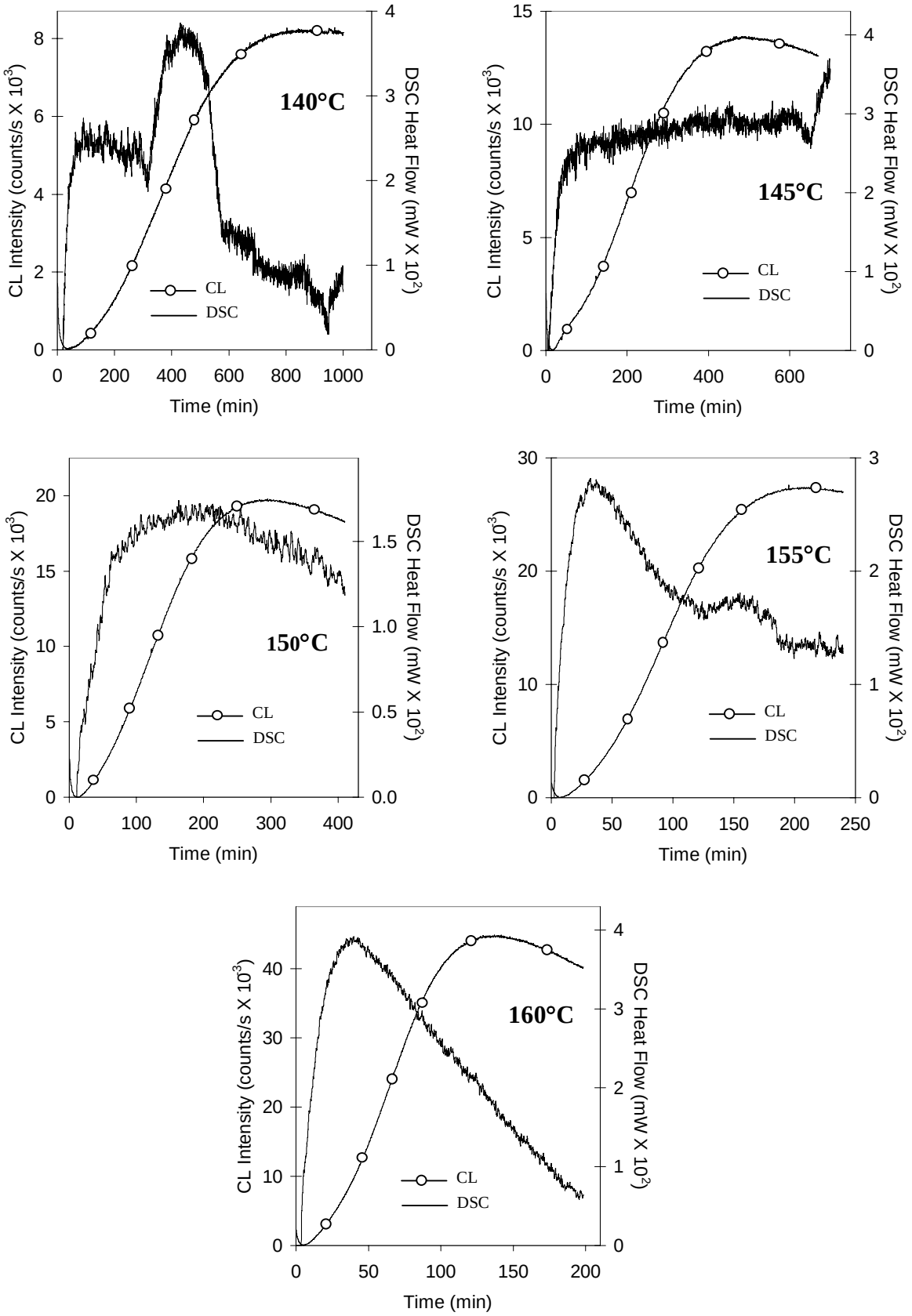

Figure 4.5: Simultaneous CL/DSC of methyl terminated PA-6 under oxygen at 140°C, 145°C, 150°C, 155°C and 160°C.

Table 4.1: Time to maximum for CL and DSC curves produced from the oxidation of PA-6 samples.

Sample	Temp. (°C)	CL t_{max} (min)	DSC t_{max} (min)	Difference (%)
COOH	140	176	33	81
	145	87	17	80
	150	58	16	72
	155	34	8.5	75
	160	21	6	71
NH_2	140	573	544	5.0
	145	476	463	2.8
	150	335	331	1.2
	155	195	192	1.8
	160	143	142	0.8
CH_3	140	858	-----	-----
	145	489	-----	-----
	150	295	163	45
	155	207	35	83
	160	136	38	72

The maximum intensities of the CL and DSC curves for the methyl terminated sample occur at a much later time than those for the carboxylic terminated sample at the respective temperatures. However, the percent difference between the CL and DSC curves is approximately the same for the two different samples at the respective temperatures. At 155°C and 160°C the differences between the CL and DSC curves of the carboxylic terminated sample are 75% and 71% respectively, while the

relative differences for the methyl terminated sample are 83% and 72% respectively. This similarity of differences between the CL and DSC curves provides added support to the notion that both samples undergo the same mechanism of oxidation, suggested by the normalized plot (in reduced coordinates) of the CL data in Figure 4.2.

In stark contrast to the carboxylic terminated and methyl terminated samples, there is practically no difference between the CL and DSC curves of the amine terminated sample. For example, at 155°C and 160°C the differences are 1.8% and 0.8% respectively. This supports the proposal that amine end groups cause PA-6 to oxidize via a different mechanism (as discussed previously) to that of PA-6 terminating in either carboxylic or methyl groups.

4.4.2.1 Discussion of Difference Between CL and DSC Curves

When heat flow is plotted against CL intensity up to the heat flow maximum (Figure 4.6) it is apparent that direct proportionality between the two types of curves does not exist for any of the three different types of PA-6 samples. Even for the amine terminated sample, where for all purposes the two types of curves seemed to coincide, curvature is obvious when the two types of curves are plotted against each other. However, when the square of the heat flows are plotted against CL intensity (Figure 4.6) a linear relationship can be seen for all three types of samples. This suggests that the mechanisms resulting in heat flow and CL are connected for the same sample. It does not in any way suggest that the mechanisms between samples are the same.

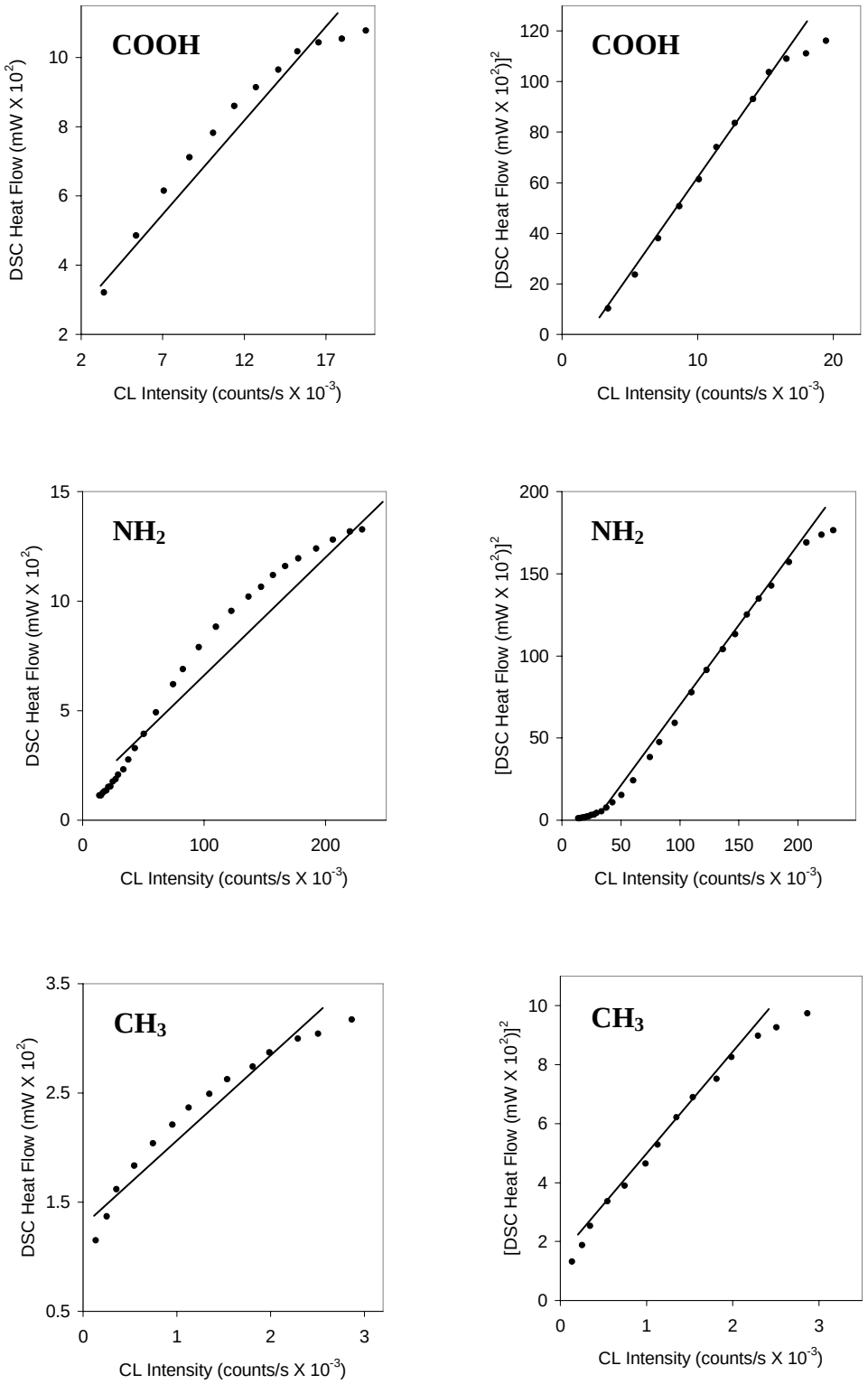

Figure 4.6: Plots of heat flows versus CL intensity and square of heat flows versus CL intensity for carboxylic, amine and methyl terminated PA-6 samples oxidized at 150C under an oxygen atmosphere.

A DSC heat flow curve gives the instantaneous rate of oxidation ($d[O_2]/dt$) and so it is proportional to [ROOH]. From Figure 4.4 we see that the CL intensity curves and the DSC heat flow curves coincide for amine terminated PA-6 samples. Therefore, when amine end groups are present:

$$I_{CL} \approx d[O_2]/dt \approx k''[ROOH]$$

From section 2.2.1.3 the CIEEL mechanism proposes that:

$$I_{CL} = k[ROOH][A] \approx k''[ROOH]$$

where A is an easily oxidized functional group present in excess.

Thus in the case of amine terminated PA-6 the CIEEL mechanism occurs directly and the CL profile is that of [ROOH] versus time. The amine groups are in excess so they function as 'A' in the CIEEL mechanism.

Figures 4.3 and 4.5 show that the CL intensity curves and the DSC heat flow curves do not coincide for carboxylic or methyl terminated PA-6 samples. Therefore, when amine groups are absent:

$$I_{CL} \neq d[O_2]/dt$$

However, Figure 4.7 illustrates that for carboxylic terminated PA-6 the DSC curve is equivalent to the first derivative of the CL intensity curve. Therefore, when amine groups are absent:

$$dI_{CL}/dt \approx d[O_2]/dt \approx k''[ROOH]$$

Consequently, in the absence of amine end groups, the CIEEL mechanism cannot operate until an easily oxidisable luminescent oxidation product is formed. In such a case:

$$I_{CL} = k[C{=}O] = \int_0^t [ROOH]dt$$

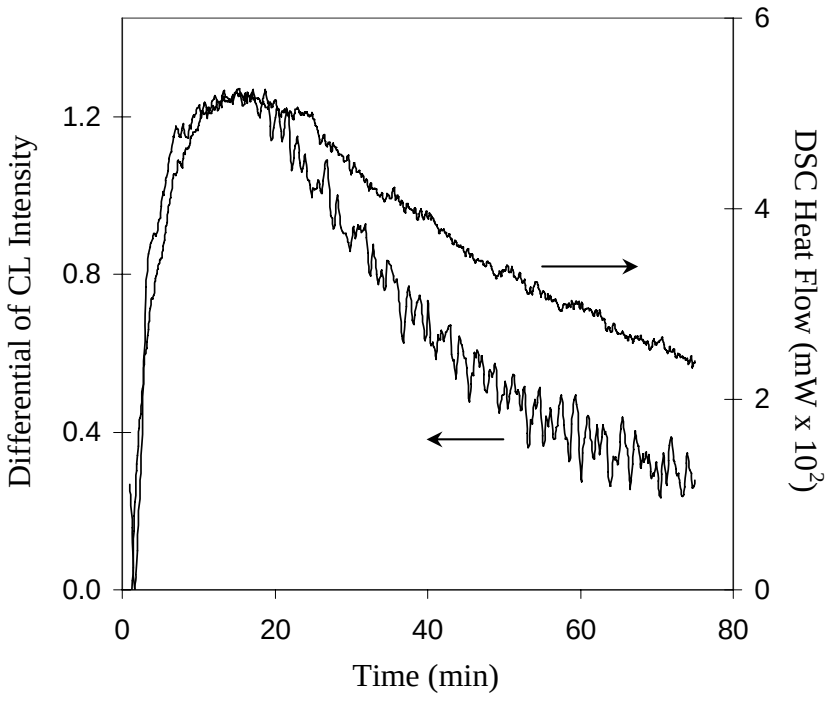

Figure 4.7: Comparison of the DSC heat flow curve and the first derivative of the CL intensity curve obtained simultaneously from a carboxylic terminated PA-6 sample oxidized at 150°C

It should be noted that for amine terminated PA-6 the first derivative of the CL intensity curve does not coincide with the DSC heat flow curve (Figure 4.8).

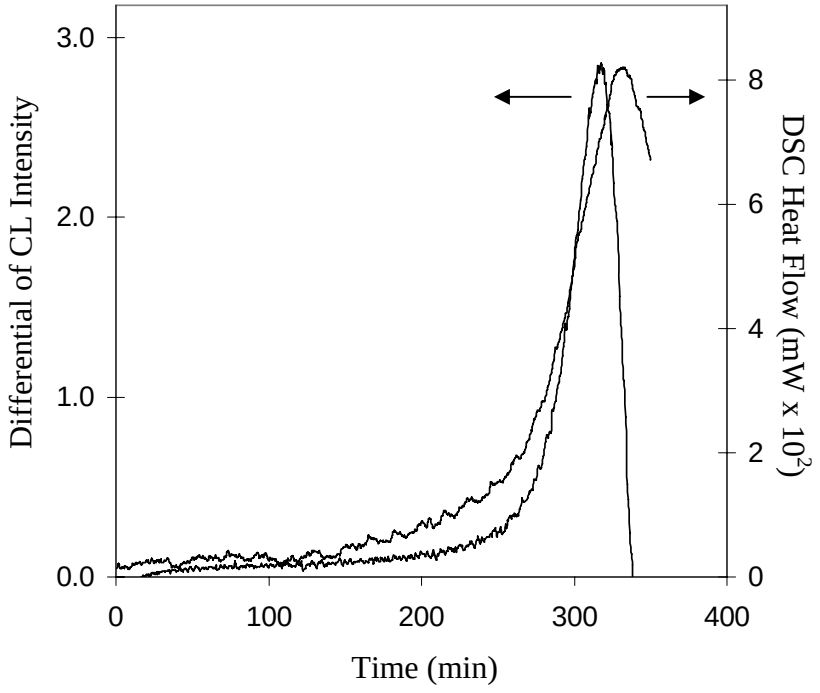

Figure 4.8: Comparison of the DSC heat flow curve and the first derivative of the CL intensity curve obtained simultaneously from an amine terminated PA-6 sample oxidized at 150°C

4.5 Conclusions

The differences in the oxidative mechanisms and stabilities, as a result of the end groups, for PA-6 were made obvious by a comparison of CL curves obtained at 150°C.

Both the CL and heat flow curves had the same basic shape for only amine end groups. In the case of amine terminated PA-6 samples the CL intensity was proportional to the heat flow curve. For PA-6 samples terminating in end groups other than amine end groups, the time to maximum intensity for the two types of curves differed by approximately 70% to 80%. When amine end groups were absent it was the first derivative of the CL intensity that was proportional to the heat flow curve. Thus in the case of amine terminated PA-6 a CIEEL mechanism occurs directly and the CL profile is that of [ROOH] versus time. While, in the absence of amine end groups, the CIEEL mechanism cannot operate until an easily oxidisable luminescent oxidation product is formed.

4.6 References

(1) Wendlandt, W., *Thermal Methods of Analysis*, 3rd Ed., John Wiley, New York, 1986.

(2) Hohne, G. W. H.; Hemminger, W.; Flammershein, H. J., *Differential Scanning Calorimetry an Introduction for Practitioners*, 1st Ed., Springer, Berlin, 1996.

(3) Billingham, N. C.; Bott, D. C.; Manke, A. S., *Developments in Polymer Degradation - 3*, Grassie, N. (ed), Applied Science Publishers, London, 1981.

(4) Blakey, I.; George, G. A., *Macromolecules*, **34** (2001) 1873.

(5) Karstens, T.; Rossbach, V., *Makromol. Chem.*, **190** (1989) 3033.

(6) Zimmerman, J., *Polyamides*, Kroschwitz, J. I. (ed), Wiley, New York, 1990.

(7) Marechal, P.; Legras, R.; Dekoninck, J. M., *J. Polym. Sci., Part A: Polym. Chem.*, **31** (1993) 2057.

(8) Gijsman, P.; Tummers, D.; Janssen, K., *Polym. Degrad. Stab.*, **49** (1995) 121.

(9) Lanska, B., *Polym. Degrad. Stab.*, **53** (1996) 89.

(10) Lanska, B., *Eur. Polym. J.*, **30** (1994) 197.

(11) Lanska, B.; Matisova-Rychla, L.; Brozek, J.; Rychly, J., *Polym. Degrad. Stab.*, **66** (1999) 433.

(12) Matisova-Rychla, L.; Lanska, B.; Rychly, J.; Billingham, N. C., *Polym. Degrad. Stab.*, **43** (1994) 131.

(13) Allen, N. S.; Harrison, M. J.; Follows, G. W.; Matthews, V., *Polym. Degrad. Stab.*, **19** (1987) 77.

(14) Pavlov, N. N.; Kudryavtseva, G. A.; Abramova, I. M.; Vasil'eva, V. A.; Zezina, L. A.; Kazaryan, L. G., *Polym. Degrad. Stab.*, **24** (1989) 389.

(15) Reimschuessel, H. K.; Dege, G. J., *J. Polym. Sci., Part A-1*, **8** (1970) 3265.

(16) Lanska, B.; Doskocilova, D.; Matisova-Rychla, L.; Puffr, R.; Rychly, J., *Polym. Degrad. Stab.*, **63** (1999) 469.

(17) Allen, N. S., *Chem. Soc. Revs.*, **15** (1986) 373.

(18) Levchik, S. V.; Weil, E. D.; Lewin, M., *Polym. Int.*, **48** (1999) 532.

(19) Rossbach, V.; Karstens, T., *Chemiefasern/Textilind.*, **40** (1990) E44.

(20) George, G. A., *Polym. Degradation Stab.*, **1** (1979) 217.

(21) Matisova-Rychla, L.; Rychly, J.; Tiemblo, P.; Gomez-Elvira, J.M.; Elvira, M., *Macromol. Symp.*, **214** (2004) 261.

(22) Lanska, B.; Matisova-Rychla, L.; Rychly, J., *Polym. Degradation Stab.*, **61** (1998) 119.

(23) Lanska, B.; Matisova-Rychla, L.; Rychly, J., *Polym. Degradation Stab.*, **72** (2001) 249.

(24) Matisova-Rychla, L.; Rychly, J., *J. Polym. Sci., Part A*, **42** (2004) 648.

(25) Cerruti, P.; Rychly, J.; Matisova-Rychla, L.; Carfagna, C., *Polym. Deg. Stab.*, **84** (2004) 199.

(26) Matisova-Rychla, L.; Lanska, B.; Rychly, J., *Ang. Makromol. Chem.*, 216 (2003) 169.

5. CL Imaging

5.1 Abstract

CL Imaging was used to map the occurrence and extent of oxidation across samples of PA-6 (which terminate in predominantly carboxylic, amine or methyl end groups respectively) to display the influence end groups have on the homogeneous or heterogeneous nature of PA-6 oxidation. CL images were also obtained from samples deliberately doped with adipic acid (chosen because of the known effect of the carboxylic acid end groups on the oxidation rate). The contaminating adipic acid was added to produce an exaggerated zone for initiation of oxidation.

5.2 Introduction

The oxidation of polyolefins has been shown to progressively spread across the polymer like an infection through a population. The initiation sites are clusters of hydroperoxides which are generated by the redox reaction of residual Ziegler Natta catalyst. The catalyst generates a mobile species, possibly the hydroperoxy radical, that is responsible for spreading the infection.[1-4]

PA-6 is a condensation polymer that has none of the features of polyolefins except that it too is oxidatively unstable. It does not contain the obvious impurities that cause the heterogeneous oxidation in polyolefins.[5,6] However the end groups in PA-6 could be considered to be impurities, as chapter 4 illustrated that end groups have a significant effect on the thermo-oxidation of PA-6. Carboxylic end groups were shown to greatly increase the rate of oxidation, while amine end groups acted to stabilize the polymer against oxidation. These observations support the literature sited in section 1.3.3. Therefore, the carboxylic groups possibly act in an analogous fashion to the impurities in polypropylene that cause heterogeneous oxidation. The polymer in the direct vicinity of the amine end groups would be less likely to undergo oxidation than polymer that does not have the stabilizing effect of the amine end group. PA-6 end groups could also coalesce to form discrete zones of impurities within the polymer.

A study by Cerruti *et al*[17] used adipic acid to exaggerate the effect of carboxylic end groups on the oxidation of a model diamide. Via CL curves they were able to show

the addition of adipic acid (i.e. an increase in carboxylic endgroups) shortened the oxidation induction time of the model diamide.

CL Imaging is a technique that has been used to spatially study the oxidation and the oxidative spreading of polymers. Fleming and Craig[7] conducted the first CL Imaging study of polymer oxidation with an investigation into the lateral variation of CL due to micro-crack formation in pre-aged hydroxyl terminated polybutadiene. They found a different temperature dependence of the CL from the preoxidized surface compared to the regions of the newly formed cracks. Early CL imaging studies also investigated the concentration gradients of antioxidants in thermally aged elastomers[8] and the spectral resolution from luminescent materials[9]. Increased CL intensity was also observed around a stressed part of a PA-6 sample when a uniaxial strain was applied at room temperature.[10]

Lacey and Dudler were the first to simultaneously measure the induction time of differently stabilized PP films.[11] They also demonstrated, via CL Imaging, that oxidation can spread through polypropylene film.[12] This was achieved by placing an unstabilized film on the edge of a thin strip of stabilized film. The oxidation was perceived to spread down the film of oxidized polymer as the anti-oxidant was consumed.

Through CL Imaging, oxidation has been shown to spread through the gas phase from polymer particle to polymer particle[13,14] and oxidation was seen to spread from an initially oxidized region of a polymer to the remainder of the polymer with time[13]. The oxidation profiles for a sample of PA-6,6 were estimated by Ahlblad et al[15].

Recently, CL Imaging experiments were conducted on unstabilized and stabilized samples of PA-6.[16] Each sample contained approximately 350 mmol kg^{-1} of carboxylic end groups and 130 mmol kg^{-1} of amine end groups. The CL intensity was found to be virtually homogeneous across the surface of all samples at all aging times.

This study used CL Imaging to map the occurrence and extent of oxidation across samples of PA-6 (which terminate in predominantly carboxylic, amine or methyl end groups respectively) to display the influence end groups have on the homogeneous or heterogeneous nature of PA-6 oxidation. CL images were also obtained from samples deliberately doped with adipic acid (chosen because of the known effect of the carboxylic acid end groups on the oxidation rate). The contaminating adipic acid was added to produce an exaggerated zone for initiation of oxidation.

5.3 Experimental

5.3.1 Materials

Three distinct PA-6 samples terminating predominantly in carboxylic, amine or methyl groups respectively were used. The synthesis and characterization of the samples are discussed in chapter 3.

5.3.2 Preparation of Films

PA-6 films were hot pressed from powder at 130°C under 25 ton using a 100 μm thick mold. The desired section of film was obtained from the middle of the pressed film with a scalpel. The films were 100 ± 10 μm thick.

5.3.3 CL Imaging

The PA-6 film was inserted into the sample chamber on an aluminium pan. The chamber was flushed with nitrogen for 30 mins before the sample was heated to 215°C to soften and adhere it to the aluminium pan. The temperature of the chamber and sample was then lowered to the oxidation temperature of 150°C while still under a nitrogen atmosphere. Once the temperature had stabilized the gas was switched to oxygen with a flow rate of 50 mL/min. The light emitted during oxidation was measured by a CCD camera, which produced images of the CL intensity distribution. The CL Images were integrated over 4 minute intervals.

5.4 Results and Discussion

It was very important to preheat the sample and ensure the entire film was in contact with the aluminium pan in order to achieve an even temperature profile. If the film was not preheated the corners and sides of the film would curl away from the

aluminium pan and result in temperature gradients, which led to the observation of uneven oxidation in the CL images.

5.4.1 Uncontaminated Films

If carboxylic end groups do act in an analogous fashion to the impurities in polypropylene that cause heterogeneous oxidation then the CL images of the carboxylic terminated sample should display hot spots of oxidation very early on. Oxidation should then be observed to spread from the hot spots to the remainder of the sample. The opposite would be expected for the amine terminated sample. As oxidation proceeds, spots of low intensity should be detected where the amine groups are positioned relative to the rest of the film. Unlike the carboxylic and amine terminated samples, which are expected to lead to heterogeneous oxidation, the methyl terminated sample would be expected to result in homogeneous oxidation as no significant contribution towards oxidation come from the methyl end groups.

Figures 5.1, 5.2 and 5.3 display CL images obtained during the oxidation of the carboxylic, amine and methyl terminated samples respectively. The nature of oxidation appears to be homogeneous for each sample, as the CL intensity essentially increases uniformly across all samples.

The results in Figures 5.1 and 5.2 do not necessarily imply that the oxidation of carboxylic or amine terminated PA-6 does not take place heterogeneously with respect to the end groups. It is highly likely that, even if the end groups do coalesce,

there are sufficient end groups to be dispersed across all pixels of the CCD camera. The area contributing to the CL intensity of each pixel would then be oxidizing heterogeneously but the CL intensity recorded by the pixel would show that whole area of polymer to be undergoing a certain level of homogeneous oxidation. Therefore, the scale of heterogeneity resulting from the end groups could be smaller than what is possible to be spatially measured by the pixels of the CCD camera.

Even if the scale of heterogeneity were large enough to be measured by the CCD camera the chances of observing heterogeneous oxidation are reduced due to the large thickness of the films. The number of domains that the detector can observe increases with increasing thickness. Therefore, heterogeneous oxidation might be occurring but that fact may be obscured for thicker films.

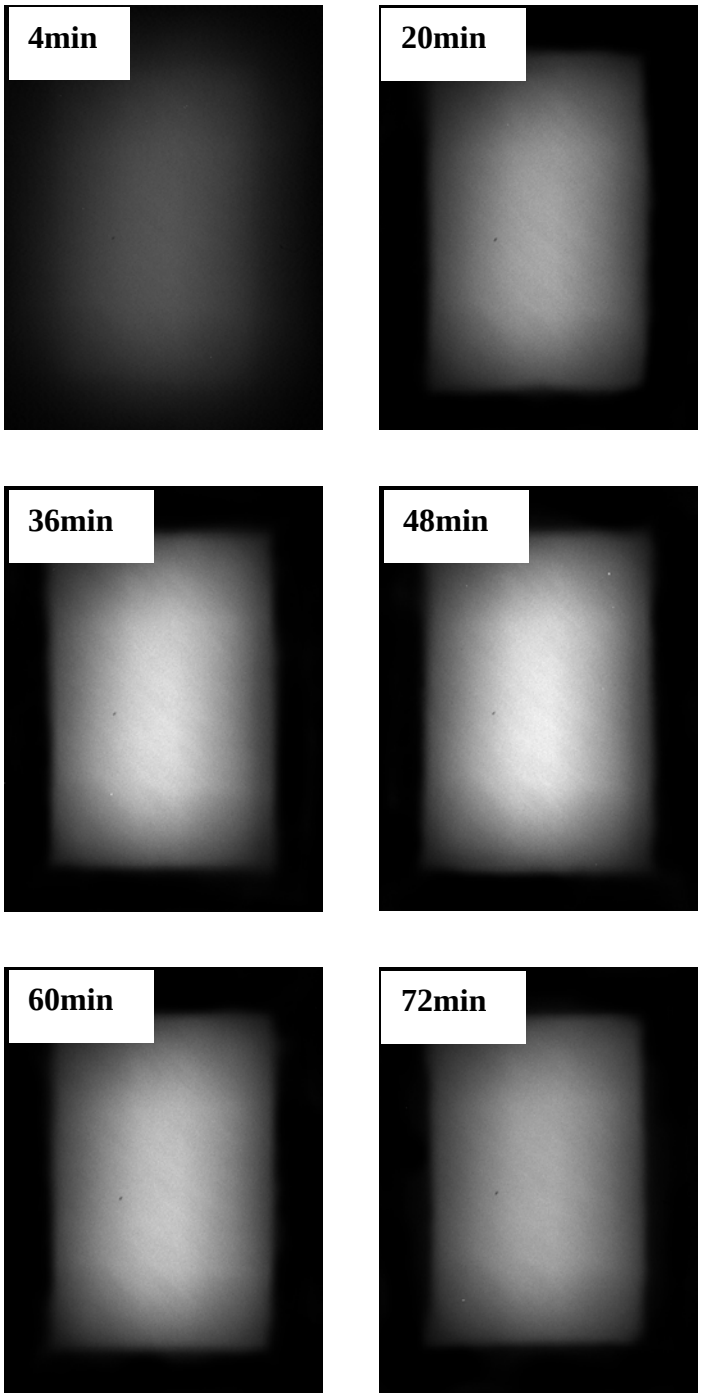

Figure 5.1: CL Images during the oxidation of carboxylic terminated PA-6 at 150°C with an oxygen flow rate of 50 mL/min.

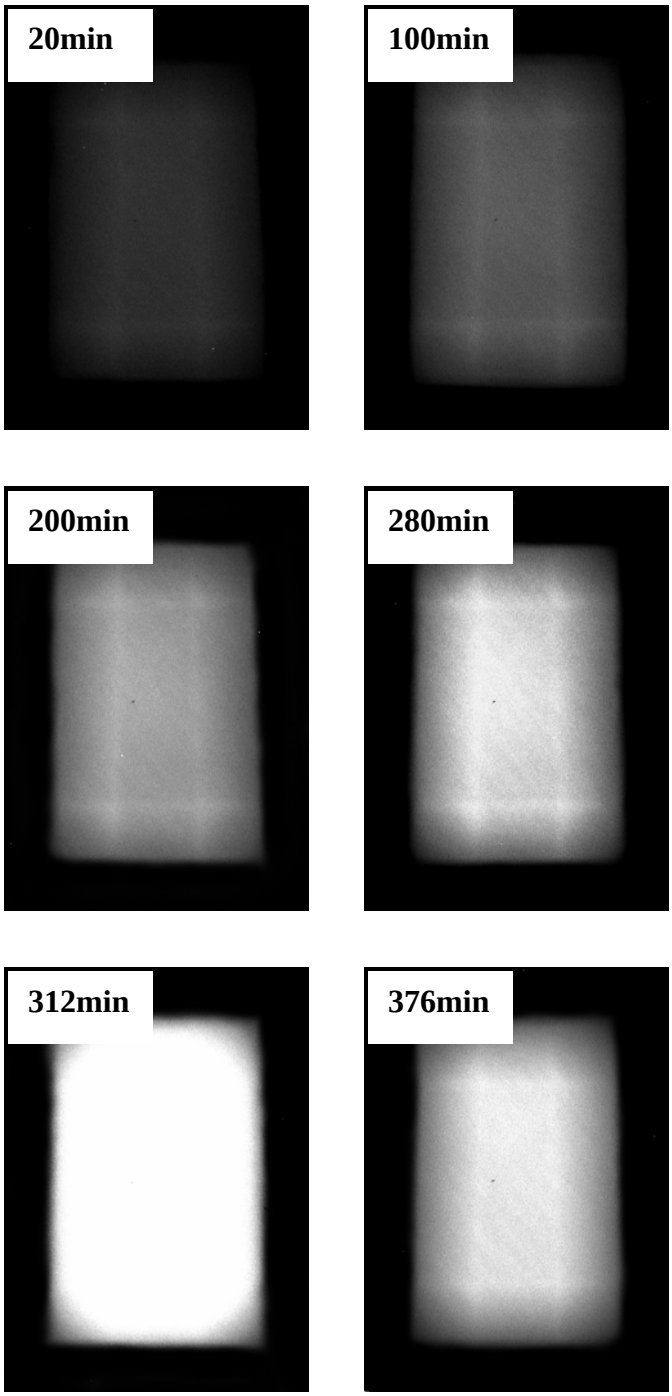

Figure 5.2: CL Images during the oxidation of amine terminated PA-6 at 150°C with an oxygen flow rate of 50 mL/min.

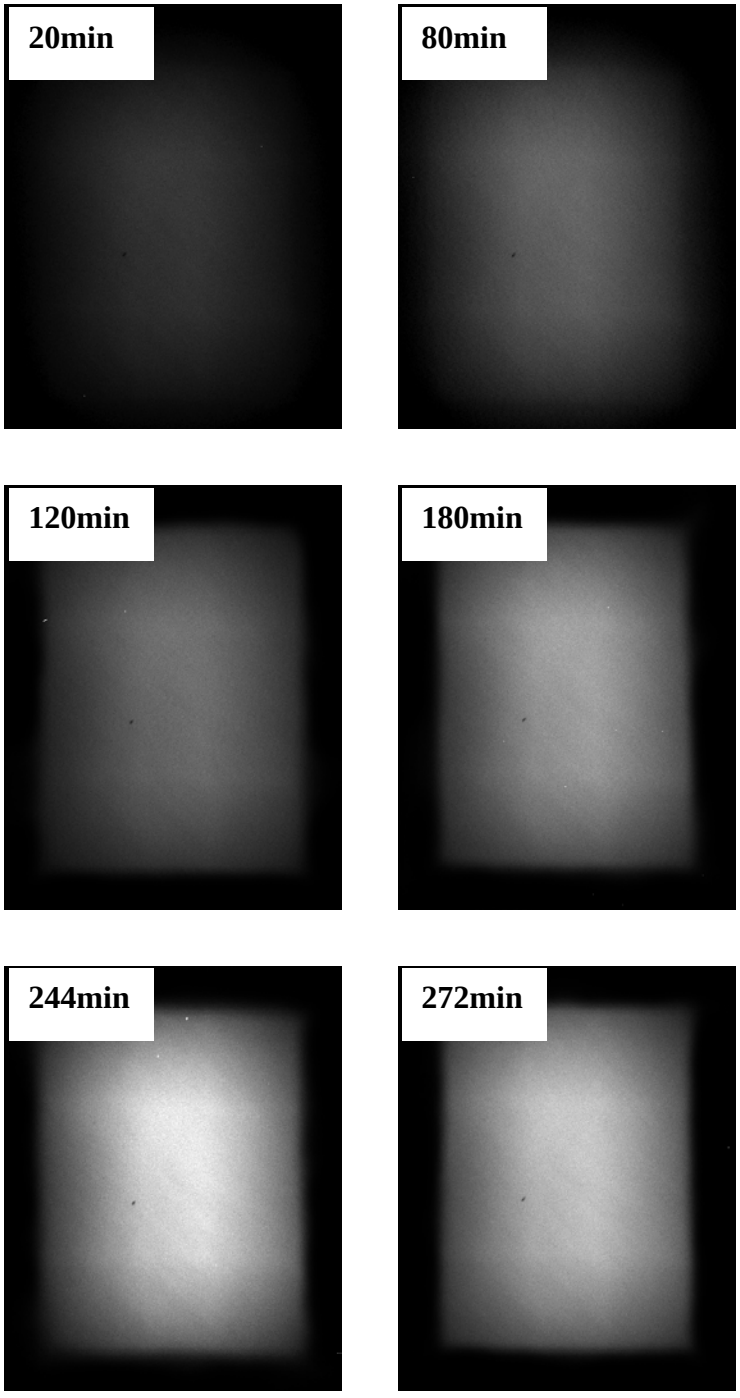

Figure 5.3: CL Images during the oxidation of methyl terminated PA-6 at 150°C with an oxygen flow rate of 50 mL/min.

5.4.2 Doped Films

The previous section illustrated that the scale of oxidative heterogeneity caused by the end groups in PA-6 is likely to be less than can be monitored by CL Imaging. The initiating zone that might be caused by carboxylic end groups needs to be exaggerated to a size greater than the resolution of the instrument. To achieve this each film of PA-6 that terminated in a different end group was doped with a small granule of adipic acid. CL images obtained during the oxidation of carboxylic, amine and methyl terminated PA-6 samples doped with adipic acid are displayed in Figures 5.4, 5.5 and 5.6 respectively.

The CL intensity for the carboxylic terminated PA-6 sample increases uniformly across the film with no sign of increased oxidation around the position of the adipic acid. The maximum rate of oxidation for the doped carboxylic terminated film occurred at approximately the same time as the uncontaminated film, indicating that the adipic acid had little or no effect on the oxidation of that sample. However, the CL images obtained during the oxidation of doped amine and methyl terminated samples clearly show that hot spots of oxidation occur where the adipic acid had been placed. These hot spots occur almost from the start of oxidation. The intensity of the hot spot intensifies considerably above the level of intensity emitted by the remainder of the film. Oxidation can be seen to spread from the doped zone through the remainder of the film. In one of the images a high rate of oxidation can be observed across both films. The oxidation is then perceived to recede from the area of the initial hot spot up to the other end of the films.

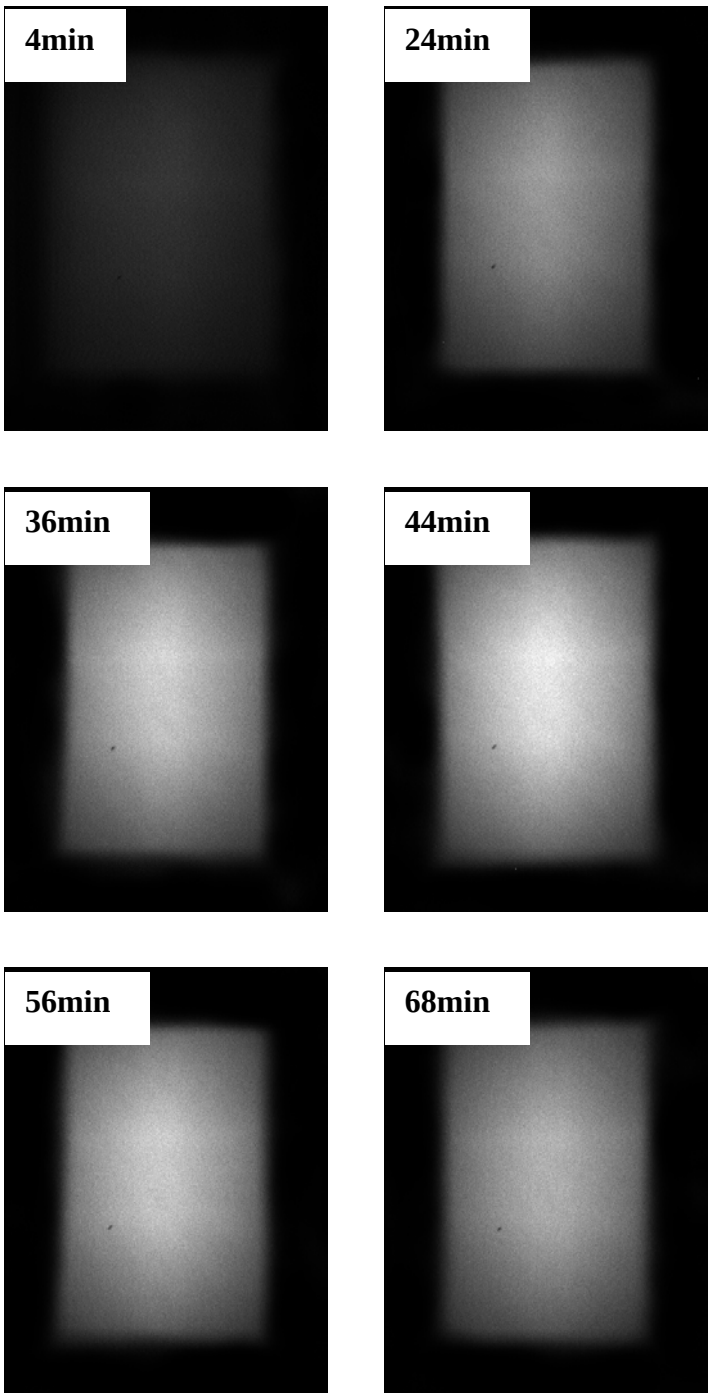

Figure 5.4: CL Images during the oxidation of carboxylic terminated PA-6 contaminated with adipic acid at 150°C with an oxygen flow rate of 50 mL/min.

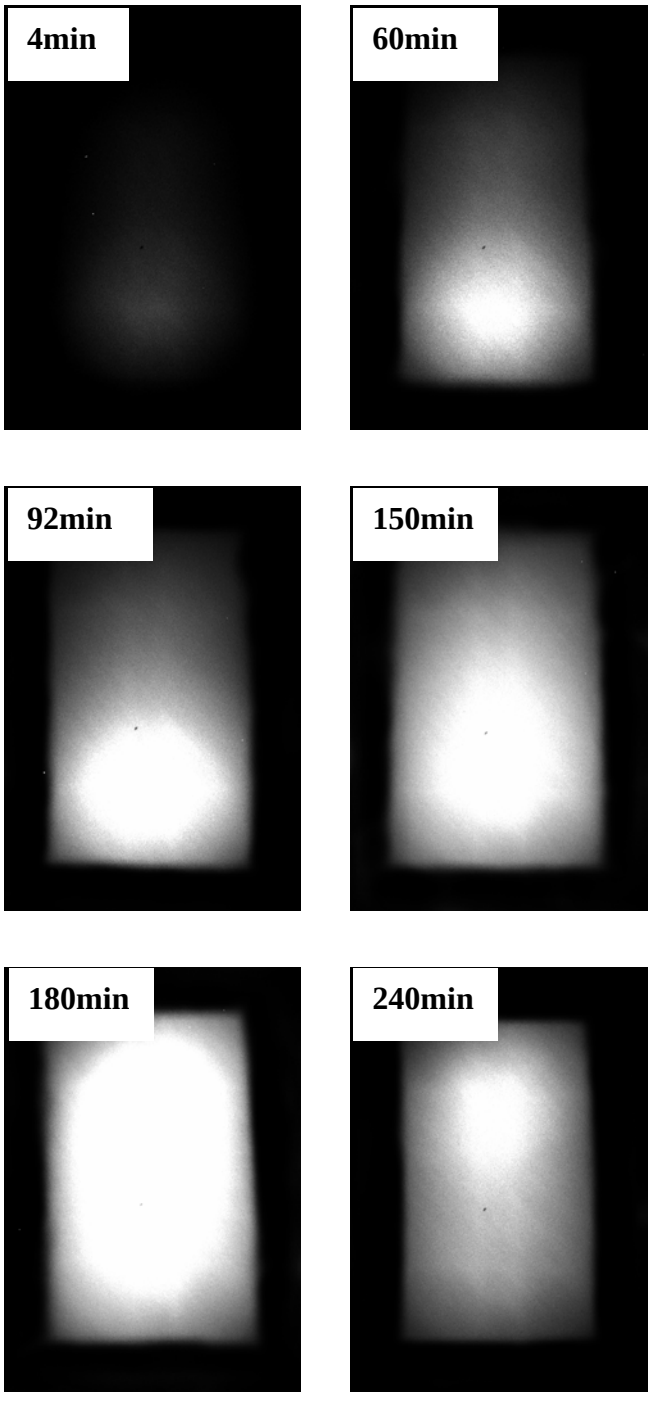

Figure 5.5: CL Images during the oxidation of amine terminated PA-6 contaminated with adipic acid at 150°C with an oxygen flow rate of 50 mL/min.

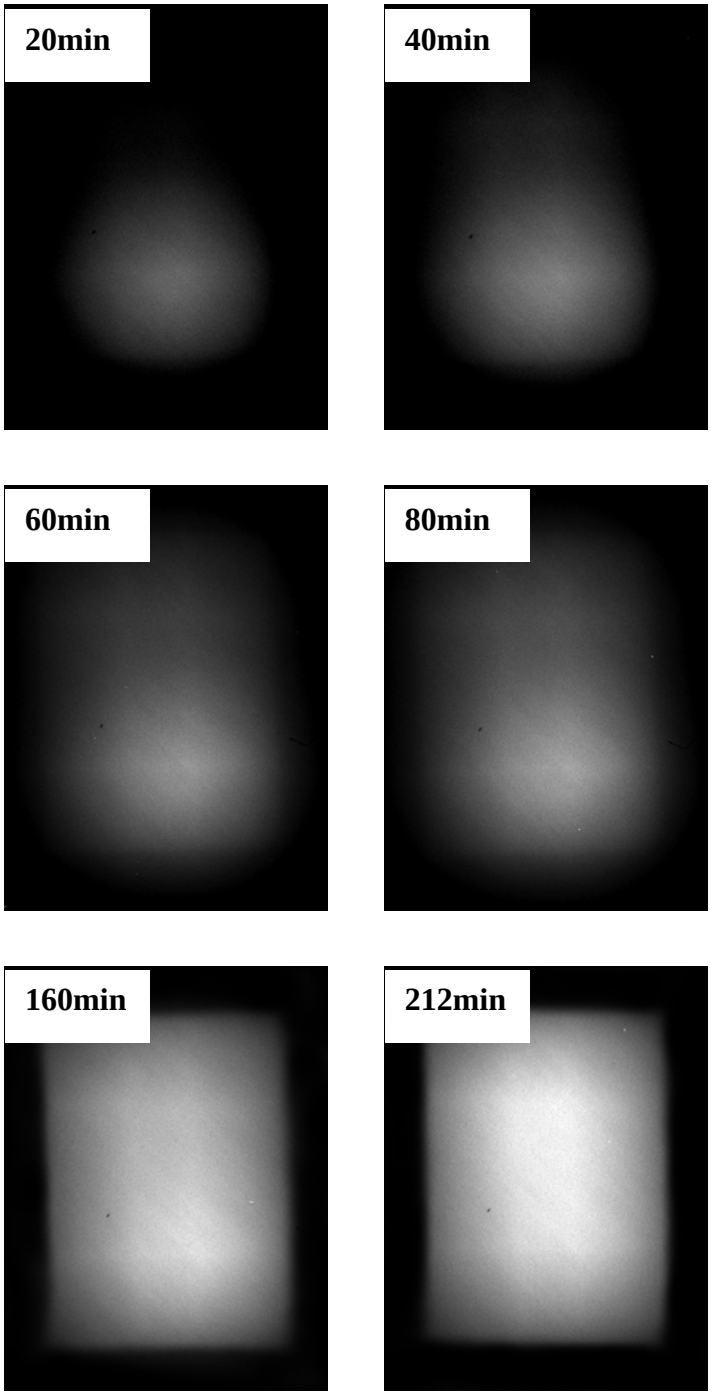

Figure 5.6: CL Images during the oxidation of methyl terminated PA-6 contaminated with adipic acid at 150°C with an oxygen flow rate of 50 mL/min.

A hot spot is not observed when the carboxylic terminated sample is doped with adipic acid because the concentration of carboxylic end groups within the PA-6 sample alone is sufficient to produce a comparable effect to the high concentration of adipic acid. The end groups are distributed such that the rate of oxidation across the sample appears homogeneous when monitored by CL Imaging.

The oxidation rates of uncontaminated amine and methyl terminated samples are relatively low for a long period of time when compared to the carboxylic terminated sample. This is because the amine end groups help to stabilize the polymer against oxidation and the methyl end groups play no part in the oxidation mechanism, while the carboxylic end groups increase the oxidation rate by catalyzing the decomposition of hydroperoxides.

When the adipic acid is placed on the films of the amine and methyl terminated samples it reacts with the amine end groups and therefore removes their capacity to stabilize against oxidation. Residual adipic acid, like the carboxylic end groups, catalyzes the decomposition of hydroperoxides in that area. The result is an increase in the rate of oxidation in the area of polymer that is in contact with the adipic acid. The oxidation hot spots are so active they are able to initiate oxidation in the neighboring polymer.

The rate at which oxidation is spread to the neighboring polymer far exceeds the rate at which the reminder of the polymer oxidizes. Therefore oxidation can be observed to spread from the hot spot through the entire film. The time at which the maximum rate of oxidation occurs across a contaminated film is significantly shorter than

observed for uncontaminated films. The observed spreading from the area of the amine and methyl terminated PA-6 samples in contact with the adipic acid implies that oxidation is initiated by carboxylic end groups and that oxidation does in fact spread from that initiating site.

The spreading of oxidation from the area of PA-6 doped with adipic acid can also be illustrated by the construction of line maps. As demonstrated in Figure 5.7, a line of pixels positioned through the center of the doped zone and across the entire length of the film was selected. The value of each pixel was related to the pixel's position in order to create the line maps.

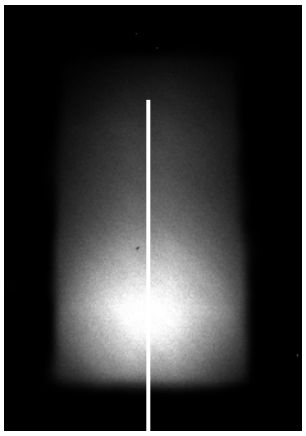

Figure 5.7: Illustration for the selection of pixels that contribute to the construction of line maps.

Line maps for the amine terminated and methyl terminated PA-6 films doped with adipic acid are displayed in Figures 5.8 and 5.9 respectively. Each line map corresponds to an image in either Figure 5.5 or 5.6. In both cases bright emission is observed slightly below 400 units on the pixel position axis early in the oxidation of

the films. As oxidation proceeds the intensity at that position increases. The width of the peak at this position also increases with oxidation time.

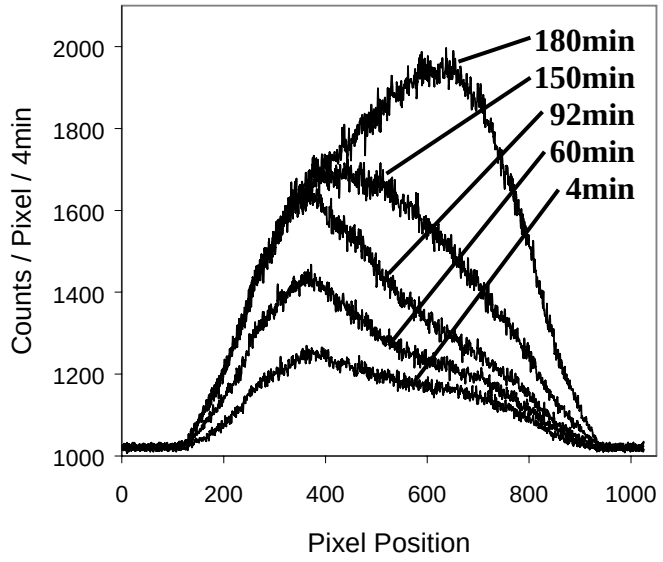

Figure 5.8: Line maps indicating the shift of light emission with oxidation time across an amine terminated PA-6 film doped with adipic acid.

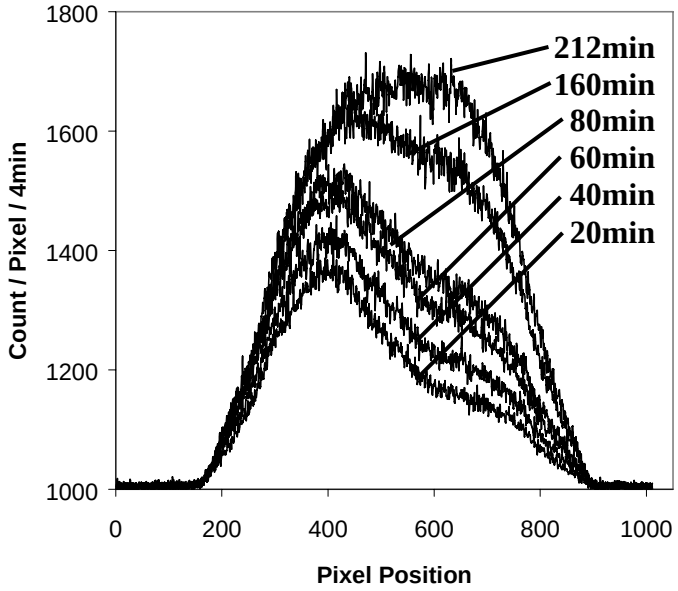

Figure 5.9: Line maps indicating the shift of light emission with oxidation time across a methyl terminated PA-6 film doped with adipic acid.

The increasing width of the peaks in figures 5.8 and 5.9 could be a measure of the oxidation front moving across the film. However, Figures 5.1 to 5.3 illustrate that some level of oxidation occurs almost as soon as oxygen is admitted to non-doped PA-6 films. This level continues to increase with time. It is possible to plot this oxidation front by noting, from the line maps the change in slope which corresponds to the boundary between the bright CL emission and the background emission. In this sample the front progresses at 0.14 μm/s which may be compared with Dudlers study of stabilized PP film where it varied from 0.17 to 0.56 μm/s depending on the type of stabilizer.[12]

5.5 Conclusions

CL images obtained at various oxidation times from PA-6 films indicate that the nature of oxidation for PA-6 was homogeneous regardless of the type of end group present in the polymer. When films of carboxylic terminated PA-6 were doped with adipic acid the oxidation again appeared to be homogeneous. However heterogeneous oxidation occurs when films of amine and methyl terminated PA-6 are doped with adipic acid. The initial zone of oxidation resulting from the contact with adipic acid is so active that the oxidation spreads from that area to the remainder of the polymer. Therefore, certain end groups can be said to cause PA-6 to undergo heterogeneous oxidation. The distribution of the end groups within the film make the scale of oxidative heterogeneity in the uncontaminated films smaller than the resolution of the CCD camera.

5.6 References

(1) George, G. A.; Celina, M., *Homogeneous and Heterogeneous Oxidation of Polypropylene in Handbook of Polymer Degradation*, Halim Hamid, S. (ed), Marcel Dekker, New York, 2000.

(2) Blakey, I.; George, G. A., *Polym. Deg. Stab.*, **70** (2000) 269.

(3) Blakey, I.; George, G. A., *Macromolecules*, **34** (2001) 1873.

(4) Goss, B.; Barry, M. D.; Birtwhistle, D.; George, G. A., *Polym. Deg. Stab.*, **72** (2001) 271.

(5) Kroschwitz, J. I.; Howe-Grant, M., *Kirk-Othmer, Encyclopedia of Chemical Technology, 4th Ed.*, John Wiley & Sons, Inc., Brisbane, 1996.

(6) Zimmerman, J., *Polyamides*, Kroschwitz, J. I. (ed), Wiley, New York, 1990.

(7) Fleming, R. H.; Craig, A. Y., *Polym. Deg. Stab.*, **37** (1992) 173.

(8) Mattson, B.; Kron, A.; Reitberger, T.; Craig, A.; Fleming, R., *Polymer Testing*, **11** (1992) 357.

(9) Mendenhall, G. D.; Fleming, R. H., *Rev. Sci. Instrum.*, **64** (1993) 3425.

(10) Hosoda, S.; Seki, Y.; Kihara, H., *Polymer*, **34** (1993) 4602.

(11) Lacey, D.; Dudler, V., *Polym. Deg. Stab.*, **51** (1996) 115.

(12) Lacey, D.; Dudler, V., *Polym. Deg. Stab.*, **51** (1996) 101.

(13) Celina, M.; George, G. A.; Lacey, D. J.; Billingham, N. C., *Polym. Deg. Stab.*, **47** (1995) 311.

(14) Ahlblad, G.; Reitberger, T.; Terselius, B.; Sternberg, B., *Polym. Deg. Stab.*, **65** (1999)

(15) Ahlblad, G.; Forsstroem, D.; Stenberg, B.; Terselius, B.; Reitberger, T.; Svensson, L.-G., *Polym. Degrad. Stab.*, **55** (1997) 287.

(16) Forsstrom, D.; Reitberger, T.; Terselius, B., *Polym. Degrad. Stab.*, **67** (2000) 255.

(17) Cerruti, P.; Carfagna, C.; Rychly, J.; Matisova-Rychla, L., *Polym. Deg. Stab.*, **82** (2003) 477.

6. FTIR Emission

6.1 Abstract

The effect of end groups on the thermo-oxidative degradation of PA-6 under an oxygen atmosphere at a temperature of 150°C was investigated, in situ, by infrared emission spectroscopy (FTIES). The PA-6 samples studied terminated predominantly in carboxylic, amine or methyl groups respectively. Sequences of FTIES spectra collected at specified time intervals during the course of PA-6 oxidation were turned into oxidation product profiles. The differences between spectra related to significant points on the oxidation profiles were compared in an attempt to elucidate the chemical or physical changes occurring in the samples during oxidation.

6.2 Introduction

FTIR emission spectroscopy (FTIES) is a sensitive technique where the infrared radiation emitted from heated materials is directly analyzed by an FTIR spectrometer.[1] The basic principles of FTIES are outlined in section 2.1. The fact that samples need to be heated for FTIES makes the technique ideal for the real time *in situ* analysis of polymer oxidation.

Only a relatively small amount of literature on the use of FTIES for studies on polymer degradation exists.[2-7] However, Celina et al[2] have recently displayed the ease at which spectroscopic information from a variety of samples undergoing degradation at elevated temperatures can be acquired by simply detecting the time dependant IR emission originating from samples as they degrade. George et al[3,4] have shown that it is possible, via FTIES, to obtain quantitative oxidation product profiles as a function of time.

The most significant FTIR studies on PA-6 degradation were conducted by Do et al[8]. They found that the application of thermal energy to PA-6 results in an increase in the number of non hydrogen-bonded amide groups (originally from the amorphous region). The crystallinity-sensitive ratio I_{930}/I_{1123}, where I_{930} and I_{1123} are the intensity of the bands representing the crystalline and amorphous phases respectively, increased due to annealing.

Their IR spectra also indicated that many different types of carboxylic groups were formed during oxidation. Svoboda et al[9] investigated the condensation products of thermal degradation of PA's by FTIR. They too found that crystallinity increased due to annealing however stated that prolongation of heating times led to the destruction of the macromolecules and formation of predominantly amorphous degradation products. Characterization of the degradation products suggested that both vinyl and nitrile end groups were present.

Chapters 4 and 5 illustrated that end groups have a significant effect on both the rate and heterogeneous nature of PA-6 thermo-oxidation. It is evident that so far nobody has performed a detailed FTIR analysis on the effect of end groups on the thermo-oxidation of PA's. It has been the aim of this study to determine by FTIES the behavior and structural changes of PA-6 that occur due to end groups during thermo-oxidation.

6.3 Experimental

6.3.1 Materials

Three distinct PA-6 samples terminating predominantly in carboxylic, amine or methyl groups respectively were used. The synthesis and characterization of the samples are discussed in chapter 3. TFE was purchased from Sigma Aldrich Australia and used as received. Each sample was prepared to a concentration of 10 mg/mL in TFE.

6.3.2 FTIES of PA-6 Samples

The FTIES instrument has been previously described.[5] Briefly, the FTIES consists of a BioRad FTIR spectrometer with an emission cell replacing the IR source. The emission cell consists of a platinum hotplate which has its temperature controlled by a Eurotherm temperature controller. Infrared radiation emitted from the hotplate is reflected onto an off axis ellipsoidal gold plated mirror into the spectrometer. A standard liquid nitrogen cooled MCT detector was used.

PA-6 films were formed on the platinum hotplate by applying 0.05mL of PA-6 solution to the hotplate and then heating the hotplate to 70°C under a nitrogen atmosphere to remove the TFE. FTIES spectra were collected in single beam mode and averaged over 32 scans with a resolution of 4 cm^{-1}. Sequences of spectra were collected at specified time intervals during the course of PA-6 oxidation at 150°C in an oxygen atmosphere with a flow rate of 0.2 L min^{-1}. The raw data of the FTIES was converted to an emissivity spectrum (the equivalent of an absorption spectrum) by subtraction of a platinum background and calculating the ratio of the result to a reference graphite spectrum minus the platinum background.

6.4 Results and Discussion

6.4.1 Comparison of Unaged PA-6 Samples

The IR spectra for the three different PA-6 samples, terminating predominantly in carboxylic, amine or methyl groups respectively, are displayed in figure 6.1. All three spectra were collected with the samples heated to 150°C under a nitrogen atmosphere. As expected, little difference can be observed between the IR spectrum of each sample because, as illustrated in Chapter 3, the three different types of PA-6 samples are very comparable with the only noticeable difference being that of their endgroups.

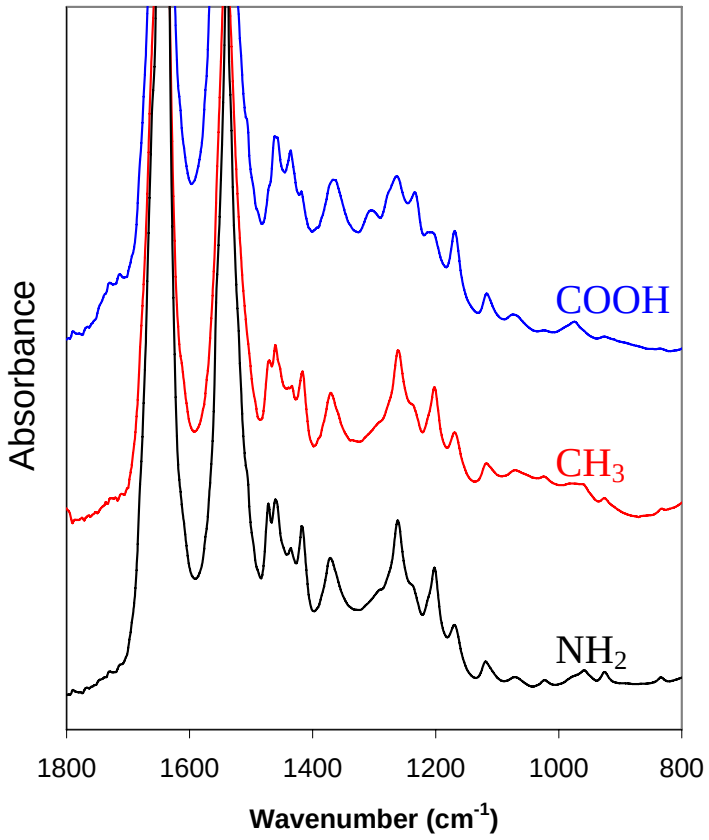

Figure 6.1: FTIES Spectra of PA-6 samples terminating predominantly in carboxylic, amine or methyl endgroups obtained at 150C under nitrogen.

An additional band due to carboxylic endgroups, can be seen from approximately 1700 to 1750 cm^{-1} in the spectrum of the carboxylic terminated sample which is not present in the spectra of the other two samples. This band is relatively broad as it consists of both free carboxylic end groups and carboxylic endgroups that have hydrogen bonded with amide groups in the macromolecules backbone. Although it is not clear in figure 6.1 the amide bands in the spectrum for the amine terminated sample are slightly more intense than observed for the other two samples. This is simply because of the extra number of free NH_2 groups.

Small discrepancies in peak ratios can be seen in the band of 1200-1500 cm^{-1} for the carboxylic terminated sample compared to the other two types of samples. However, figure 6.2 demonstrates that these peaks play no significant part in the oxidation of PA-6 in this study.

6.4.2 FTIES During Thermo-Oxidation of PA-6 Samples

A typical spectrum of an oxidised sample of PA-6 can be seen in figure 6.2 where a comparison is made between a sample of methyl terminated PA-6 before oxidation and after it had been oxidized for 300 minutes.

The most noticeable change in the spectrum caused by oxidation can be observed as an increase in the broad band of wavelengths between 1700-1800 cm^{-1}. This band represents an increase in carbonyl groups (aldehydes, ketones, carboxylic acids, *N*-

acylamides, and α,β-unsaturated carbonyl compounds) formed during the oxidation process.

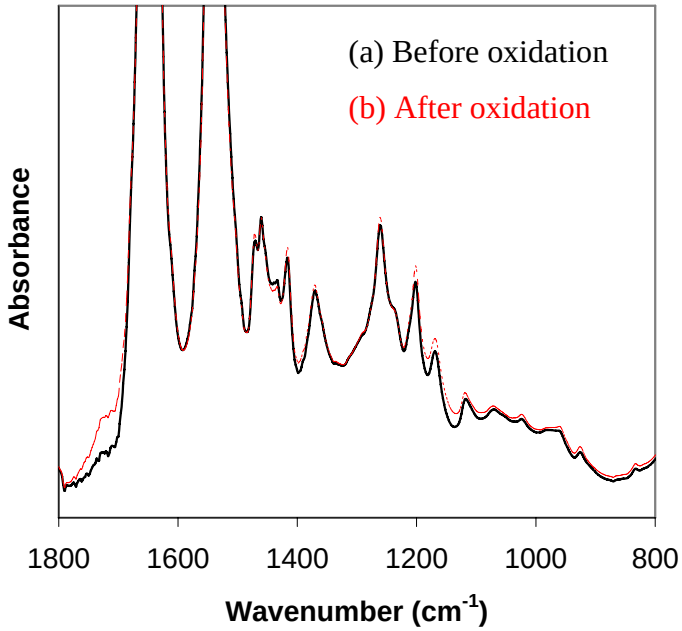

Figure 6.2: FTIES Spectra of amine terminated PA-6 samples (a) before oxidation and (b) after 300 minutes of oxidation at 150°C.

The peak at 1240 cm^{-1} remains relatively unchanged during oxidation and can therefore be used as an internal standard. Plotting the ratio of the area under the band from 1700–1800cm^{-1} to the area under the peak at 1240 cm^{-1} against time results in an oxidation product profile (figure 6.3).

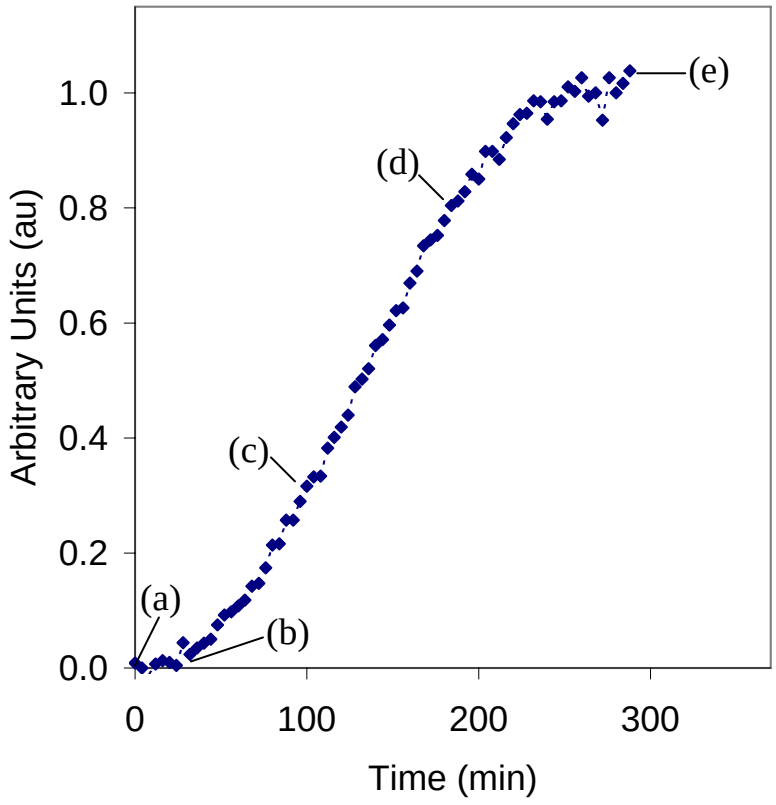

Figure 6.3: Oxidation product profile of amine terminated PA-6 oxidised at 150°C.

The shape of the oxidation product profile, which illustrates the build up of carbonyl groups, appears similar to the shape of the CL curve displayed in figure 4.1. Each point on the CL curve is related to the number of photons emitted during the oxidation of the sample, while each point of the oxidation product profile in figure 6.3 relates to an FTIES spectrum.

Therefore, in theory it should be possible to obtain more information from a point in figure 6.3 than from a point in the CL curve. For example, a comparison of spectra related to significant points on the oxidation profile should aid to elucidate the chemical or physical changes occurring in the sample during oxidation.

Figure 6.4 presents the difference spectra relating to the points (a) to (e) highlighted on the oxidation product profile in figure 6.3.

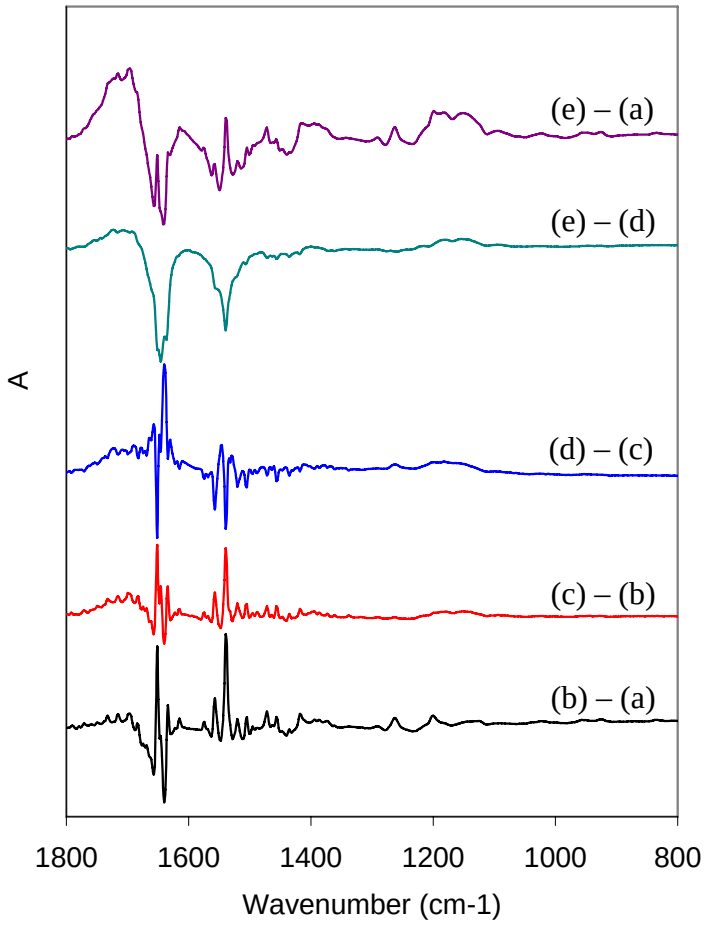

Figure 6.4: Changes in the FTIES spectrum during the oxidation at 150°C of an amine terminated sample of PA-6. Spectra (a) to (e) relate to the points highlighted in figure 6.3.

Until point (d) it appears the only significant changes in the spectra are due to peak shifts most likely caused by increased thermal energy and an increase in the carbonyl band between 1700-1800 cm^{-1}. From (d) to (e) there is a strong decrease in the amide bands and a further increase in the carbonyl group band. However, there are no other

changes to aid in the elucidation of the mechanism. This lack of information is prevalent in all samples of PA-6 tested regardless of endgroup type.

When comparing the oxidation product profiles constructed from FTIES spectra for PA-6 samples terminating in all three types of endgroups to the CL curves obtained at the same oxidation temperature for the respective endgroups we see the oxidation product profiles are proportional to the CL curves (figures 6.5 to 6.7).

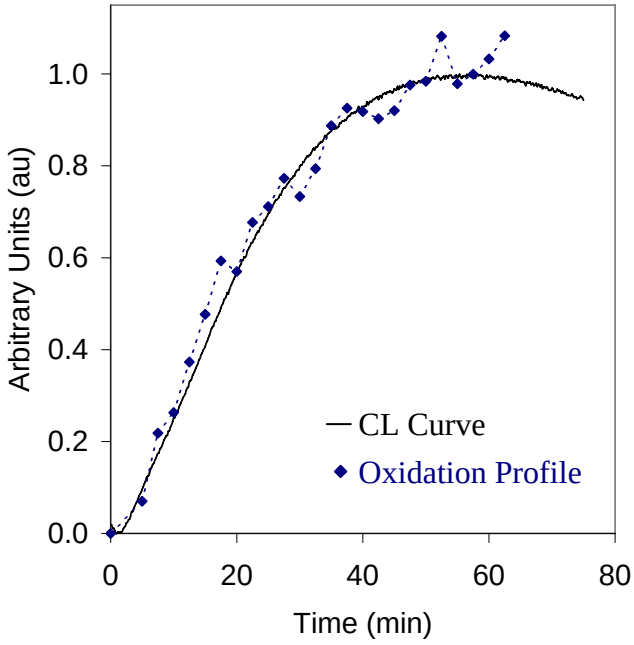

Figure 6.5: Comparison of oxidation product profile and CL intensity curve for carboxylic terminated PA-6 oxidised at 150°C.

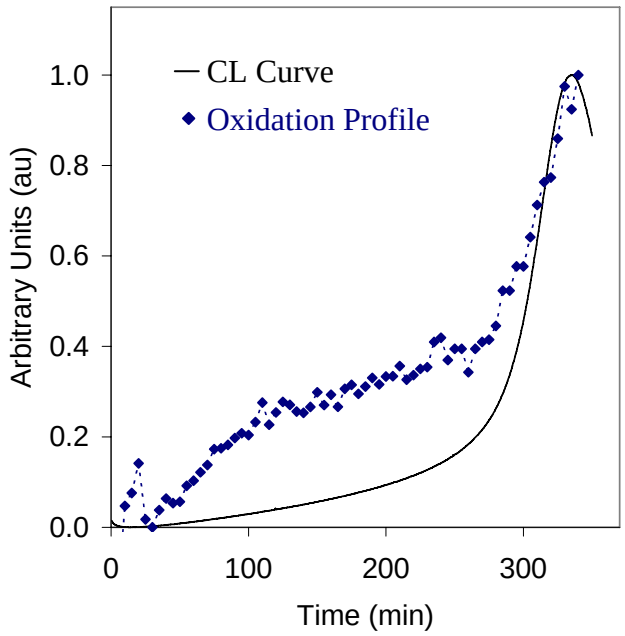

Figure 6.6: Comparison of oxidation product profile and CL intensity curve for amine terminated PA-6 oxidised at 150°C.

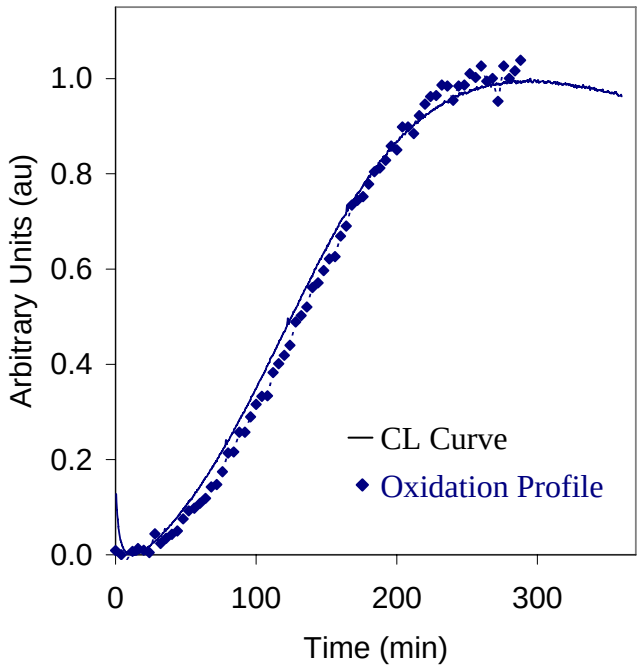

Figure 6.7: Comparison of oxidation product profile and CL intensity curve for methyl terminated PA-6 oxidised at 150°C.

It should be noted that some disagreement occurs between the curves over the first 100 minutes in figure 6.6. The initial shape of the oxidation curve is the opposite of what is expected. As illustrated in figures 1.6 and 1.13 the excess amine endgroups are predicted to react with and remove some of the oxidation products, which should be represented in the oxidation product profile as an almost zero gradient section of curve.

Blakey and George[4] showed via kinetic analysis that if classical mechanisms such as the Russell mechanism or bimolecular decomposition of peroxides (refer to figures 1.5 and 2.4) were to account for CL emission as is classically believed then the intensity of the CL curve should be proportional to the hydroperoxide concentration. They also showed via kinetic analysis that the concentration of carbonyls at any given time is proportional to the integral of the hydroperoxide concentration. This led them to hypothesize that the carbonyl growth curve should be proportional to the integral of the CL intensity vs time curve. However, their experimental results contradicted their hypothesis with the carbonyl growth curve being proportional to the CL intensity curve and not its integral.

Further work by Blakey *et al*[10] led them to rule out energy transfer from triplet states as being significant in CL emission. However, they provided experimental evidence for a Chemically Induced Electron Exchange Luminescence (CIEEL) mechanism as the route for photon emission in polyolefins. The mechanism assumes polyolefin peroxides react with an easily oxidizable luminescent oxidation product.

The CIEEL mechanism could account for the results obtained in this current study on PA-6. The CL profile is proportional to the oxidation product profile because luminescence is dependant on the formation of an easily oxidizable luminescent oxidation product.

6.5 Conclusions

FTIES spectra of PA-6 samples after high extents of oxidation show little deviation from the spectra of unoxidized PA-6 samples regardless of endgroup. The only significant changes appear to be an increase in the carbonyl bands between 1700 and 1800 cm^{-1} and a decrease in the amide bands. There is no other information to aid in the elucidation of the mechanism of PA-6 oxidation and certainly no indication of the role that endgroups play in the mechanism.

Oxidation product profiles can be prepared from the time resolved FTIES spectra. Such profiles are proportional to CL curves regardless of the endgroup type. This result supports the CIEEL mechanism as proposed for Polyolefins by Blakey and George[10].

6.6 References

(1) Willis, H. A., *Laboratory Methods in Vibrational Spectroscopy*, Willis, H. A., Van Der Maas, J. H., Miller, R. G. J., John Wiley and Sons, New York, 1987.

(2) Celina, M.; Ottesen, D. K.; Gillen, K. T.; Clough, R. L., *Polym. Degrad. Stab.*, **58** (1997) 15.

(3) George, G. A.; Vassallo, A. M.; Cole-Clarke, P. A.; Celina, M., *Die Angew. Makromol. Chem.*, **232** (1995) 105.

(4) Blakey, I.; George, G. A., *Macromolecules*, **34** (2001) 1873.

(5) George, G. A.; Celina, M.; Vassallo, A. M.; Cole-Clarke, P. A., *Polym. Deg. Stab.*, **48** (1995) 199.

(6) DeBlase, F. J.; Compton, S., *Appl. Spec.*, **454** (1991) 611.

(7) Celina, M.; Gillen, K. T.; Wise, J.; Clough, R. L., *Radiation Phys. and Chem.*, **48** (1996) 613.

(8) Do, C. H.; Pearce, E. M.; Bulkin, B. J.; Reimschuessel, H. K., *J. Polym. Sci., Part A: Polym. Chem.*, **25** (1987) 2409.

(9) Svoboda, M.; Schneider, B.; Stokr, J., *Collect. Czech. Chem. Commun.*, **56** (1991) 1461.

(10) Blakey, I.; Billingham, N. C.; George, G. A., *Macromolecules*, (accepted 2001)

7. MALDI-TOF MS Method Development

7.1 Abstract

Methods for the MALDI-TOF analysis of various PA-6 samples were developed. The samples included PA-6 samples terminating predominantly in carboxylic, amine or methyl groups.

The optimum instrumental settings and sample preparation techniques for the MALDI-TOF MS analysis of each sample was determined by a systematic reduction of variables. Experimental settings such as type of mass analyzer, accelerating voltage and laser power, and preparation conditions such as matrix, solvents, sample and matrix concentrations, cationization agents and application methods were all varied.

7.2 Introduction

Hillenkamp and Karas developed matrix assisted laser desorption/ionization time of flight mass spectrometry (MALDI-TOF MS) in 1988 for the analysis of large biomolecules.[1,2] MALDI-TOF MS is a soft ionization technique that allows the measurement of intact molecular ions. The basic principles of MALDI-TOF MS are discussed in section 2.4. Unlike some other MS techniques, MALDI-TOF MS can measure molecular ions above 100,000 Da with virtually no fragmentation.[3-6] However, the first investigation on polymers with MALDI-TOF MS was not performed until 1992.[3-5]

MALDI-TOF MS has been applied to the analysis of polymers over the last few years with increasing success.[7] The MALDI-TOF MS spectra of polymers can provide a great deal of important information in the mass range where single polymer chains are resolved, e.g. mass of the constituent repeating units, composition of end groups, chemical distributions (i.e. different functional groups, different sequences of monomers or different sequence length), and structural heterogeneities (i.e. linear, cyclic, grafted or branched segments).[8-12]

There is no general rule on how to select the ideal instrumental settings or sample preparation for the MALDI-TOF MS analysis of a given polymer. The selection is still a matter of experimentation that must be worked out for each polymer. Variables to consider are experimental settings such as linear or reflectron mass analyzer, accelerating voltage and laser power, and preparation conditions such as matrix, solvents and cationization agents.

This chapter presents the method development for the MALDI-TOF analysis of PA-6 samples.

7.3 Experimental

7.3.1 Materials

Three distinct PA-6 samples terminating predominantly in carboxylic, amine or methyl groups respectively were used. The synthesis and characterization of the samples are discussed in chapter 3. All solvents, matrices and cationization agents were obtained from commercial sources and appropriately purified if required. The more significant matrices, solvents and cationization agents used are listed in Table 7.1.

7.3.2 MALDI-TOF MS Instrumentation and Spectrum Acquisition

A Micromass TOF Spec E spectrometer was used to acquire the mass spectra. The instrument was equipped with a nitrogen laser (λ=337 nm) to desorb and ionize the samples. Samples were deposited and dried onto a stainless steel target. A video camera was attached to the instrument that enabled real time images to be displayed on a TV monitor, which aided in the aiming of the laser at specific locations within a target area. The accelerating voltage used was 20 kV. All spectra were collected in the reflectron mode and were the sum of no less than 200 laser shots. External mass

calibration was applied, based on a number of points that both bracketed and fell within the mass range of interest. Numerous combinations of matrix, solvent, cationization agent and concentrations were investigated.

Table 7.1: Various factors trialed during method development for MALDI-TOF MS analysis of PA-6.

MATRIX	**SOLVENTS**
Sinapinic acid	2,2,2-trifluoroethanol
α-cyano-4-hydoxycinnamic acid	Water
2,5-dihydroxybenzoic acid	Acetonitrile
β-indole acrylic acid	Acetone
2-(4-hydroxyphenylazo)benzoic acid	**CONCENTRATION** (mg/mL)
Dithranol	0.1
2,5-dihydroxybenzoic acid	1
CATIONIZATION AGENT	10
NaCL	100
LiI	
AgTFA	

7.4 Results and Discussion

The results in this chapter are set out such that the optimum methodology determined for the MALDI-TOF MS analysis of PA-6 samples is displayed first. Significant variables

contributing to the methodology (e.g. experimental settings and preparation conditions) will then be discussed in greater detail.

7.4.1 Optimum Method for PA-6 Analysis by MALDI-TOF MS

The same method was found to be optimal for the MALDI-TOF MS analysis of PA-6 samples that differed by end group species. The outline for this method is provided below.

> PA-6 solutions were prepared to a concentration of 10 mg/mL in TFE. The matrix (HABA) was also prepared to a concentration of 10 mg/mL in TFE. Equal amounts of these solutions were mixed and approximately 2 μL of this combined solution was applied to a stainless steel plate and air-dried. Samples were measured in reflectron mode and the spectra generated by summing a minimum of 200 laser shots.

An example of a typical spectrum obtained from a PA-6 sample via this method is illustrated in Figure 7.1, which displays the MALDI-TOF MS spectrum of amine terminated PA-6. The spectrum is typical of a polymer with a high polydispersity. From the inset it can be seen that the spectrum is composed of a number of series of peaks. The peak-to-peak distance for each series of peaks is approximately 113 Da, which reflects the mass of a PA-6 repeat unit. The three most intense series of peaks correspond to protonated, sodium cationized and potassium cationized forms of the same species. Two series of peaks with relatively low intensity indicate a small level of impurity within the sample. For examples of MALDI-TOF MS spectra for carboxylic and methyl terminated PA-6 using this method see figures 3.4 and 3.6 respectively.

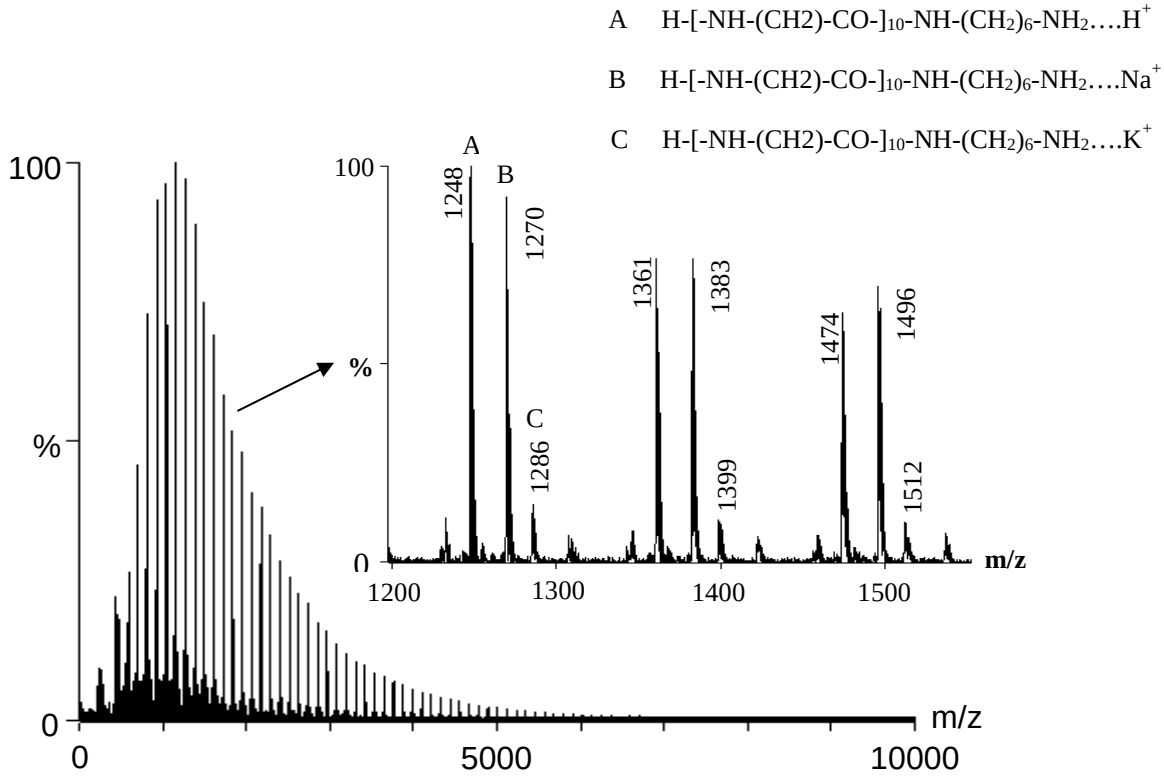

Figure 7.1: MALDI-TOF mass spectrum of amine terminated PA-6, where the three most intense series of peaks in the inset, labeled A, B and C, represent protonated, sodium cationized and potassium cationized chains of the same species.

7.4.2 Matrix Selection

The choice of the matrix is possibly the most important factor in the MALDI-TOF MS analysis of a sample. However, the first question should be: is a matrix really required? Laser desorption (LD) is capable of producing intact molecular ions up to a few thousand Da. When looking at Figure 7.2, which is the LDI-TOF MS of amine terminated PA-6 prepared via the optimal method with the omission of the matrix, the answer to the previous question is yes a matrix is definitely required.

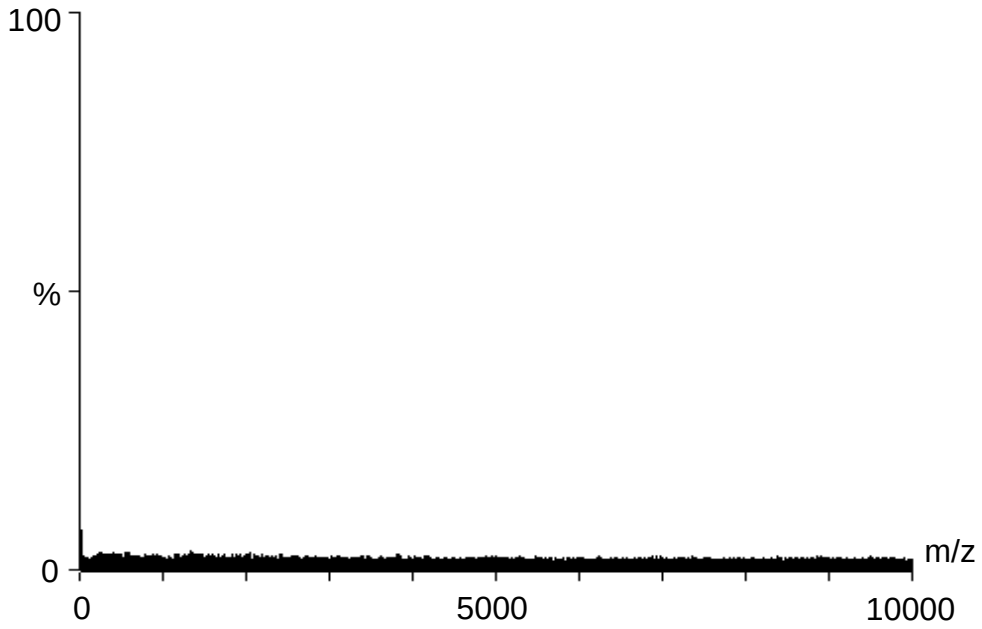

Figure 7.2: LDI-TOF mass spectrum of amine terminated PA-6 (i.e. without matrix).

Numerous matrixes were examined in order to select the most effective for the MALDI-TOF MS measurements. Most matrixes produced a spectrum like that of Figure 7.3 where the MALDI-TOF MS spectrum is dominated by peaks associated with the matrix and peaks representing the sample are only just visible. The results indicated that HABA, used to obtain the spectrum in figure 7.1, provides a MALDI-

TOF MS spectrum with the most abundant ion intensity. Therefore, HABA was selected as the matrix for the analysis of PA-6.

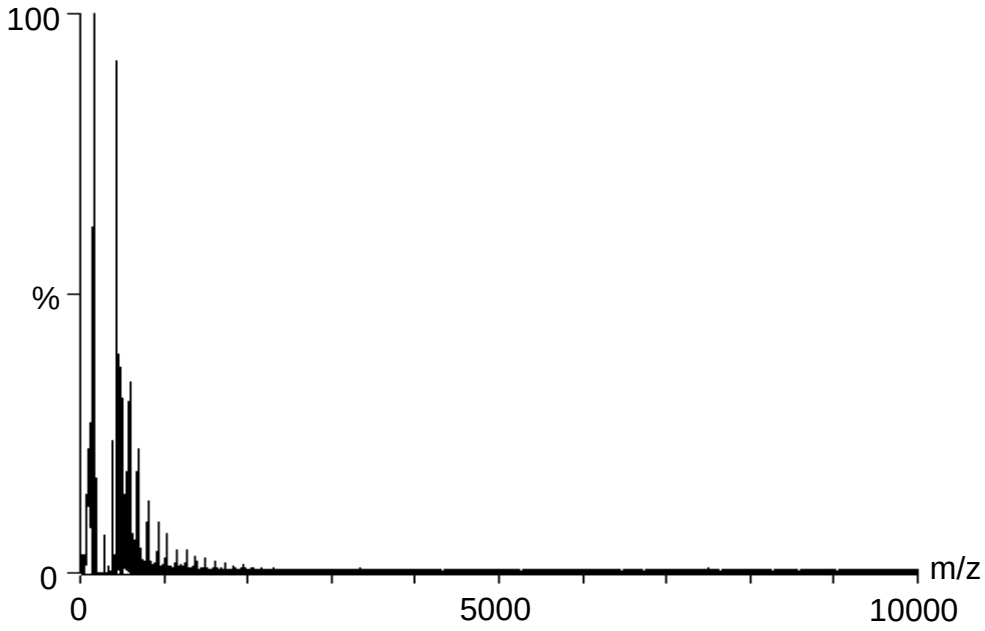

Figure 7.3: MALDI-TOF mass spectrum of amine terminated PA-6, where a-cyano-4-hydoxycinnamic acid was used at the matrix.

7.4.3 Solvents

A solvent suitable for dissolving a matrix might not be appropriate for dissolving the sample under investigation and vice versa. This is even more pronounced when the sample is a polymer such as PA-6, where only a handful of organic solvents can dissolve it. For example, acetone is regularly used to prepare a solution of HABA, while TFE is used to prepare a solution of PA-6.

A number of binary systems were trialed for PA-6/matrix combinations. TFE was always used to dissolve the PA-6 sample while acetone, water and acetonitrile, to name a few, were used to dissolve the matrixes. Although the ion intensity was high for the majority of binary solvent systems a significant mass discrimination against the larger oligomers and a variation in the polymer distribution was observed (see Figure 7.4) for all binary solvent systems investigated.

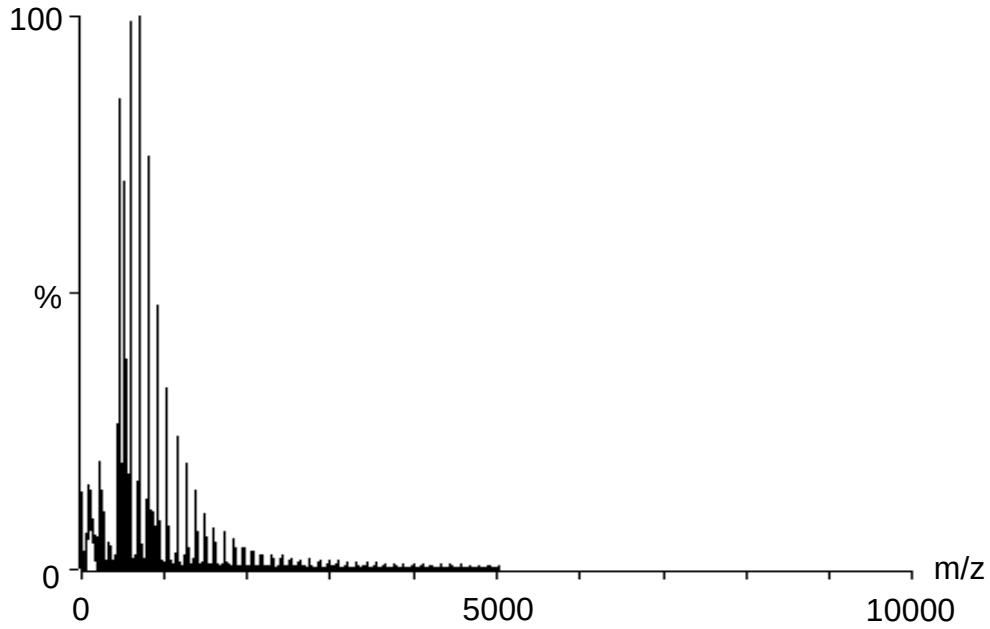

Figure 7.4: MALDI-TOF mass spectrum of amine terminated PA-6 obtained via the use of a binary solvent system, where the PA-6 was dissolved in TFE and the HABA was dissolved in acetone.

The optimum result was obtained when the same solvent (TFE) was used to dissolve both sample (PA-6) and matrix. The combination of PA-6 and HABA, both dissolved in TFE, was determined to be the most suitable for MALDI-TOF MS of PA-6.

7.4.4 Concentrations of PA-6 and Matrix

The optimum concentrations of PA-6 and HABA were chosen simply by comparing the spectra obtained for different combinations of the concentrations listed in table 7.1. 10 mg/mL of PA-6 and 10 mg/mL of HABA were found to be the optimum concentrations and ratio when applying approximately 2 μL of a combined solution to the sample plate. If a lower ratio of PA-6 was used then insufficient sample would be present and the ion intensity for the PA-6 would decline (Figure 7.5). Too little matrix also caused the same effect.

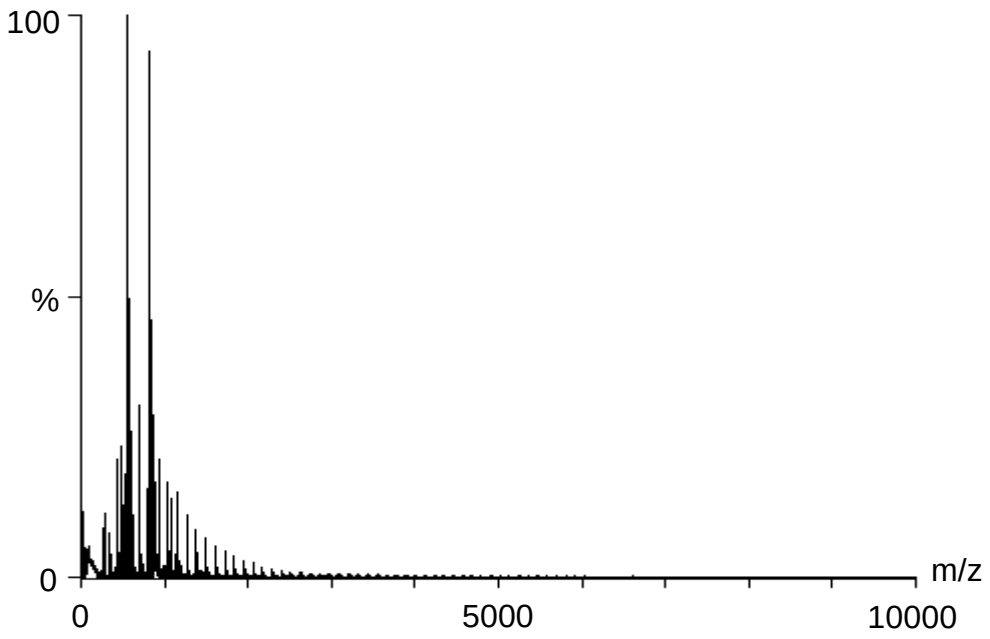

Figure 7.5: MALDI-TOF mass spectrum of amine terminated PA-6 obtained when the concentration of PA-6 was 1mg/mL and the concentration of HABA was 10 mg/mL.

7.4.5 Deposition

The most commonly employed approach for sample preparation for MALDI-TOF MS has been to deposit a solution of matrix and a solution of sample onto a substrate. This can be done one of two ways. The solutions can be mixed prior to deposition or deposited separately onto the substrate. The sample is then allowed to dry before being placed into the instrument.

The MALDI-TOF MS spectra obtained when the solutions were mixed prior to deposition were far superior to those obtained after the solutions were deposited separately. Figure 7.6 shows a MALDI-TOF MS spectrum from a sample where the PA-6 and HABA solutions were deposited separately. The PA-6 oligomers do not appear to have ionized at all. This observation is likely to be due to the fact that HABA and PA-6 precipitate at different rates as the drop dries. Therefore, much of the PA-6 sample is not co-deposited with the HABA and hence cannot be desorbed and ionized. This effect is exaggerated when the solutions are applied separately.

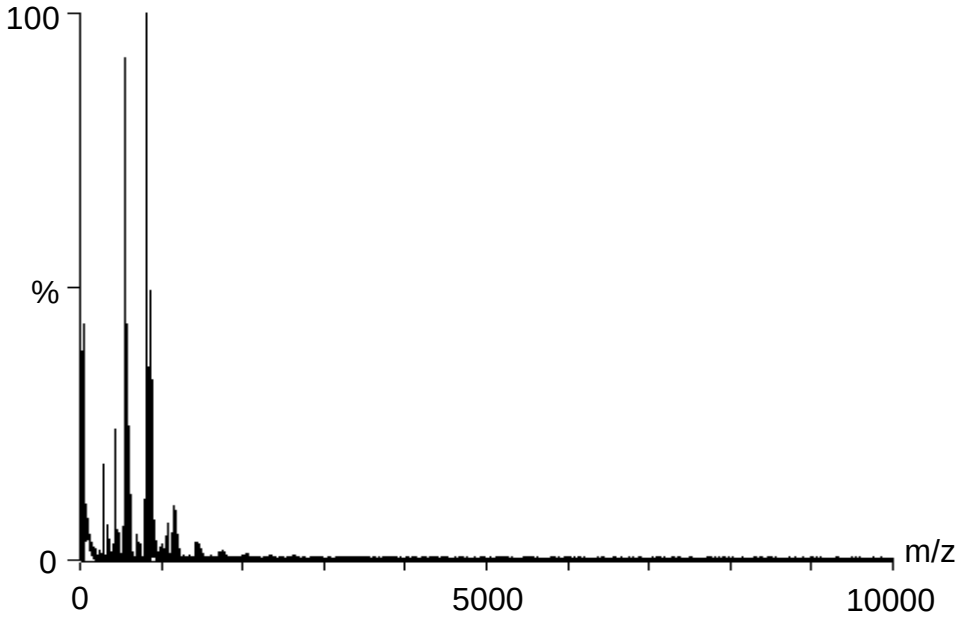

Figure 7.6: MALDI-TOF mass spectrum of amine terminated PA-6 obtained after the solutions of PA-6 and HABA were deposited separately.

7.4.6 Cationization Agents

Polymers are often not readily protonated in MALDI and are instead observed as complexes or adducts with alkali or transition metal ions. Therefore, metal ions are often added to enhance cationization. In Figure 7.1 three series of intense peaks, which correspond to protonated, sodium cationized and potassium cationized forms of PA-6 oligomers, can be observed. Therefore, PA-6 appears to protonate and cationize with sodium and potassium readily even without the further addition of cationization agents. However, various cationization agents were trialed in the anticipation that the PA-6 oligomers would preferentially cationize with the added metal ion. This would reduce the complexity of the spectrum because in the ideal result there would only be one peak per species instead of three. If the MALDI-TOF MS spectrum of oxidized PA-6 were to contain 10 different species then without preferential cation attachment there would be 30 peaks to identify instead of 10.

The addition of Na^+ had no significant effect. The intensity of the peaks representing the sodiated form of the oligomers was slightly increased over the peaks for other cations. However, the complexity of the spectrum was not greatly reduced. The addition of Ag^+ to the sample only resulted in increasing the complexity of the spectrum. An additional peak for the silver cationized peak was observed, the intensity of which was not significantly greater than observed for any other cation. The greatest effect came from the addition of Li^+ (Figure 7.7). The PA-6 oligomers have a much higher affinity for the Li^+ than for H^+, Na^+ or K^+, which is illustrated by the presence of only one significant series of peaks for the PA-6 oligomers. Unfortunately the addition of Li^+ causes the ion intensity for the PA-6 peaks to be

considerably decreased. As a consequence, the addition of cationization agents is omitted from the methodology.

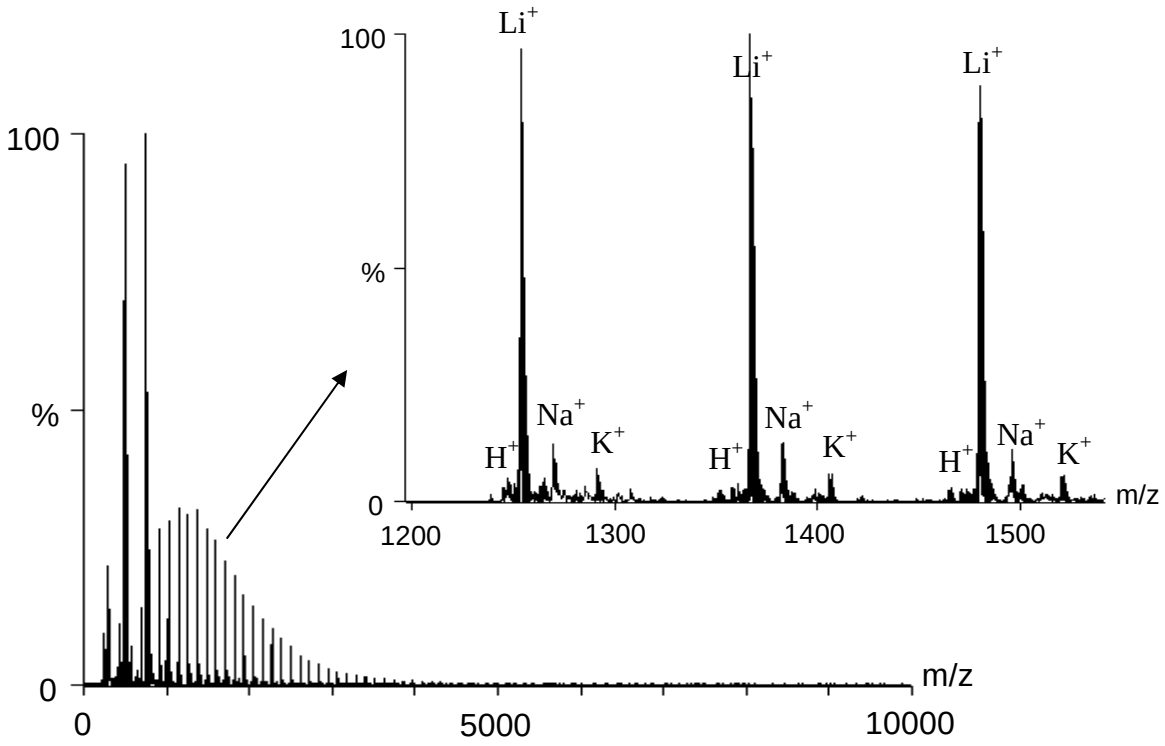

Figure 7.7: MALDI-TOF mass spectrum of amine terminated PA-6 obtained after the addition of Li^+ as a cationization agent.

7.4.7 Instrument Settings

MALDI-TOF MS spectra were always collected in the reflectron mode due to the relatively low molecular weight of the samples. The accelerating voltage was always set to 20 kV and the laser energy was adjusted from acquisition to acquisition.

7.5 Conclusions

The same MALDI-TOF MS method was found to be the optimal method for all non-oxidized and oxidized samples of PA-6. The best MALDI-TOF MS spectra for each sample were collected when:

- Sample solutions were prepared to a concentration of 10 mg/mL, of both PA and HABA (matrix), in TFE. Approx. 2 μL of this combined solution was applied to a stainless steel plate and air-dried.

- All samples were measured in reflectron mode and the spectra generated by summing a minimum of 200 laser shots.

7.6 References

(1) Karas, M.; Bachmann, D.; Bahr, U.; Hillenkamp, F., *Int. J. Mass Spectrom. Ion Processes*, **78** (1987) 53.

(2) Hillenkamp, F.; Karas, M.; Beavis, R. C.; Chait, B. T., *Anal. Chem.*, **63** (1991) 1193.

(3) Danis, P. O.; Karr, D. E.; Mayer, F.; Holle, A.; Watson, C. H., *Org. Mass Spectrom.*, **27** (1992) 843.

(4) Karas, M.; Bahr, U.; Deppe, A.; Stahl, B.; Hillenkamp, F., *Macromol. Chem., Macromol. Symp.*, **61** (1992) 397.

(5) Danis, P. O.; Karr, D. E.; Westmoreland, D. G.; Piton, M. C.; Christie, D. I.; Clay, P. A.; Kable, S. H.; Gilbert, R. G., *Macromolecules*, **26** (1993) 6684.

(6) Schriemer, D. C.; Li, L., *Anal. Chem.*, **68** (1996) 2721.

(7) Rader, H. J.; Schrepp, W., *Acta Polym.*, **49** (1998) 272.

(8) Pasch, H.; Unvericht, R.; Resch, M., *Angew. Makromol. Chem.*, **212** (1993) 191.

(9) Schadler, V.; Spickermann, J.; Rader, J.; Wiesner, U., *Macromolecules*, **29** (1996) 4865.

(10) Spickermann, J.; Rader, H. J.; Mullen, K.; Muller, B.; Gerle, M.; Fischer, K.; Schmidt, M., *Macromol. Rapid Commun.*, **17** (1996) 885.

(11) Montaudo, G.; Montaudo, M. S.; Puglisi, C.; Samperi, F., *J. Polym. Sci., Part A: Polym. Chem.*, **34** (1996) 439.

(12) Kruger, R. P., *GIT Fachz Lab.*, **3** (1995) 189.

8. MALDI-TOF MS of Oxidized PA-6

8.1 Abstract

The MALDI-TOF MS method developed in chapter 7 was utilized to investigate the oxidative degradation of PA-6. Samples of PA-6 were thermally oxidized for various intervals of time. The relative extent of oxidation for each sample analyzed by MALDI-TOF MS was examined via chemiluminescence.

Degradation products of PA-6 can be ionized and detected by MALDI-TOF MS, but it is only possible to detect the occurrence of degradation products by MALDI-TOF MS after considerable oxidation as measured by chemiluminescence. As a result, the identification of the species formed during oxidation was not possible because by the time oxidation products could be observed, the starting PA-6 material had undergone a number of oxidative processes.

8.2 Introduction

The simultaneous CL-DSC results obtained in chapter 4 highlighted the changes that occur in the oxidative stabilities and mechanisms of PA-6 as a result of altering the end groups of PA-6. It was proposed that when amine end groups were abundant in the PA-6 sample a chemically induced electron exchange luminescence (CIEEL) mechanism could occur directly but when amine end groups were absent the CIEEL mechanism could not operate until an easily oxidisable luminescent oxidation product was formed.

CL Imaging was used in chapter 5 to map the occurrence and extent of oxidation across samples of PA-6 to display the influence end groups have on the homogeneous or heterogeneous nature of PA-6 oxidation. It was concluded that certain end groups could be said to cause PA-6 to undergo heterogeneous oxidation.

Despite the large amount of literature[1-8] about the thermo-oxidative degradation of PA-6, the techniques used so far to monitor the early stages of the oxidative degradation have not provided clear evidence for the structures of the species produced. MALDI-TOF MS spectra are obtained from the desorption of intact polymer chains and allows the direct determination of the individual species contained in the polymer.[9] Carroccio *et al* have used MALDI to analyse photo-oxidative degraded samples of PA-6[11] and PA-6,6[12]. Although the samples studied had undergone extensive degrees of degradation they were able to provide information on the structure of some degradation products and draw maps of the photodecomposition mechanisms for the respective PA's.

The aim of this chapter was to apply the MALDI-TOF MS method developed in chapter 7 for the analysis of PA-6 in order to investigate the nature of the degradation products in the different stages of oxidation and therefore gain further insight into the mechanisms proposed in the previous chapters.

8.3 Experimental

8.3.1 Materials

PA-6 samples terminating predominantly in carboxylic, amine or methyl groups were used. The synthesis and characterization of the samples are discussed in chapter 3. TFE and HABA where analytical grade reagents purchased from Sigma Aldrich Chemical Company (Australia) and used as received.

8.3.2 Oxidation and Chemiluminescence of Samples

Approximately 5 mg of each sample was placed into a CL apparatus. The CL apparatus used has been described elsewhere.[10] Photon counts were accumulated every 10 seconds during thermo-oxidation at 150°C under oxygen with a flow rate of 50 mL/min.

8.3.3 MALDI-TOF MS Instrumentation and Spectrum Acquisition

Sample solutions were prepared to a concentration of 10 mg/mL, of both PA and HABA (matrix), in TFE. Approx. 2 μL of this combined solution was applied to a stainless steel plate and air-dried. A Micromass TOF Spec E spectrometer was used to acquire the mass spectra. The instrument was equipped with a nitrogen laser (λ=337 nm) to desorb and ionize the samples. The accelerating voltage used was 20 kV. The laser energy was maintained slightly

above threshold. All spectra were collected in the reflectron mode and were the sum of no less than 200 laser shots. External mass calibration was applied, based on a number of points that both bracketed and fell within the mass range of interest.

8.4 Results and Discussion

The carboxylic terminated PA-6 was of relatively high molecular weight and most probably of high polydispersity. As a result, the MALDI-TOF MS spectrum of the non-oxidized sample (Figure 3.4) was poor. The detector was flooded with the lower molecular weight chains causing the signal to noise ratio to be low. The consequence was that oxidation products could not be detected until extremely high amounts of oxidation had occurred. Detection of the oxidation products from methyl terminated PA-6 was also not possible. This was most likely due to the number of oxidation products being too numerous causing the signal to noise to again be below the level of detection. The best results were obtained for amine terminated

PA-6. The process of how this type of sample undergoes azomethine condensation was discussed in section 1.3. By undergoing azomethine condensation the number of products is kept low which results in a greater signal to noise and the detection of oxidation products.

Figure 8.1 illustrates how four samples were each thermooxidatively degraded at 150°C under an oxygen atmosphere to different extents as displayed on the CL curve. These degraded samples were then analysed by MALDI-TOF MS.

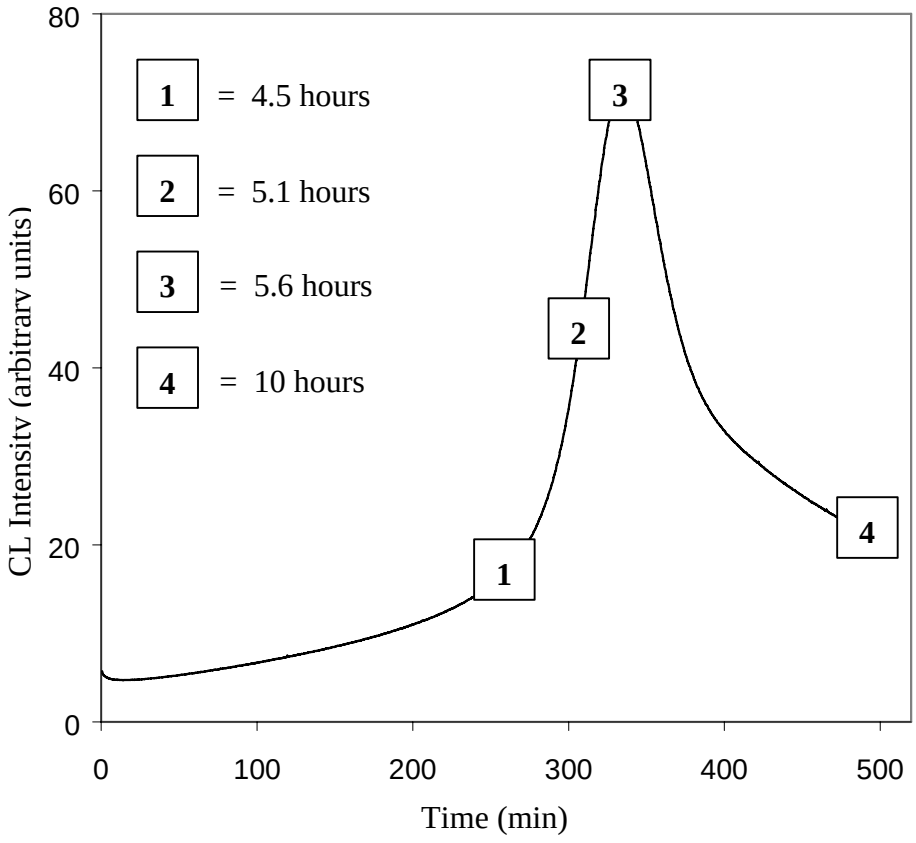

Figure 8.1: Chemiluminescence curve for amine terminated PA-6 at 150°C under an oxygen atmosphere

Figures 8.2 to 8.5 displays the MALDI-TOF MS spectra for amine terminated PA-6 samples oxidized to the positions indicated on the CL curve in Figure 8.1.

No significant peaks due to degradation can be detected in the sample after 4.5 hours of thermo-oxidation. However, after 5.1 hours of degradation peaks around 1262 Da, 1298 Da and possibly at 1276 Da due to degradation become visible. The degradation products grow to be quite visible after 5.6 hours of degradation; the most noticeable being detected around 1262 Da, 1276 Da and 1298 Da. In addition, there are numerous peaks consistent with a complex degradation process at the maximum of the CL curve. After 10 hours of thermo-oxidative degradation the differences in the spectrum compared to an unoxidized sample is very apparent. There is a peak on every mass unit consistent with the high extent of degradation. It also illustrates that degradation products of Nylon 6 can be ionized and detected by MALDI-TOF MS.

Therefore, it is only possible to detect the occurrence of degradation products after considerable oxidation as measured by chemiluminescence. By the time oxidation products could be observed the starting PA-6 material had undergone a number of oxidative processes which meant that the identification of the species formed was not possible.

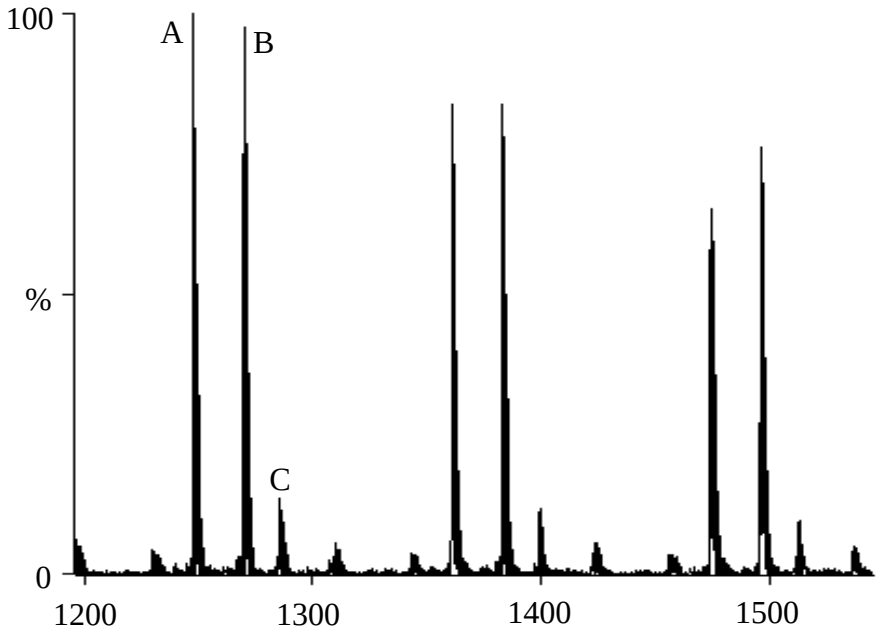

Figure 8.2: MALDI-TOF MS spectrum of amine terminated PA-6 after 4.5 hours of thermo-oxidative degradation at 150°C in oxygen.

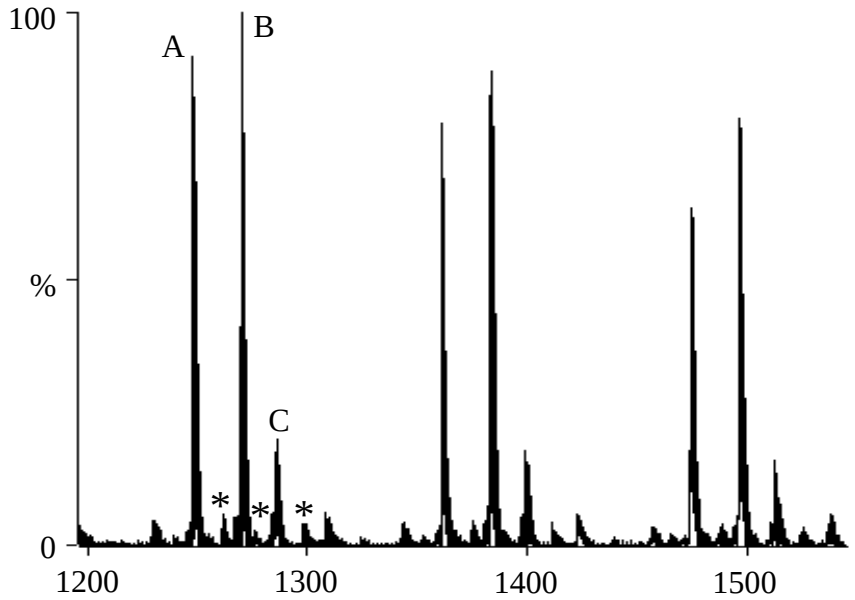

Figure 8.3: MALDI-TOF MS spectrum of amine terminated PA-6 after 5.1 hours of thermo-oxidative degradation at 150°C in oxygen. * indicates degradation product.

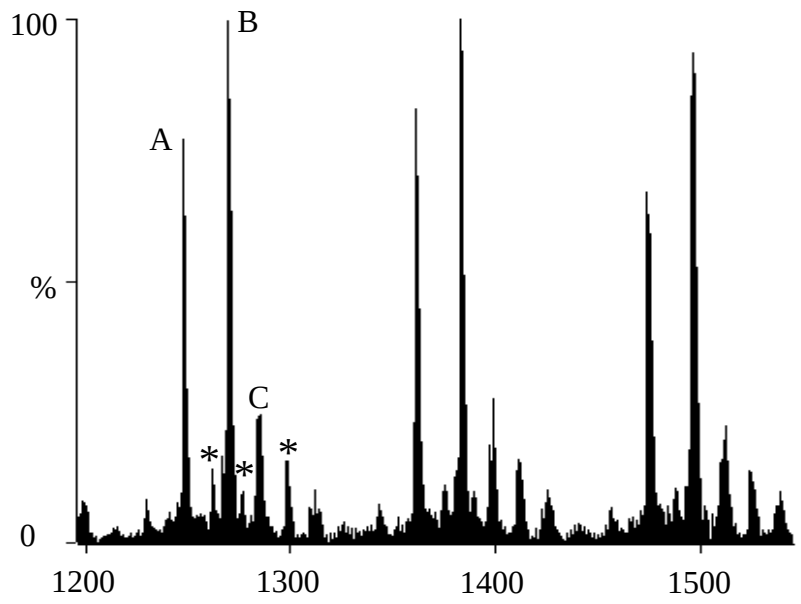

Figure 8.4: MALDI-TOF MS spectrum of amine terminated PA-6 after 5.6 hours of thermo-oxidative degradation at 150°C in oxygen. * indicates degradation product.

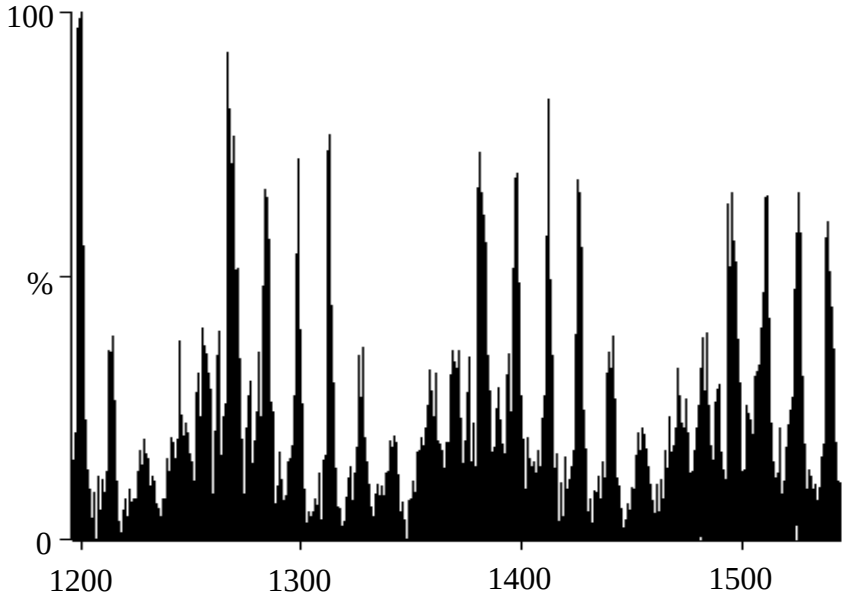

Figure 8.5: MALDI-TOF MS spectrum of amine terminated PA-6 after 10 hours of thermo-oxidative degradation at 150°C in oxygen.

8.5 Conclusions

The MALDI-TOF MS spectra of highly degraded samples were consistent with a complex degradation process. Therefore, degradation products of PA 6 can be ionized and detected by MALDI-TOF MS. However, it is only possible to detect the occurrence of degradation products by MALDI-TOF MS after considerable oxidation as measured by chemiluminescence. This limitation is most likely due to the large polydispersity of the sample produced by oxidation.

Identification of the species formed was not possible. By the time oxidation products could be observed the starting PA-6 material had undergone a number of oxidative processes.

8.6 References

(1) Sharkey, W. H.; Mochel, W. E., *J. Am. Chem. Soc.*, **81** (1959) 3000.

(2) Levantovskaya, I. I.; Kovarskaya, B. M.; Dralyuk, G. V.; Neiman, M. B., *Vysokomol Soedin*, **6** (1964) 1885.

(3) Karstens, T.; Rossbach, V., *Makromol. Chem.*, **190** (1989) 3033.

(4) Levchik, S. V.; Weil, E. D.; Lewin, M., *Polym. Int.*, **48** (1999) 532.

(5) Gijsman, P.; Kroon, M.; Vanoorschot, M., *Polym. Deg. Stab.*, **51** (1996) 3.

(6) Forsstrom, D.; Terselius, B., *Polym. Degrad. Stab.*, **67** (1999) 69.

(7) Forsstrom, D.; Svensson, L.-G.; Terselius, B., *Polym. Degrad. Stab.*, **67** (2000) 263.

(8) Forsstrom, D.; Reitberger, T.; Terselius, B., *Polym. Degrad. Stab.*, **67** (2000) 255.

(9) Rader, H. J.; Schrepp, W., *Acta Polym.*, **49** (1998) 272.

(10) Celina, M.; George, G. A.; Billingham, N. C., *Polym. Deg. Stab.*, **42** (1993) 335.

(11) Carroccia, S.; Puglisi, C.; Montudo, G., *Macromol.*, **36** (2003) 7499.

(12) Carroccia, S.; Puglisi, C.; Montudo, G., *Macromol.*, **37** (2004) 6037.

9. Conclusions

A technique that simultaneously measures chemiluminescence (CL) and heat flow (DSC) was used to study the isothermal oxidation of unstabilized PA-6 samples at temperatures ranging from 140°C to 160°C. The differences in the oxidative mechanisms and stabilities, as a result of the end groups, for PA-6 were made obvious by a comparison of CL curves. Both the CL and heat flow curves had the same basic shape for each type of end group. In the case of amine terminated PA-6 samples the CL intensity was proportional to the heat flow curve. Yet, for PA-6 samples terminating in end groups other than amine end groups, the time to maximum intensity for the two types of curves differed by approximately 70% to 80%. When amine end groups were absent it was the first derivative of the CL intensity that was proportional to the heat flow curve. Thus in the case of amine terminated PA-6 a CIEEL mechanism occurs directly and the CL profile is that of [ROOH] versus time. While, in the absence of amine end groups, the CIEEL mechanism cannot operate until an easily oxidisable luminescent oxidation product is formed.

CL images obtained at various oxidation times from PA-6 films indicated that the nature of oxidation for PA-6 appeared to be homogeneous regardless of the type of end group present in the polymer. When films of carboxylic terminated PA-6 were doped with adipic acid the oxidation again appeared to be homogeneous. However heterogeneous oxidation occurs when films of amine and methyl terminated PA-6 are

doped with adipic acid. The initial zone of oxidation resulting from the contact with adipic acid is so active that the oxidation spreads from that area to the remainder of the polymer. Therefore, it is proposed that carboxylic end groups may cause PA-6 to undergo heterogeneous oxidation. The distribution of the end groups within the film makes the scale of oxidative heterogeneity in the uncontaminated films smaller than the resolution of the CCD camera.

FTIES spectra of PA-6 samples after high extents of oxidation show little deviation from the spectra of unoxidized PA-6 samples regardless of endgroup. The only significant changes appear to be an increase in the carbonyl bands between 1700 and 1800 cm^{-1} and a decrease in the amide bands. There is no other information to aid in the elucidation of the mechanism of PA-6 oxidation and certainly no indication of the role that endgroups play in the mechanism. Oxidation product profiles can be prepared from the time resolved FTIES spectra. Such profiles are proportional to CL curves regardless of the endgroup type. These results are consistent with a CIEEL mechanism.

The same MALDI-TOF MS method was found to be the optimal method for analysis of all non-oxidized and oxidized samples of PA-6. The best MALDI-TOF MS spectra for each sample were collected when: sample solutions were prepared to a concentration of 10 mg/mL of both PA and HABA (matrix) in TFE; approx. 2 μL of this combined solution was applied to a stainless steel plate and air-dried; and all samples were measured in reflectron mode and the spectra generated by summing a minimum of 200 laser shots.

The MALDI-TOF MS spectra of highly degraded samples were consistent with a complex degradation process. This illustrated that degradation products of PA 6 can be ionized and detected by MALDI-TOF MS. However, it is only possible to detect the occurrence of degradation products by MALDI-TOF MS after considerable oxidation as measured by chemiluminescence. This downfall is most likely due to the large polydispersity of the sample produced by oxidation. Identification of the species formed was not possible. By the time oxidation products could be observed the starting PA-6 material had undergone a number of oxidative processes.

10. Future Work

Results from this work suggest that end groups could be a site within the polymer that leads to heterogeneous oxidation. Although results indicated that oxidation could in fact be spreading from carboxylic end groups, the distribution of the end groups through the polymer makes the scale of oxidative heterogeneity smaller than the resolution of the CCD camera employed. Therefore, an instrument with a resolution greater than the scale of oxidative heterogeneity needs to be employed in order to map the chemical and physical heterogeneities occurring as a result of the end groups. The most sensitive technique for nano- to micro-metre scale mapping of such heterogeneities would be lateral force measurements (LFM) during Atomic Force Microscopy (AFM).

Contact AFM, where the tip is in constant contact with the sample, can be destructive towards the sample. The use of non-contact AFM means that soft samples are unaffected, however the presence of water layers on the surface of most polymers results in imaging of the surface of the liquid. This has been overcome by using intermittent contact or tapping AFM with the cantilever vibrating at its resonant frequency. In this mode a greater variation in surface topography may be accommodated. A further development has been to measure the twisting of the cantilever due to changes in forces parallel to the surface. This lateral force measurement (LFM) enables edge-enhanced images to be obtained where there is a change of the surface composition. By performing LFM and AFM simultaneously it

is possible to separate effects due to surface topography from those due to surface composition. Therefore this technique could be used to determine the dimensions of the heterogeneous domains caused by the end groups of PA-6 and observe the progressive oxidation growth to give an absolute measure of the rate of spreading.

It has recently been demonstrated that it is possible to perform Chemical Force Microscopy (CFM) by using chemically modified AFM tips. Self assembled monolayers (SAM's) are produced by depositing appropriate long chain thiols terminating in specific functional groups onto silicon AFM tips that have been freshly coated with gold. The functionalised tips discern similar species present on the surface of a substrate by the different adhesive and frictional forces. By choosing the appropriate functional groups for the AFM tip it should be possible to not only determine the dimensions of the heterogeneous zones but also gain some insight into their composition during relatively low extents of oxidation.

Degradation products could only be detected via MALDI-TOF MS after considerable oxidation as measured by chemiluminescence. Size exclusion chromatography (SEC) could be utilized to either narrow the polydispersity of the unoxidized samples or extract degradation products early in the degradation process. Either option or the combination of both could increase the possibility of early detection via MALDI-TOF MS.